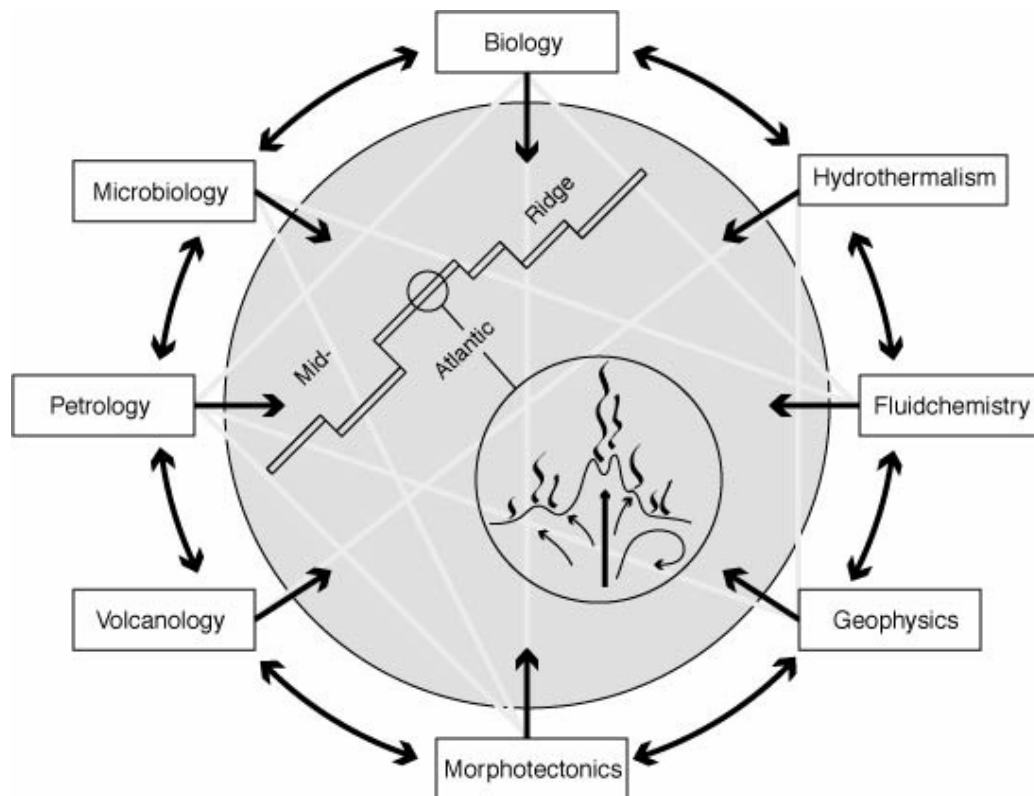


Mid-Atlantic Expedition 2009

FS METEOR Cruise No. 78, Leg 2

Mantle to ocean on the southern Mid-Atlantic Ridge (5°S - 11°S) (MAR-SÜD V)

02.04.2009 Port of Spain – 11.05.2009 Rio de Janeiro



SPP 1144: “From Mantle to Ocean: Energy, Material and Life Cycles at Spreading Axes”.

Content

		Page
2.1	Participants	3
2.2	Research Program	5
2.3	Narrative of the Cruise	7
2.4	Preliminary Results	13
2.4.1	ROV Kiel 6000 Deployments	13
2.4.2	AUV-Dives	15
2.4.3	Geological Observations and Sampling	21
2.4.4	Physical Oceanography	37
2.4.5	Fluid Chemistry	44
2.4.6	Gases in Hydrothermal Fluids and Plumes	48
2.4.7	Microbial Ecology	52
2.4.8.	Hydrothermal Symbioses	56
2.4.9	Volatile Organohalogens	59
2.4.10	Temperature Measurements of Hydrothermal Fluids	64
2.4.11	Bathymetry	67
2.5.	Journey Course and Weather	71
2.6	References	73
2.7	Acknowledgments	74

Appendix

A 2.1	Stationlist	A 1
A 2.2	ROV Station Protocols	A 4
A 2.3	Rock Sampling Protocol M78/2: Inside Corner High at 5°S	A 56
A 2.4	Fluid Chemistry	A 64
A 2.5	Gas Chemistry	A 72
A 2.6	Microbiology	A 74
A 2.7	Animals Collected During M 78/2 for Symbioses Research	A 81
A 2.8	Temperature Measurements of Hydrothermal Fluids	A 83

2.1 Participants

Leg M 78/2

1.	Seifert, Richard, Dr.	Fahrtleiter / <i>Chief Scientist</i>	IfBM Uni-HH
2.	Abegg, Friedrich, Dr.	ROV	IFM-GEOMAR
3.	Borowski, Christian, Dr.	Zoologie / Symbiosen	MPI Bremen
4.	Breuer, Christian	Schwefel-Isotope	Univ. Münster
5.	Foster, Andrew	ROV	Schilling
6.	Garbe-Schönberg, Dieter, Dr.	Fluidprobenahmesysteme	Univ. Kiel
7.	Herrlich, Sascha	Gase / Fluidchemie	IfBM Uni-HH
8.	Hinz, Claus	ROV	IFM-GEOMAR
9.	Huusmann, Hannes	ROV	IFM-GEOMAR
10.	Klevenz, Verena	Fluidchemie	JUB
11.	Koepke, Jürgen, Dr.	Petrologie	Uni-Hannover
12.	Köhler, Janna	Ozeanographie	UBU
13.	Lackschewitz, Klas, Dr.	AUV	IFM-GEOMAR
14.	Laternus, Frank, Dr.	Gase / Fluidchemie	IfBM Uni-HH
15.	Meissner, Daniela	Fluidchemie	JUB
16.	Mertens, Christian, Dr.	Ozeanographie	UBU
17.	Perner, Mirjam, Dr.	Mikrobiologie	BKF Uni-HH
18.	Petersen, Sven, Dr.	Petrographie / Bathymetrie	IFM-GEOMAR
19.	Pieper, Martin	ROV	IFM-GEOMAR
20.	Rodriguez, Pablo	ROV	CSIC
21.	Rothenbeck, Marcel	AUV	IFM-GEOMAR
22.	Rychlik, Nicolas	Mikrobiologie	BKF Uni-HH
23.	Schirnack, Carsten, Dr.	AUV/ROV/Bathymetrie	IFM-GEOMAR
24.	Sticklus, Jan	AUV	IFM-GEOMAR
25.	Strauss, Harald, Prof. Dr.	Schwefel-Isotope	Univ. Münster
26.	Suck, Inken, Dr.	ROV	IFM-GEOMAR
27.	van der Heijden, Karina	Hydrothermale Symbiosen	MPI Bremen
28.	Warmuth, Marco	Gase / Fluidchemie	IfBM Uni-HH
29.	Truscheit, Thorsten	Wetterfunktechnik	DWD
30.	Rentsch, Harald	Wetterfunktechnik	DWD

*Participating Institutions***IfBM Uni-HH**

Universität Hamburg
Institut für Biogeochemie und
Meereschemie
Bundesstr. 55
D-20146 Hamburg, Germany

IFM-GEOMAR

Leibniz-Institut für Meereswissenschaften
Wischhofstr. 1-3
D-24148 Kiel, Germany

MPI-Bremen

Max-Planck Institut für Marine
Mikrobiologie
Celsiusstr. 1
D-28359 Bremen, Germany

Univ. Münster

Westfälische Wilhelms-Universität
Münster
Geologisch-Paläontologisches Institut
Corrensstr. 24
D-48149 Münster, Germany

Schilling

Schilling Robotics, Davis, California,
U.S.A.

Univ. Kiel

Christian-Albrechts-Universität Kiel
Institut für Geowissenschaften
Ludewig-Meyn-Str. 10
D-24118 Kiel, Germany

JUB

Jacobs University Bremen
School of Engineering and Science
P.O. Box 752561
D-28725 Bremen, Germany

Univ. Hannover

Leibniz Universitaet Hannover
Institut fuer Mineralogie
Callinstr. 3
30167 Hannover, Germany

UBU

Universität Bremen
Institut für Umweltphysik
PF 330440
D-28334 Bremen, Germany

BKF Uni-HH

University of Hamburg
Biocenter Klein Flottbek
Microbiology and Biotechnology
Ohnhorststr. 18
D-22609 Hamburg, Germany

CSIC

Unidad de Tecnología Marina, CSIC. Paso
Marítimo de la Barceloneta, Spain

DWD

Deutscher Wetterdienst
Geschäftsfeld Seeschifffahrt, Germany

2.2 Research Program

This cruise was the last scheduled within the DFG Special Priority Program 1144 to the major study site at 5° to 11°S, on the southern Mid-Atlantic Ridge (MAR), following the investigations performed during and subsequent to cruises M62/5, CD169, M64/1, M68/1, and L'Atalante II 2008. Work focused on cross-disciplinary core questions of the SPP 1144:

- How does the energy and mass transfer from the mantle into the ocean take place?
- What are the time scales on which processes at spreading axes occur?
- How does the regional geology influence and control vent fluid composition and spatial and temporal changes in hydrothermal fluxes?

To answer these questions, a comprehensive set of data and samples was obtained from 4 hydrothermally active areas:

- Vents around 4°48'S: Found and sampled for the first time in 2004 during cruise M64/1, these vents provide a wide variety of fluid types, habitats and geological settings to investigate the linkages between magmatism, fluid circulation and ecosystems in the deep sea.
- Inside corner high at 5°S: There is mounting evidence that the deep crust also plays an important role in hydrothermal circulation and that water in the deep crust can strongly influence magmatic processes. Earlier studies during M47/2 and L'Atalante 2008 have shown the presence of good lower crustal exposures on an inside corner high just south of the 4°48'S vent fields.
- The 'Nibelungen' field hosting the 'Drachenschlund' black smoker vent found during M68/1 at 8°18' S/13°30'W in 2915 m water depth. This is one of the few known ultramafic-hosted systems, the first of its kind to be found on the southern MAR.
- Lilliput Vent Fields at 9°32'S: Discovered during M64/1, this area located in much shallower water than the 4°48'S vents provides an ideal compliment, enabling the influence of water depth on hydrothermal and biological processes to be investigated in a systematic way for the first time.

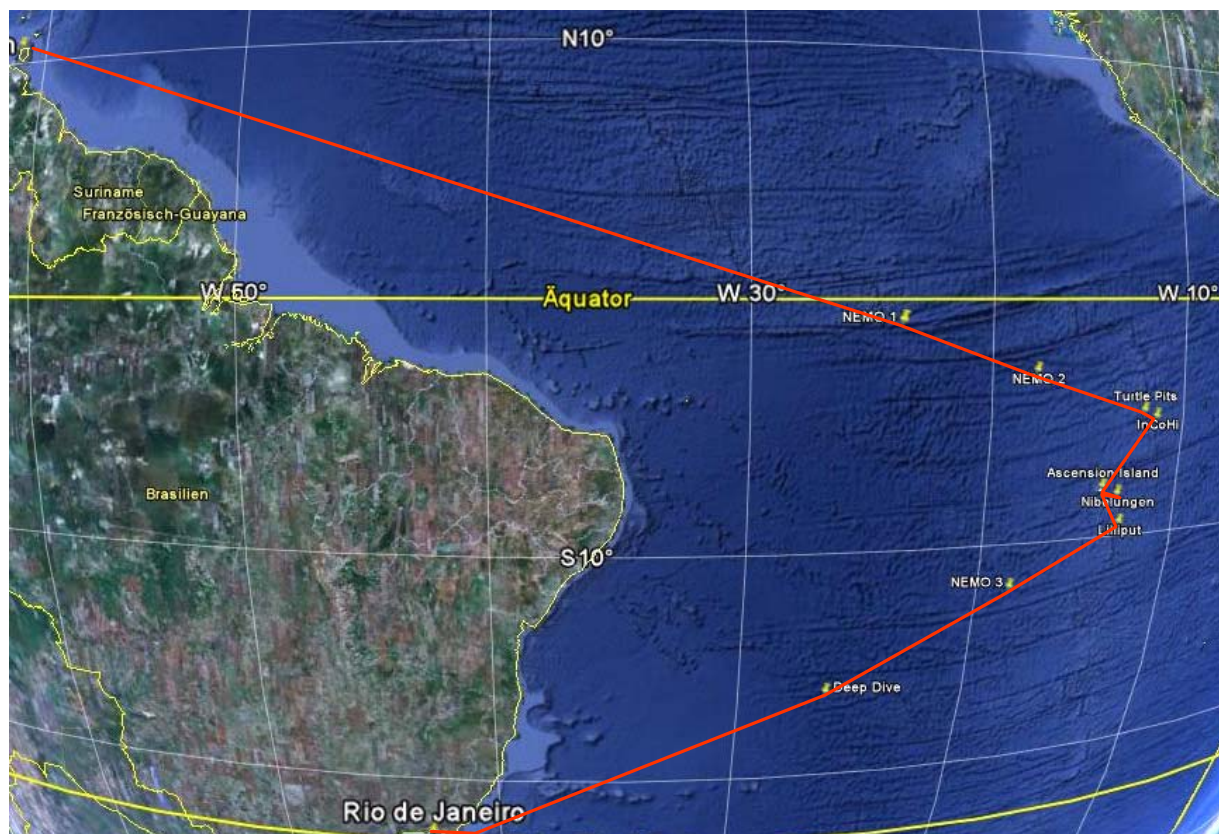
The work comprised measurements at individual vents (ROV "Kiel 6000", IFM-GEOMAR), detailed plume mapping (AUV, CTD) and integrated analysis of the flow field (CTD, moorings, AUV). The investigation of trace metals and dissolved gases (including signatures of stable isotopes) for fluids of distinct vents carried on the time series investigation started in 2005 and should contribute significantly to understand the evolution of the vent systems.

Methodologies applied to obtain data and samples were:

- A Remotely Operated Vehicle (ROV Kiel6000, IFM-GEOMAR) for ocean floor investigations and sampling of microbial mats and water samples including the application of a profiler to obtaining geochemical profiles of the upper sediment layer *in-situ*;
- an Autonomous Underwater Vehicle (AUV Abyss, IFM-GEOMAR) for plume mapping and high resolution bathymetry;

- CTD/Carousel water sampler equipped with ADCP and Back Scatter Sensor for profiling and sampling of the water column;
- Wax corer (VSR) for sampling basaltic glasses;
- Multi Beam Echo-Sounding (EM 120) surveys for bathymetry.

In total, 87 stations were performed within the 17.5 working days including 16 ROV-dives, 23 sediment stations (VSR), 22 water stations (CTD), and about 1000nm of profiling (multi beam echo sounding).



Track of R/V METEOR cruise M78/2 (satellite map: Google Earth)

2.3 Narrative M78/2

(Richard Seifert)

01. to 14.04.

FS Meteor left Port of Spain, the Capital of Trinidad And Tobago, with a delay of one day against schedule, April 2nd at noon aiming to the active hydrothermal areas located at 04°48'S, 012°22'W on the Mid Atlantic Ridge (MAR). This delay was caused by a belated arrival of the team responsible for the mobilization of the ROV Kiel6000 and the AUV Abyss, planned to start at March 28th. The transatlantic flights missed to be in time for the connecting flights from Bridgetown (Barbados) to Port of Spain and the vanguard had to stay overnight on Barbados. Moreover, no work was also possible during the 29th when the harbor of Port of Spain was closed for a security check in view of the near visit of the U.S. president Barack Obama. Thus, unloading of containers and mobilization of heavy gear had to be postponed to the 30th, when also the rest of the scientific party arrived save and sound on board. Work proceeded well and could be closed by a successful harbor test of the ROV in the morning of April 2nd. During the 3100 nm long transit to the hydrothermal sites at the MAR, concentrations of halogenated organic compounds in the atmosphere and the surface waters were continuously measured by a team of the IfBM, University of Hamburg. The objective of this work, performed under the auspicious of the excellence cluster CLISAP, is to shed light on the relevance of tropical coastal zones for the atmospheric burden of halogenated molecules. FS Meteor crossed the equator in the early morning of April 11th. To avoid any hindrance of the work ahead by force majeure, we took care to enter the southern hemisphere with the whole crew being orderly baptized. We had a nice time during the ceremony and the following party. This Easter will for sure be memorized as one having been very special and enjoyable. At April 12th the first of three Argo Floats launched on behalf of the BSH at 1°S, 24°W. At this opportunity, a launch and recovery test was performed using a dummy of the AUV. Also at April 12th, recording of bathymetry and water currents were started using the ship based EM 120 and ADCP, respectively. A second Argo Float was launched Easter Monday at 03°S, 18°W.

15.04.

After having reached the working area in the early morning, a CTD station was carried out to record a sound velocity profile. Due to entrained water in the main plug, the station had to be abandoned. It followed the first ROV station aimed to take fluid samples of the smokers at the "Turtle Pits" vent field. However, the ROV had to be brought back on deck before any work could be realized due to loss of hydraulic oil. Thereafter, three transponders needed to navigate the AUV were deployed and located in the working area at 5°S.. Having done this successfully, the first CTD station could be completed. The day ended by CTD stations including water sampling for Helium and other gases, and a wax corer (VSR) station.

16.04.

Volcanic glass and rock chips were recovered by VSR until morning. Then, the AUV was launched for detailed mapping of the area south of "Turtle Pits". To problems with the parameterization of the new propeller the station aborted. We thus performed a second ROV-

dive but faced similar problems than the day before. However, during about 1 hour bottom time we could get a mussel sample. A following attempt to calibrate the AUV-propeller failed as the vehicle could not get its position properly. Obviously, the GPS-system was, at least partly, damaged.

17.04.

Night work proceeded by one CTD followed by a VSR station. From 07:30 until 14:00, the first part of the bathymetric data of the working area was recorded by the EM 120 system of Meteor. Next, the 50th dive of the ROV Kiel 6000 was on schedule. Main objective of this dive was to learn whether we had overcome those problems faced during the earlier dives. Though started with cautious expectations, it became an enjoyable and fruitful jubilee dive. Going down at Comfortless Cove, we quickly found the black smoker "Sisters Peak". A sample of about 30kg of massive sulfide could successfully be placed on the porch of the ROV. Flying on, we entered "Golden Valley" again an impressive and beautiful sight with mussels densely covering the walls of an about 3 m wide fissure. The ROV was based in front a white colored hill, assumed to represent rocks overgrown by bacteria. When trying to sample these microbial mats by a net, we cracked the surface and hot smoke merged from the hole destroying the net. The hill showed to be composed of massive hydrothermal sulfides and to contain hot fluids below a thin sulfide crust. This observation sheds new light on the processes supporting the dense hydrothermal fauna at "Golden Valley". After having sampled mussels using a second net, a chunk of basaltic rocks with abundant mussels attached could be secured. The ROV was recovered at 22:00 on deck and CTD work followed.

18.04.

After having performed two CTDs and one VSR, the ROV was applied to investigate the Turtle Pits vent field including the smokers One Boat, Two Boats, and Southern Tower which all three emitting extremely hot fluids. The smokers were found shortly after bottom view, however, sampling of fluids became a severe problem. All sources emitting the desired hot fluids were located at the upper zone of these smokers being several meters in height and none was easy to reach by the vehicle. However, we finally succeeded to obtain two Ti-Majors samples from One Boat chimney and to realize a temperature measurement by KIPS showing extraordinary high temperatures exceeding 400°C. This was made possible by the skilled work of the ROV-team until midnight when the ROV was regained on board Meteor. Thank you for the successful dive!

19.04.

The day was highlighted by the first complete ROV-dive focused on biological work (ROV 287). At early morning, the AUV was launched together with a Zodiak. To overcome the problem in obtaining sufficient satellite data for positioning, we intended to hold a signal amplifier close to the AUV-GPS-antenna. However, after trying hard we had to give up due to the extraordinary bad weather conditions. An extended pressure low caused stronger, permanently turning winds together with a high sea stage of 2-3 m. It rained almost the whole day. Two VSR stations could be realized until the ROV was sent to the water at 14:30 aiming to land close to the low-temperature vent fields Golden Valley and Clueless to find a place

offering diffuse outflows of warm waters and abundant easy to reach mussel patches. After the ROV touched bottom, no such place could be found while searching for about 4 hours. However, then an appropriate sampling station were discovered. after having decided to extend the dive time until 23:00, including temperature measurements fluid sampling by KIPS and implanting “Die Fast” and gathering mussels.

20.04.09

While the ROV needed a day of maintenance after the extensive work it performed during the last days, the day started with the 2 CTD located south of Turtle Pits and a VSR. At 08:00, the AUV was given another try by circumnavigating the hardly working GPS-unit by attaching an amplifier to the AUV-antenna from a Zodiac until the vehicle had got the position was ready to dive. Though this was successful, the AUV moved to slow as no proper parameters were still available for the propeller and dive had to be abandoned. During the attempt to change these parameters for a second try, some problems with entrained water into the amplifier came to light and thus the station work with the AUV had to be stopped. Thus, we proceeded bathymetry by the EM 120 to complete the area map until 23:00. to go on with CTD stations.

21.04.

CTD work and a successful VSR preceded a ROV-dive dedicated to the “Red Lion” hydrothermal system. After launching the ROV at 08:00, the four smokers “Shrimp Farm”, “Tannenbaum”, “Mephisto”, and “Sugarhead” were found without problems. All of them appeared to be more active compared to the observations in 2006 and 2008. Fluid temperatures of 353°C were measured at “Tannenbaum” and “Mephisto”, and the latter was sampled by KIPS, whereas an attempt with a Ti-Major failed. Thereafter, the ROV fled SSE in direction to “Comfortless Cove” vent field for observing several elevated structures, which were found to be small pillow mounts. Along the about ½ nm long pass, a frequent change between pillow lava, lobate lava (overlying hacky lava), hacky lava and sheet flows was observed. Following a prominent fissure striking about 10°, we entered “Golden Valley” and, south of it, most probably “Clueless”. After the ROV was recovered on deck at 20:30, work proceeded by oceanography.

22.04.

Having completed a CTD and a VSR station, a last try was undertaken to get the AUV on track for mapping. However, though trying hard two times we failed. Thus, we have to wait until the vehicle is fixed by spare parts we shall obtain at Ascension Island. At noon, the ROV was launched to investigate the smoker “Sister Peak” and especially the diffuse hydrothermal field “Clueless”, both located in the area “Comfortless Cove”. With the help of an improved Posidonia under water navigation system and the experience from the last dive, we could quickly find the locations and accomplish the entire suite of planned work. This mainly concerned microbiological studies and investigations of mussels, shrimps and their symbionts.

23.04.

During the early day, one CTD and one VSR were followed by a try to release a mooring placed about on year ago. However, no mooring came in sight at sea surface. After sunrise we released and collected the three AUV-transponders deployed 8 days ago.

The seventh ROV-station, made possible by the skilled work of the ROV-Team, led us from the hydrothermal area "Turtle Pits" located in the south of the working area along a about ½ nm track to the black smoker "Sister Peak". The ROV touched bottom directly within the field of active and extinguished smokers of "Turtle Pits". An attempt to obtain a sample of hot fluid had to be aborted as no appropriate parking position could be found for the ROV. We could not find a place where the sight was not hindered by smoke or the top of the vehicle was not endangered by the exhaling hot fluids. Thus we headed to three little mounds located about 260m north of "Turtle Pits" crossing a mussel field at vents of shimmering waters.. The mounds were found to be composed of hydrothermal precipitates. One appeared to be a mound of massive sulfides much larger than all other sites so far observed in the working area, even no black smoke but only vents of shimmering water could be found. The other two are most probably composed of iron oxides rich in silicic acid and represent a late hydrothermal stage with emanations of fluids prone in hydrogen sulfide and metals but enriched in silica. After the exiting view on these mounds we turned east to cross mainly fairly sedimented basalt sheet flows suggested to originate from south east. After about 300m the morphology became much rougher with sheets of lobate lava, jumbled lava, lava domes, sky lights, and pillars. We continued flying NNE heading to "Sister Peak" and observed several mussel patches where warm waters emerged from the sea floor and a pillow mount about 100m south of Sister Peak.

24.04.

Until early morning, the bathymetric map of the area harboring the active hydrothermal fields "Red Lion", "Comfortless Cove", and Turtle Pits by ship based EM 120 system. At 06:00 we steamed to the next working area, the Inside Corner High located at 5°S and launched the ROV. The dive concentrated on the upper zone of the high and started traversing 500m along an about 30m thick mylonitic horizon to continue by exploring the top of the structure. Beside comprehensive footage we gained 17 rock samples. From the evaluation of this material more insight into the processes responsible for the generation of the huge elevated complexes found at the edge between the spreading zone and transform faults are expected. After recovery of the ROV at 22:00, time until morning was covered by bathymetric mapping of the area.

25.04.

In the early morning Meteor started the about 240 nm long transit to Ascension Island. The evening was used for a barbeque on deck.

26.04.

Having arrived at Ascension Island at sunrise, a TV team of 4 persons were embarked in exchange for 4 scientists and Meteor steamed to the hydrothermal working area "Nibelungen" with the active site "Drachenschlund". After arrival at noon, the ROV was launched aimed to get samples of hot fluids emitted from the smoking crater "Drachenschlund", one of the few hydrothermal sites hosted by ultramafic rock, and, of inactive chimney structures present in its

surrounding. Work was very much adapted to the requests of the TV-team also taking pictures within the control container of the ROV. A sample of an inactive chimney was recovered for investigation of the biological decomposition of massive sulfides at the seafloor. The night was spent in recording a bathymetric map.

27.04.

A second try to obtain samples from the “Drachenschlund” by using a spear, an about 2 m long steel baton with the KIPS-nozzle on top hold by the Rickmaster of ROV was successful. However, the ROV was requested to leave water at sun down, and thus remained for some hours at 300m depth, not to the benefit of the samples. Bathymetric mapping of the “Nibelungen” area occupied the night.

28.04.

The day was dedicated to filming until 17:00 when the TV-team disembarked to Ascension Island. With the again completed scientific team FS Meteor steamed heading to the last working area “Lilliput”, an active hydrothermal region with common occurrence of diffuse venting accompanied by rich vent fauna and especially symbiotic mussels.

29.04.

Having arrived at “Lilliput” by early morning, two transponders for the planned AUV work were located and the AUV was launched. Though the AUV started the mission properly, it aborted after about 1 hour, most probably due to data overload. We thus sent down the ROV to the hydrothermal field “Main Lilliput”, where diffuse outflows and associated fauna had been discovered at 1500 m depth during cruise M64/1 in 2005. While the ROV having quickly found the active sites was underway to survey the surroundings of “Lilliput”, the AUV was launched for a second time with the multibeam system switched off. The AUV-team, having tried really hard throughout the cruise, became finitely rewarded by a successfully completed 7 hours long mission, gorgeous! Also the ROV worked perfectly. An extended program on the biology of vent mussels was realized and we started an investigation on the influence of tides on diffuse sources and the associated microbiology. In this context, an instrument was located in a selected vent for recording temperature over an extended time period of days. Both, ROV and AUV were recovered on deck at about 21:00. CTD work including a Tow-yo was done through the night and dedicated to the exploration of a hot hydrothermal vent within the blown up ridge segment “Lilliput” is located on.

30.04.

Today’s ROV-dive started in the northeast of “Lilliput” at 09°32.6’S, 013°12.8’W and went south exploring the westerly arm of the mound chains west of “Lilliput” down to 09°33.15’S. We observed unsedimented pillow lavas, lava flows and jumbled lavas cut by deep and up to 10m wide N to S striking fissures. Then we turned east to enter “Limtoc” showing occurrences of iron-oxides and lava sheets with skylights and even larger collapse structures. We finally went to “Main Lilliput” for sampling. During the ROV dive, the AUV mapped the area centered at 09°31.3’S, 013°11.8’W for Eh and turbidity anomalies 50m above seafloor, where last night’s CTD work had shown enhanced turbidity and decreased Eh-values. The

night was covered by CTD work, aimed to obtain more information for searching a hot hydrothermal vent by ROV the following day.

01.05.

After the early morning was covered by bathymetry, the ROV was launched at “Main Lilliput” to proceed with the studies on tidal effects. Having done this, the ROV flew about 2 nm to the north east where indications of possible hot venting had emerged from CTD records and last day’s AUV-mapping by anomalies in turbidity and Eh values. In parallel, the AUV performed another mission in that area by mapping Eh values flying at a water depth of 1530m. However, the ROV survey of the northeastern corner of “Lilliput” showed basaltic lava of enhanced age (as deduced from considerable coverage by sediment) penetrated by N - S striking faults, but no signs of any hydrothermal activity. The night was spent trying to obtain more information on hot venting by two CTD Tow-Yos.

02.05.

A thorough evaluation of the data obtained by CTD and AUV bearing indications for a possible presence of a hot source in the northeastern part of “Lilliput” led to the decision to truncate the search. We could not narrow the area where the hot source should be located sufficiently to allow finding it by ROV with good chance. Moreover, at least part of the observed anomalies appeared to be possibly related to resuspension of sediments. Thus, the last ROV-dive started at “Main Lilliput” and went south across “Limtoc” and “Roman City” to investigate the so far unknown southernmost area.

During the ROV dive, the AUV recorded a high resolution bathymetry of the “Lilliput” area. Further on, CTD stations were performed on the “Roman City”, “Limtoc” and “Main Lilliput” known to emit low tempered hydrothermal fluids, and the bathymetric map of region around “Lilliput” was completed using the ship based EM 120 system.

03.05.

After the bathymetric mapping, the AUV transponders were released and collected and FS METEOR left the MAR in direction to Rio de Janeiro at noon. The measurements of concentrations of halogenated organic compounds in the atmosphere and the surface waters were restarted by a team of the IfBM, University of Hamburg.

04. to 11.05.

At the evening of May 4th, the third NEMO (Argo float) was launched at 12°S, 18°30’W. The last stations of the cruise were performed May 6th 12:00 at 16°10’S, 26°20’W at water depth of 6000m. Both, the ROV and the AUV were launched to dive to their limit. While the AUV did the planned mission at 5900m, even with the multibeam echosounder system switched off, the ROV dive was stopped at 4500m due to malfunction of the propellers and severe leakage of hydraulic oil system supplying the Orion. After the end of station work, FS METEOR continued her transit at 19:45 to Rio de Janeiro to moor in Rio de Janeiro in the morning of May 11th.

2.4 Preliminary Results

2.4.1 ROV Kiel 6000 and its operation during the HYDROMAR VIII Cruise

(F. Abegg, M. Pieper, C. Hinz, H. Huusmann, I. Suck, A. Foster, P. Rodriguez, S. Petersen)

The ROV (remotely operated vehicle) Kiel 6000 is a 6000 m rated deep diving platform manufactured by Schilling Robotics LLC. As an electric work class ROV from the type QUEST, this is build no. seven, and is based at the Leibniz Institute for Marine Sciences IFM-GEOMAR in Kiel, Germany.

The whole ROV equipment was shipped to Trinidad from the previous cruise which ended in Martinique. The equipment arrived in good shape and was loaded onboard RV METEOR beginning March 30th. From then on, the whole system was set up, which was finished with the harbour test before noon 2nd of April.

The UHD vehicle is equipped with 7 brushless thrusters, with 210 kgf peak thrust each. Power is supplied through the umbilical with up to 4160V/460 Hz. The data transfer between the vehicle and the topside control van is managed by the digital telemetry system (DTSTM) which consists of two surface and four sub-sea nodes, each representing a 16-port module. Each port may be individually configured for serial, video or ethernet purposes.

The vehicle is linked to the topside control unit via a 19 mm diameter wire. No tether management system (TMS) is used. To unlink the vehicle from ship's movements, floats are attached to the umbilical. For more details please visit www.ifm-geomar/kiel6000.



Fig. 2.4.1.1: View of the ROV Kiel 6000 front with cameras, manipulators and tool sled

Tools standardly installed on the vehicle include a HDTV camera, two high-resolution colour zoom cameras and one digital still camera as well as four black and white observation cameras. Besides the video capabilities the two manipulator arms are the major tools used on this platform. One is a seven-function position controlled manipulator of the type ORION and the other one is five-function rate controlled manipulator, type RIGMASTER. Further tools include a DIGIQUARTZ depth sensor, a SIMRAD sonar system, a PNI TCM2-50 compass, a motion reference unit (MRU) containing a gyro compass, and an RDI doppler velocity log (DVL). A further tool used especially for navigation is the USBL-based IXSEA POSIDONIATM system. Additionally a SONARDYNE HOMERTM system is available as a tool for navigation within a certain area of interest which has been marked with one or more HOMER beacons.

The tool sled in the lower-most part of the vehicle is especially dedicated to take up the scientific payload. A SBE 49 FastCAT CTD is permanently mounted. Located on portside front of the tool sled is a sample tray which can be

opened hydraulically. On starboard front there is a drawer likewise hydraulically driven, which can take up probes used by the manipulator. Port aft and starboard aft are reserved for additional scientific payload which may differ from mission to mission.

During M78-2 the starboard aft side was occupied by the KIPS fluid sampling system with its sampling nozzle and temperature probe on the starboard drawer. Because of the difficult sampling conditions at the Drachenschlund site within the Nibelungen Field, an extension rod with a second KIPS nozzle was mounted on the Rigmaster manipulator. This construction allowed sampling of the 'hidden' Black Smoker. Additional tools used for scientific samples during this cruise were mussel nets, a sample box with lid, a sample barrel with lid, Die Fast I and Die Fast II, titanium major bottles, scratch shovel, Smoni, 8-channel temperature logger, passive markers and Helium sampling tubes. Details of these tools are given in the respective chapters. Occasionally, the left side was occupied by a rotary sampler which was fed by a slurp gun array.

Tab. 2.4.3.1: Summary of dives during HYDROMAR VIII

Station # M78-2	Dive No.	Date	Time Start (UTC)	At Bottom (UTC)	Off Bottom (UTC)	Time End (UTC)	ROV Bottom Time	% Bottom Time	Location
	47	02.04.2009							Harbour Test
260ROV	48	15.04.2009	11:15	13:06	13:34	14:53	00:28	12,8	Turtle Pits/Red Lion
267ROV	49	16.04.2009	13:09	14:50	16:14	17:35	01:24	31,6	Foggy Corner
274ROV	50	17.04.2009	16:32	18:07	21:19	22:45	03:12	51,5	Foggy Corner
281ROV	51	18.04.2009	16:42	18:01	23:25	00:40	05:24	67,8	Turtle Pits
287ROV	52	19.04.2009	14:39	15:55	22:17	23:27	06:22	72,3	Golden Valley
297ROV	53	21.04.2009	09:06	11:14	19:55	21:12	08:41	71,7	Red Lion
302ROV	54	22.04.2009	13:12	14:30	00:00	01:18	09:30	78,5	Clueless/Golden Valley
308ROV	55	23.04.2009	13:05	14:27	22:04	23:33	07:37	72,8	Turtle Pits
310ROV	56	24.04.2009	12:19	13:11	21:45	22:33	08:34	83,7	Inside Corner High
312ROV	57	26.04.2009	15:05	16:31	20:56	21:45	04:25	66,2	Nibelungen/ Drachenschlund
314ROV	58	27.04.2009	09:53	11:10	16:12	18:39	05:02	57,3	Nibelungen/ Drachenschlund
319ROV	59	29.04.2009	11:04	11:50	21:25	22:08	09:35	86,6	Lilliput
324ROV	60	30.04.2009	11:04	11:52	19:57	20:45	08:05	83,4	Lilliput
329ROV	61	01.05.2009	09:41	10:46	20:58	22:07	10:12	82,1	Lilliput
335ROV	62	02.05.2009	11:44	12:35	21:46	22:39	09:11	84,1	Lilliput/ Roman Ruins
343ROV	63	06.05.2009	14:43			20:05			Deep Dive Test
Total: 15 scientific dives							97:42	72,1	

Due to the perfect weather conditions, we were able to carry out 15 scientific dives, 9 in the 4°48' S and Inside Corner High area, two at the Nibelungen site (8°18' S) and 4 within the Lilliput area (9°33'S), summing up to more than 97h bottom time. The last dive was used to perform a deep dive test of the ROV Kiel 6000 at 16°9' S 26°18' W.

2.4.2 AUV dives

(K. Lackschewitz, M. Rothenbeck, J. Sticklus)

Technical description

The Autonomous Underwater Vehicle (AUV) ABYSS (built by HYDROID) from IFM-GEOMAR can be operate in water depth of up to 6000 m.

The ABYSS system comprises the AUV itself, a control and workshop container, and a mobile Launch and Recovery System (LARS) with a deployment frame that is installed at the starboard side on the afterdeck of R/V METEOR. The self-contained LARS was developed by WHOI to support ship-based operations so that no Zodiac is required to launch and recover the AUV. The LARS is mounted on steel plates which are screwed on the deck of the ship. The LARS is configured in a way that the AUV can also be deployed over the port or starboard side of the German medium and big size research vessels. The LARS is stored in a 20 ft. container during transport.

We can deploy and recover the AUV at weather conditions with a swell up to 2.5 m and wind speeds of up to 6 beaufort. For the recovery the nose float pops off when triggered through an acoustic command. The float and the ca. 25 m recovery line drift away from the vehicle so that a grappnel hook can snag the line (Fig. 1A). The line is then connected to the LARS winch, and the vehicle is pulled up (Fig. 1B). Finally, the AUV is brought up on deck and safely secured in the LARS (Fig. 1C). During M78/2 every deployment and recovery with the LARS occurred without any problems.

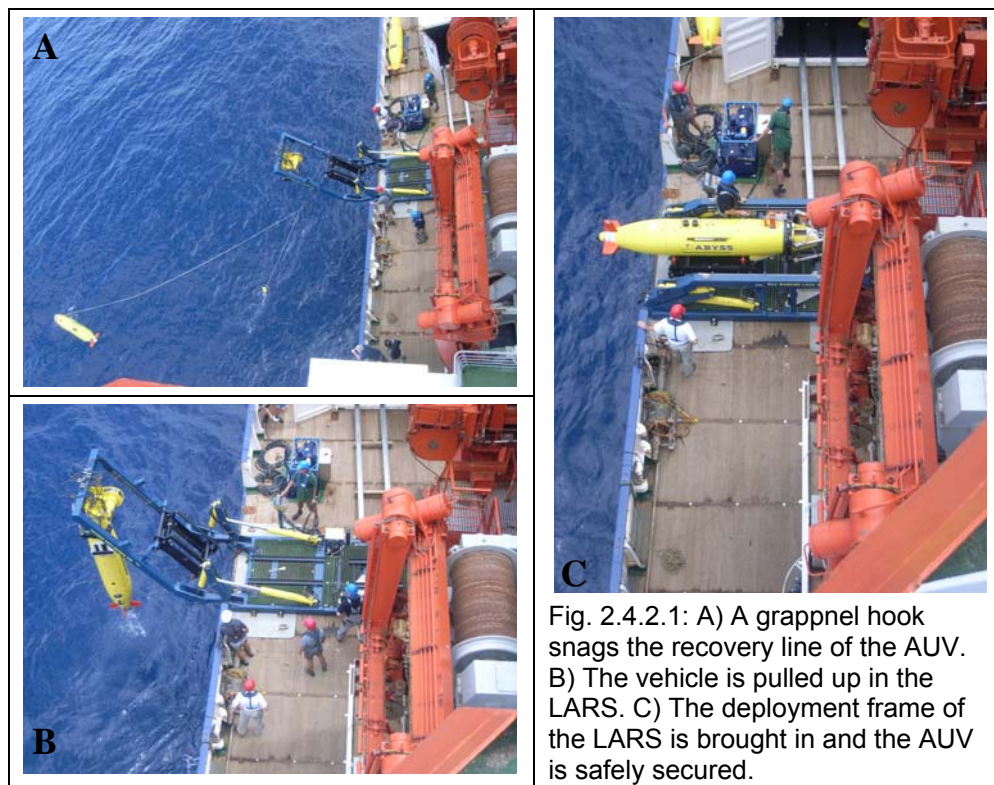


Fig. 2.4.2.1: A) A grappnel hook snags the recovery line of the AUV. B) The vehicle is pulled up in the LARS. C) The deployment frame of the LARS is brought in and the AUV is safely secured.

The vehicle consists of a tapered forward section, a cylindrical midsection and a tapered tail section. An internal titanium strongback, which extends much of the vehicle length, provides

the structural integrity and a mounting platform for syntactic foam, equipment housings, sensors and release mechanisms. The maximum vehicle diameter is 0.66 meters and the overall length is 4 meters. Vehicle weight is, depending on the payload, approximately 880 kilograms. A rectangular compartment in the midsection of the vehicle contains three pressure housings and an oil-filled junction box. Two pressure housings each contain one 5.6 kWh 29-Volt lithium-ion battery pack. The third pressure housing contains the vehicle and sidescan sonar electronics. The vehicle's inertial measurement unit and acoustic Doppler current profiler are housed in two other independent housings that are mounted forward of the 3 main pressure housings. The propulsion and control systems are located in the tail assembly, which bolts to the aft face of the vehicle strongback. The tail assembly consists of a pressure housing with motor controller electronics, and an oil-compensated motor housing. Propulsion is generated with a 24 VDC brushless motor driving a two-bladed propeller. However, some technical issues occurred due to a new propeller provided by the manufacturer. The first dive in a water depth of 3000 m during leg M78-2 has indicated errors in the given prop parameters. The problem was identified and could be successfully fixed after a few tests. As a result, the system proved to be fully operational in water depth until 5900 m during M78-2. Control is achieved with horizontal and vertical fins driven by 24 VDC brushless gear motors. The vehicle velocity range is 1.2 to 2.0 m/s, although best control is achieved at velocities above 1.5 m/s. The AUV dives descent with about 0.9 m/s whereas the ascent time is about 0.5 m/s or 1m/s if ascent weight is dropped. Together with the deployment/recovery procedure the descent to the seafloor and the ascent back to the vessel take approximately 3 hours at a water depth of 3000 m.

Sensors of the base vehicle include pressure, temperature, conductivity, optical backscatter and eH-sensor (in cooperation with Dr. Koichi Nakamura, Japan); and an inertial navigation system that is aided by an Acoustic Doppler Current Profiler (ADCP) with bottom lock capabilities.

In addition, the vehicle can be reconfigured for three different modes of operation as follows

1. Base vehicle plus RESON Seabat 7125 Multi-Beam (200/400 kHz), or
2. Base vehicle plus Electronic Still Camera & Strobe (not used during M78/2), or
3. Base vehicle plus EdgeTech Dual Frequency (110/420 kHz) Side Scan Sonar and Sub-Bottom Profiler (not used during M78/2)

All sensor information collected by the vehicle is marked with time, depth and latitude, and longitude as it is collected, facilitating the rapid and highly automated generation of maps and HTML based reports. An acoustic communication system permits the vehicle to send status messages to the surface ship containing information about the vehicle's health, its location, and some sensor data while it is performing a mission at up to 6 km below the surface. The acoustic communication system is also used to send data and redirection commands to the vehicle. The AUV utilizes electronics, control software, and the laptop based operator interface software.

The vehicle navigates autonomously using a combination of navigation methods:

- **GPS** - Works only on the surface, GPS determines the vehicle's location on Earth. GPS

determines the “initial position” before the vehicle submerges, and verifies or corrects the vehicle’s position when it surfaces during the mission. GPS also plays a critical role during INS alignment.

- **Inertial Navigation System (INS)** - After alignment on the surface, INS continuously integrates acceleration in 3 axes to calculate the vehicle’s position. It uses input from the DVL and the GPS to maintain its alignment.

Unfortunately, during M78/2 the internal GPS of the vehicle received significantly weaker satellite signals after the first AUV station. The problem couldn’t be solved although we changed the antenna and the GPS receiver and repeater boards. However, before diving an external GPS repeater was mounted over the antenna to maintain the INS alignment which worked for the remainder of the dives.

- **Doppler Velocity Log (DVL)** - Continuously measures altitude and speed over ground whenever the vehicle can maintain bottom-lock. The DVL receives temperature and salinity data from the CTD Probe to calculate sound speed. The DVL must be within range of the bottom to measure altitude and provide bottom-lock for the INS.

- **Long Baseline Acoustic Navigation (LBL)** - The vehicle can navigate using LBL navigation by computing its range to two (or more) moored acoustic transponders.

A Vehicle Interface Program (VIP), a Windows program that manages every aspect of AUV operation, include the following tasks:

- Mission planning on electronic navigation charts (customizable, multi-format)
- Real-time mission monitoring through the acoustic modem
- Real-time support-vessel position and heading through GPS and compass feeds
- Pre-mission system checkout
- Post-mission data analysis, mission play-back, and side-scan review

Navigation charts show missions during planning, operation, and review. A graphic Mission Planner lets users build mission files using drag-and-drop to position waypoints and mission objectives on the chart window, and fine-tune missions using editable text fields. Automatic error checking verifies all aspects of planned missions, and warns operators if any mission parameters are incorrect. Communication between the vehicle and the computer runs through a standard Ethernet connection, or wirelessly, using the WiFi connection.

First results

Four dives were completed in the „Lilliput“ area (9°30’S), ABYSS dives 6-9 were dedicated to hydrothermal exploration and high-resolution mapping.

ABYSS 6 (M78/2-320) did a water column investigation (e.g. hydrothermal plume survey) north of the known diffuse venting areas of Lilliput. The survey lines were conducted 120 m above the seafloor with 200 m line-spacing. The survey area showed no substantial hits on Eh, turbidity, or temperature. The survey distance was 28.7 km.

ABYSS 7 (M78/2-325) was another dive to continue exploration in the northeastern area of „Main Lilliput“. The dive was conducted at a fixed height above the seafloor (50 m) with 100 m line spacing centered on a located CTD tow-yo plume signal (see M78/2-322). The dive recorded significant Eh and turbidity signals in the northern part of the survey (Fig. 2). ABYSS flew a survey distance of 23.7 km.

Based on the results of dive 7, ABYSS 8 (M78/2-330) dive was chosen to map the plume signal further to the north. The dive was planned with a constant water depth of 1530 m and a 100 m line-spacing. In addition, we used the 200 kHz multibeam sonar for detailed bathymetric mapping on a survey distance of 32.3 km (Fig. 5B). The dive recorded significant eH and turbidity anomalies ca. 100m above the seafloor in the NW corner of the survey track but approximately 1 km NW of where the anomalies of dive 7 were detected.

ABYSS 9 (M78/2-336) was conducted to carry out high-resolution bathymetric mapping (400 kHz multibeam sonar) of the Lilliput Sites and to continue plume exploration at constant water depth of 1440 m with 80 m line-spacing.

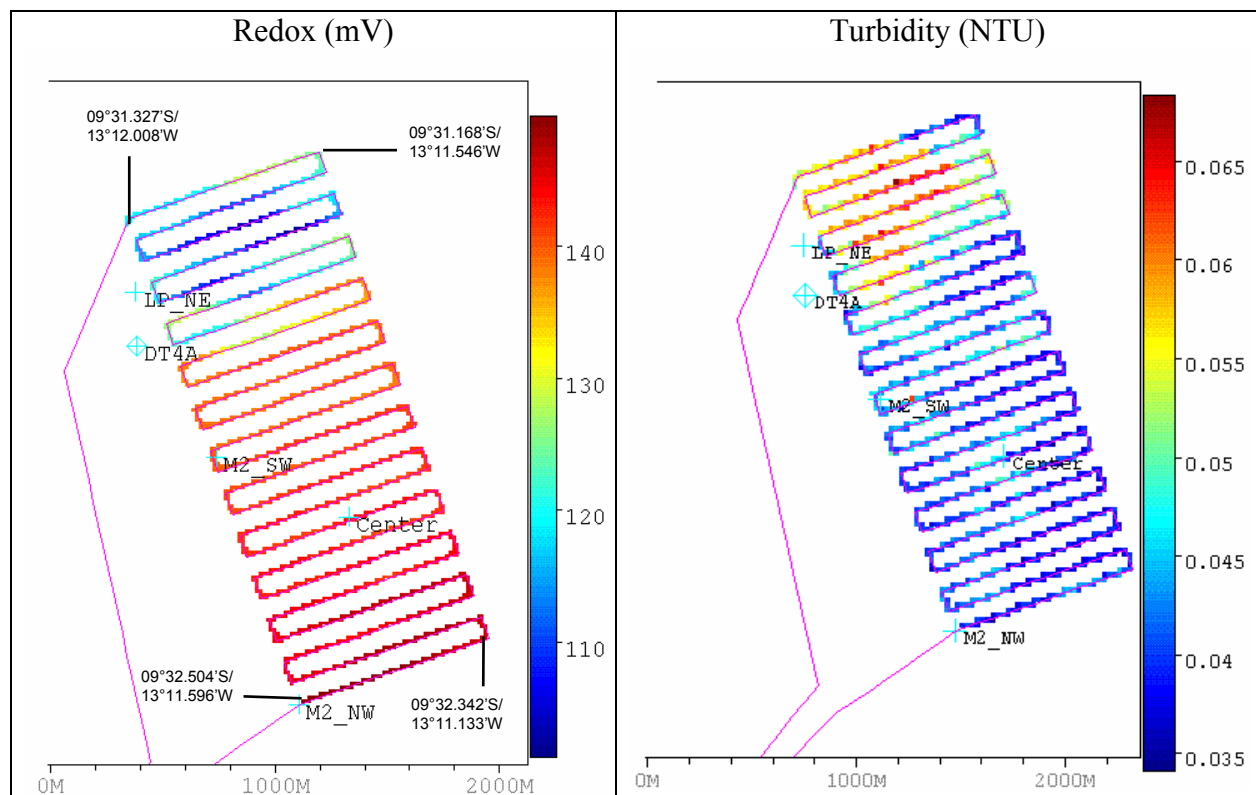


Fig. 2.4.2.2: Eh and turbidity data for ABYSS 7 dive.

From Eh and turbidity records, the two most significant hits were recorded over the „Limtoc“ and „Roman City“ diffuse venting areas (Fig.4). ABYSS surveyed 30.6 km on track during approximately 6 hours. Fig. xy shows a detailed bathymetric map of the area of the Lilliput field from the ABYSS Reson multibeam (Fig. 5A).

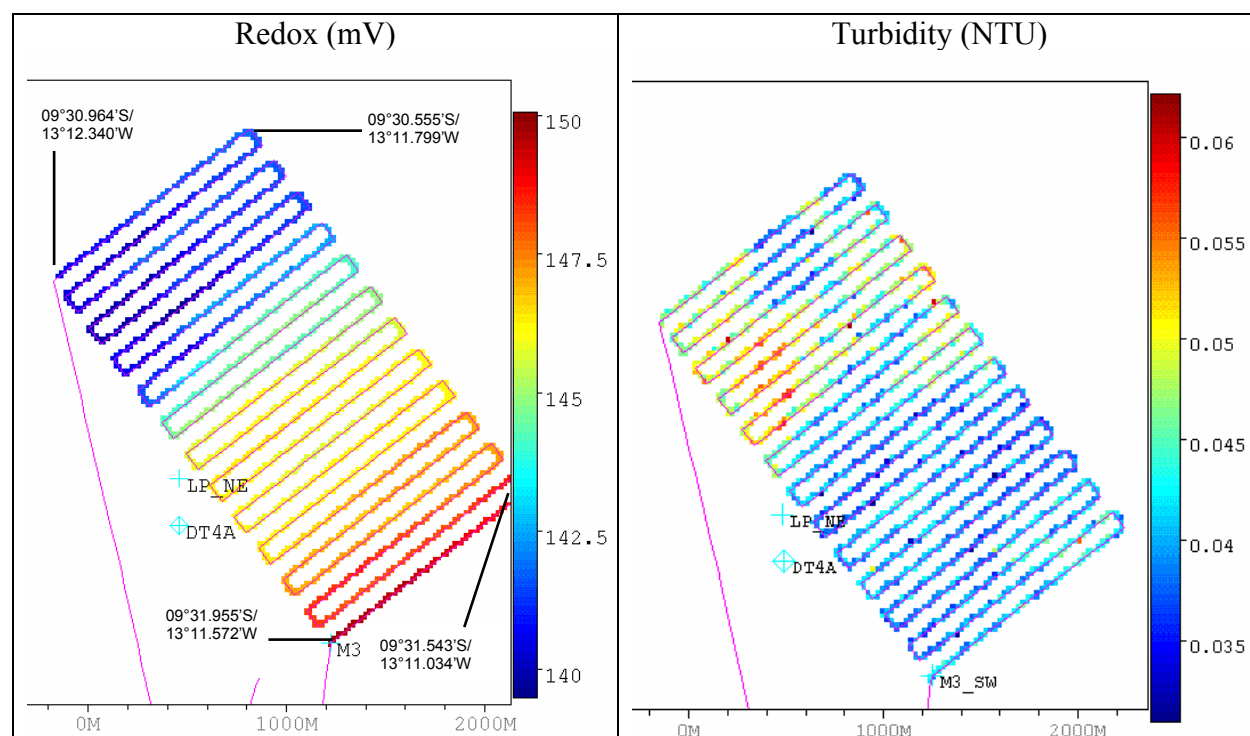


Fig. 2.4.2.3: Eh and turbidity data for ABYSS 8 dive.

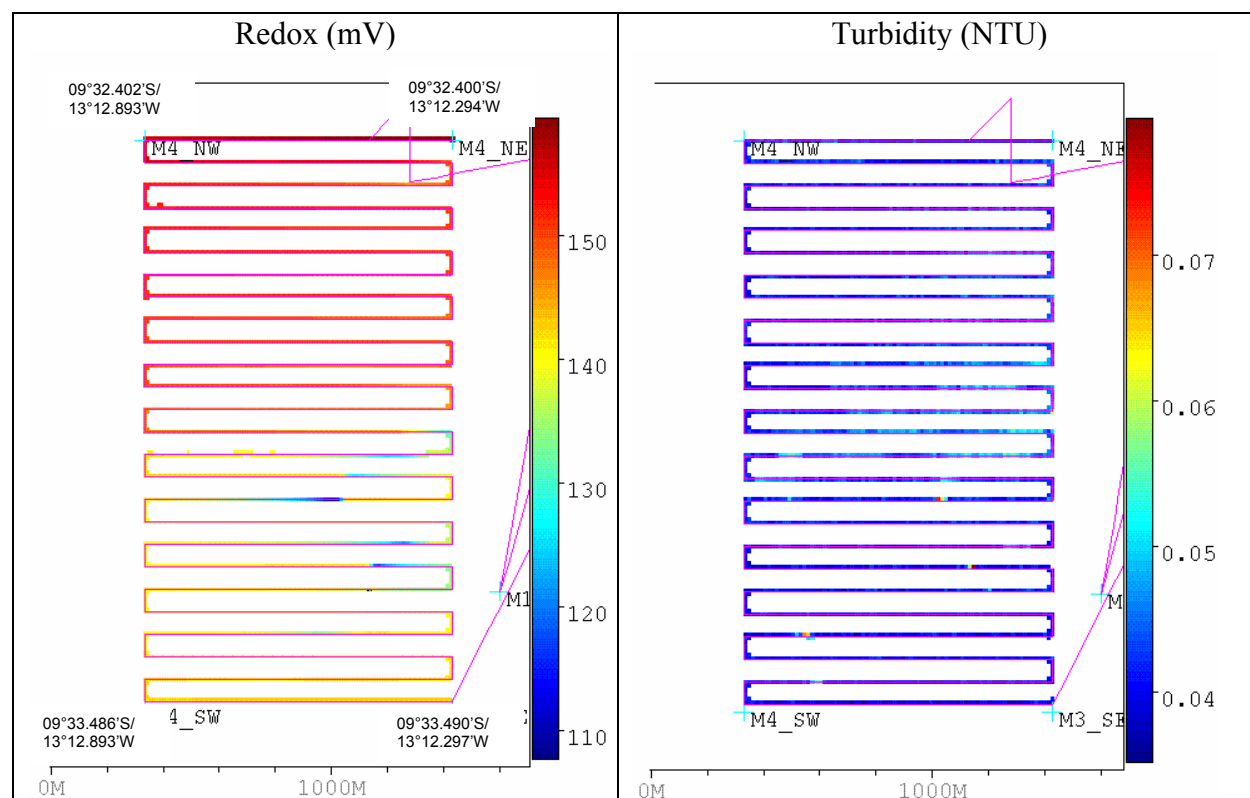


Fig. 2.4.2.4: Eh and turbidity data for ABYSS 9 dive.

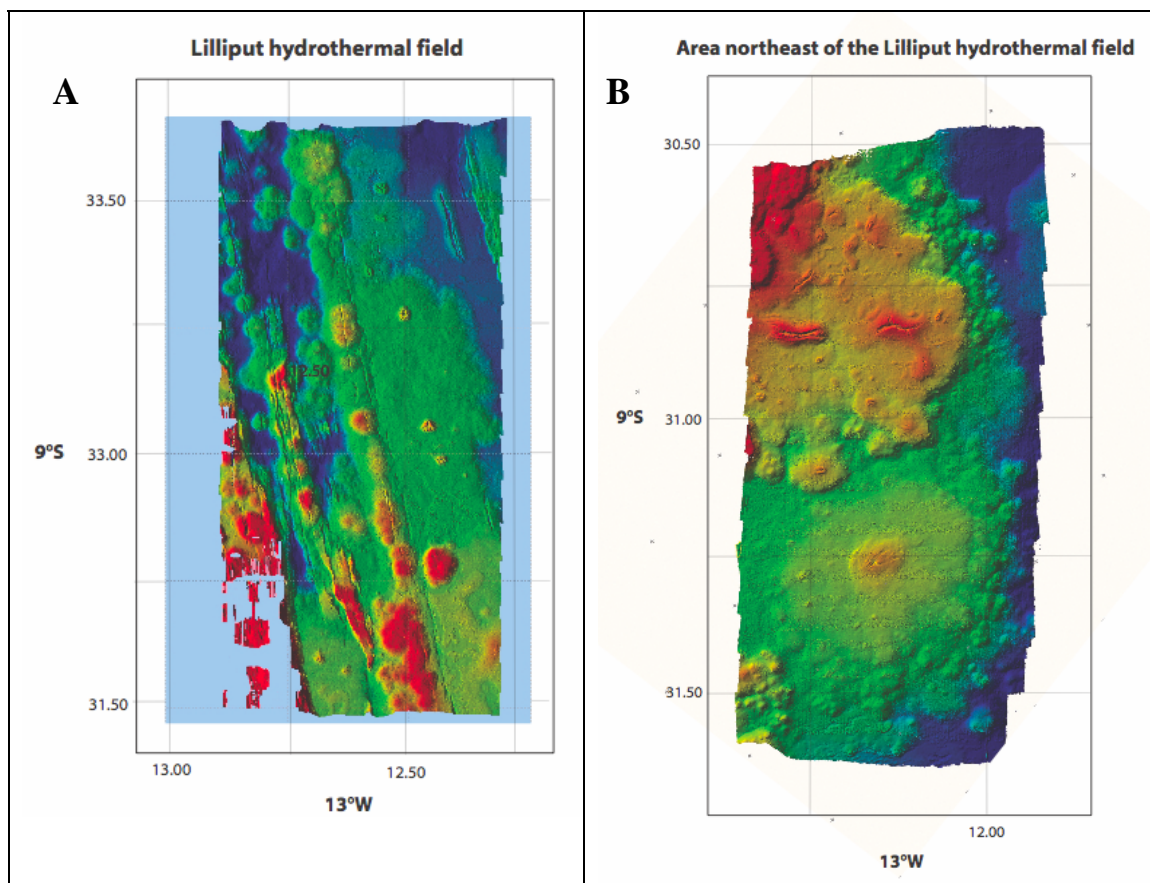


Fig. 2.4.2.5: A. High-resolution bathymetry of the Lilliput hydrothermal site. B. High-resolution bathymetry of the area northeast of the Lilliput hydrothermal site

2.4.3 Geological Observations and Sampling

J. Koepke, S. Petersen, H. Strauss, C. Breuer

This chapter describes the hard rocks recovered during the various stations as well as three subchapters dealing with the geological observations obtained during ROV dives. Three types of hard rocks were sampled during the M78/2 cruise: volcanic rocks from the rift valley, mafic and ultramafic rocks from the Inside Corner High at 5° South, and hydrothermal precipitates from the different vent systems.

2.4.3.1 Volcanic Rocks

The volcanic rocks in the region have been sampled using the wax corer (VSR stations) and the ROV. Table xy summarizes the rock samples obtained during this cruise.

Details of operations

We used "Vaseline" as medium for collecting basalt fragments, and it turned out that this material is obviously too soft at equatorial temperatures, with the risk of losing the whole vaseline mass including basalt chips out of the front tube before having the VSR back on deck. To avoid this, we used a 40 cm net held by a ~ 4 m long stick (Meteor facility) and fixed a bucket inside the net. As soon as the VSR was pulled above sea level, we held this tool under the front tube of the VSR, in order to catch the Vaseline mass in case of loosing.

We made different attempts to optimize the winch condition:

1. 5 minute stop 50 m above seafloor; then winch velocity of 1 m/s
2. 5 minute stop 20 m above seafloor; then winch velocity of 1 m/s
3. 5 minute stop 20 m above seafloor; then winch velocity of 0.5 m/s

Most VSR stations were performed with the second option.

Table 2.4.3.1 Summary of all volcanic rocks sampled during the cruise M78/2

<i>Station / Sample#</i>	<i>Lat.</i>	<i>Long.</i>	<i>Depth</i>	<i>Comment</i>
Turtle Pits area				
VSR 265	04°48.340' S	12°22.330' W	2976m	Objective: Sample small pillow mound south of Comfortless Cove; Is this a young eruptive center? Recovery: 0.1 g basalt chips (most of the sample lost)
267ROV-5	04°48.161' S	12°22.330' W	2987m	Locality "Foggy Corner" : 10 g glassy chips co-sampled in the mussel net; phenocrysts of plagioclase visible
267ROV	04°48.161' S	12°22.330' W	2987m	Locality "Foggy Corner" : Some glassy chips lying on the porch somewhere from the location "Foggy Corner"
VSR 269	04°48.479' S	12°22.209' W	2966m	Objective: Sample small pillow mound northeast of Wideawake; Is this a young eruptive center? Recovery: 50g of fresh basalt chips

<i>Station / Sample#</i>	<i>Lat.</i>	<i>Long.</i>	<i>Depth</i>	<i>Comment</i>
VSR 272	04°48.265' S	12°20.987' W	2864m	Objective: Sampling of the bathymetric minimum east of Turtle Pits. Recovery: 5g of basalt chips with some sediment
274ROV-4	04°48.166' S	12°22.280' W	2987m	Locality "Golden Valley": Several kg lava block with mussels; shows glassy rinds which were sampled separately; glass contains plagioclase phenocrysts; rock probably altered
VSR278	04°44.797' S	12°22.909' W	3110m?	Objective: Sampling of a volcanic mound in the center of the rift valley 2.5 nm north of Red Lion. No clear bottom contact; steep slope. Recovery: EMPTY, reason for this unclear; copper lever ring inside the tube damaged after operation; not clear why
VSR280	04°48.763' S	12°20.991' W	2929m	Objective: Sample elevated lava field east of Turtle Pits and south of station VSR272; is this also an older flow? Maximum cable out: 2931m; Recovery: 100g of sediment with mm-sized basalt chips.
VSR285	04°49.196' S	12°21.722' W	2890m	Objective: Sample pillow mound south of Turtle Pits; possible eruptive center for young flows at Wideawake? Maximum cable out: 2904m Recovery: Empty
VSR286	04°49.195' S	12°21.722' W	2905m	Objective: Redo previous station. Maximum cable out: 2911m Recovery: very poor; few basalt chips (less than 100 mg) and some grains of sediment suggesting an older age of the edifice.
ROV287-11	04°48.170' S	12°22.249' W	2987m	Locality: "Desperate" near "Foggy corner": 1 g glass chips found in the "Die Fast"; co-sampled
ROV287-12	04°48.170' S	12°22.249' W	2987m	Locality: "Desperate" near "Foggy corner": 1 g glass chips found in the mussel net co-sampled
ROV287	04°48.170' S	12°22.249' W		Two kg-sized blocks of altered pillow basalt with glassy rind covered with small white "Pocken (probably "Laichballen") on the surface, found on the porch; not clear from where, either "Desperate" or "Foggy corner"
VSR290	04°48.268' S	12°23.609' W	2982m	Objective: Sample lava flows west of Turtle Pits. Maximum cable out: 2987m Recovery: >10g aphyric basalt with some glass and abundant sediment

<i>Station / Sample#</i>	<i>Lat.</i>	<i>Long.</i>	<i>Depth</i>	<i>Comment</i>
VSR292	04°50.001' S	12°22.201' W	2994m	Objective: Sample ridge axis 1.5 nm to the south of Turtle Pits, filling gap in previous sampling. Maximum cable out: 2997m Recovery: ~ 1 g very fresh glass chips; aphyric
VSR296	04°45.601' S	12°22.501' W	3090m	Objective: Sample ridge axis 1.5nm to the north of Turtle Pits, filling gap in previous sampling. Depth variation on ship display \pm 3090m \rightarrow probably strong relief. Depth from friction signal at winch: 3090m Recovery: ~5g very fresh glass chips; mm-sized plagioclase crystals
VSR300	04°45.31' S	12°23.45' W	3155m	Objective: Sample volcanic high 2 nm NW of Red Lion. Maximum cable out: 3170m. Recovery: 0.1g of aphyric fresh glass chips,
VSR303	04°51.00' S	12°22.00' W	3100m	Objective: Sample ridge axis south of Turtle Pits filling sample gap of previous years. Maximum cable out: 3003m. Recovery: 5g basalt chips + few grains of sediment.
308ROV-9	04°48.174' S	12°22.228' W	2987m	Locality "Golden Valley": Several kg lava block with mussels; shows glassy rinds ; glassy chips were picked and stored separately; rock probably altered
Nibelungen area				
314ROV-10A,B	08°17.838' S	13°30.460' W	2897m	Locality: North of Drachenschlund; taken during a hard rock dive to the North; two samples taken from the same locality ; A: with glassy rind; B: heavily altered, altered glassy rind
Lilliput area				
319ROV-8	09°32.837' S	13°12.549' W		Lilliput, co-sampled with "DieFast"; 0.5 g fragments of glassy rinds; covered with Fe-oxides
319ROV-10	09°32.837' S	13°12.549' W		Lilliput, co-sampled with mussel net; 5 g fragments of glassy rinds; covered with Fe-oxides
VSR323	09°31.480' S	13°12.832' W	1508m	Objective: Sample ridge axis North of Lilliput filling sample gap of previous years. Maximum cable out: 1524m. Bottom contact at 1508m; Recovery: 10g of glassy basalt chips containing plagioclase phenocrysts (<1mm).
329ROV-4	09°32.837' S	13°12.832' W		Locality: Main Lilliput; ca. 5 g of slightly altered glassy chips covered with rusty coating







<i>Station / Sample#</i>	<i>Lat.</i>	<i>Long.</i>	<i>Depth</i>	<i>Comment</i>
335ROV	~09°33.8'S	~13°12.4'W		Locality: "South of Roman Ruins" ca. 5 g of slightly altered glassy rind; found on the porch after discovery dive to the area South of Roman Ruins; exact position not clear

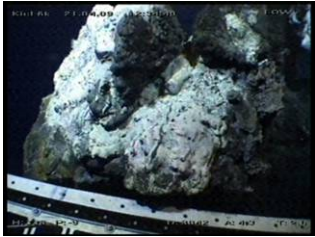






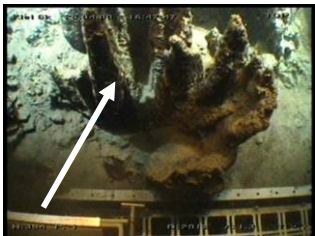


Details of sampling in the Turtle Pits working area

Sampling of the bathymetric minimum to the east of the hydrothermal fields shows the presence of sedimentary material. This suggests a rather old age of this structure indicating that this feature cannot be related to the youngest volcanic activity within the rift valley. This was later confirmed by other VSR stations also containing sediment (stations 280VSR and 286VSR). The bathymetric minimum zone to the east of Turtle Pits is clearly not the source of young lava flows in the area. These must originate from a source closer to the ridge axis (possibly the pillow mounds just outside the AUV-map?).

2.4.3.2 Hydrothermal precipitates

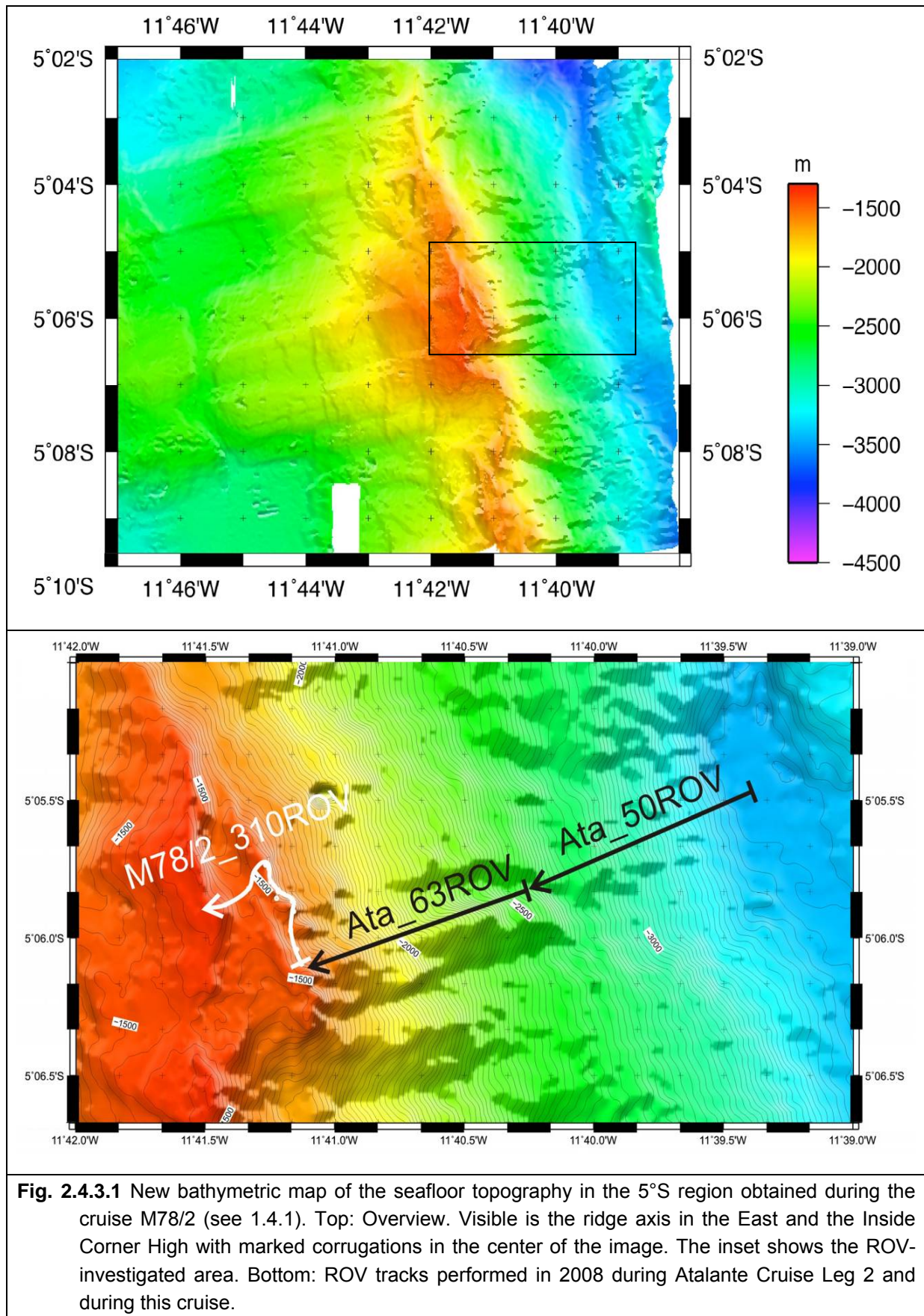
Table 2.4.3.2 Summary of all hydrothermal precipitates collected during the cruise M78/2

sample ID	location	description	bottom photo	sample photo
M78/2 274ROV-1	Sisters Peak trunk 04°48.192'S/ 12°22.310'W 2982m	beehive-like material with massive chalcopyrite core (\pm pyrite), thin sphalerite enriched layer and up to 1cm thick outer marcasite rim. Some native sulphur (microbial on the surface)		
M78/2 274ROV-2	Golden Valley 04°48.171'S/ 12°22.271'W 2986m	first evidence of sulphide formation here! outer marcasite crust with black to grey sulphide interior. Likely sphalerite, possibly some magnetite; venting from white crust after substrate was removed		
M78/2 281ROV-7	One Boat 04°48.596'S/ 12°22.422'W 2982m	with Fe-oxyhydroxide coating; accidentally recovered on ROV while parking at the chimney side.		

sample ID	location	description	bottom photo	sample photo
297ROV-1	Mephisto 04°47.843'S/ 12°22.592'W 3042m	sample from the trunk (near top) of the structure consisting of massive pyrite with minor black sphalerite and rare chalcopyrite. Outside is rimmed by marcasite with trace Fe-oxyhydroxides		
302ROV-2	Sisters Peak 04°48.192'S/ 12°22.310'W 2980m	few marcasite bits from the top taken with shovel		
308ROV-1	old mound 04°48.461'S/ 12°22.474'W 2990m	porous pyrite, recrystallized with Fe-oxyhydroxide coating from northern slope of old mound;		
308ROV-11	Sisters Peak ? 04°48.192'S/ 12°22.310'W 2980m	accidentally recovered on porch, location unsure, but likely from Sisters Peak; Zn-rich sample with thin marcasite rust	no image	
312ROV-1	Nibelungen 08°17.887'S/ 13°30.452'W 2912m	old chimney; Zn-rich core with Fe-oxyhydroxide coating; very porous and brittle		
312ROV-2	Nibelungen 08°17.866'S/ 13°30.449'W 2910m	talus from crater rim; pieces of Cu-rich material (chalcosite? 2A) as well as serpentinite (2B) and Fe-oxyhydroxides (2C); Photo right shows the crater rim, but not the actual sampling spot!		

2.4.3.3 Inside Corner High at 5° South

One ROV dive was performed to map and sample the deeper oceanic crust around 5°S (Fig. 1). We investigated the “Inside Corner High” at 5°06’S and 11°40’W (in the following ICH)



which is regarded as oceanic core complex. These are topographically high standing massifs, typically occurring at inside corners of ridge transform intersections. They are flat topped

with ridge-normal corrugations. They are believed to form by the long-lived activity of a single normal fault, thus exposing deep seated oceanic crust. The reason for strain focusing may be the presence of peridotite screens between gabbroic intrusions. They would act as rheologically weak horizons once they enter the serpentine-stability field.

Previous ROV dives

During the expedition Atalante Cruise Leg – 2 (MARSÜD IV, Ersatz MSM06/3; 07.01.08 Recife to 31.01.08 Dakar) we performed two dives with the ROV Kiel6000 (stations ATA_50ROV and ATA-63ROV) to map and sample the central part of the flank of the ICH (Fig. 2). While climbing 1900 m up the rift wall, the morphology changed from a sediment-covered floor of the rift valley to several hundred meters high, near-vertical cliffs with downdip slickensides and an abrupt transition to the flat-topped region of the core complex. The rock sampled are mainly gabbro-norites in the lower part of the rift wall with abundant oxide gabbros in the upper part of the wall. Plagiogranite infiltrations were found in three samples, diabase seems more abundant in the upper part of the rift wall. Only rare olivine-bearing gabbro was recovered. A gabbro mylonite occurs just below the top. The flat-topped region is formed by a peridotite breccia. At the rift base, a diverse suite of peridotite, peridotite mylonite, gabbro-norite and olivine gabbro was recovered. Chemical analyses revealed that the recovered rocks have a chemically evolved signature and probably formed in a high level setting with relatively rapid cooling. This is suggested by the ophitic to subophitic textures, locally coarse grained gabbro-norites (high water activity?) interleaved with microgabbros and diabbases, the presence of abundant plagiogranite infiltrations with sphene, apatite and zircon, and the occurrence of abundant ferro-gabbros. The presence of former mantle peridotite is confirmed by Cr-spinel relics (Cr# 45) and Cr-rich amphibole in one peridotite sample. The geochemical and petrological work on these rocks is still in progress. One very interesting rock was sampled at the top of our profile directly below the flattening of complex forming the roof plateau. This sample is an amphibolite-grade ultramylonite derived from a former gabbro. First geothermometric calculations reveal equilibration temperatures up to 900°C. Its position near the top of the core complex is unlikely to be a simple coincidence. Current models suggesting that core complexes are initiated as the serpentine stability field or the brittle-ductile transition is crossed seems thus not valid for the ICH at 5° South. Therefore, it was our major goal during this cruise, to find this horizon again for an appropriate mapping and sampling, in order to confirm or reject our hypothesis on high-temperatures shearing processes during the formation of this core complex.

Details of operation of dive 310ROV

Thanks to our experienced ROV pilots and their careful pre-dive preparation, we encountered no technical problems and could thus fully focus on the geological work. The ROV track, the locations for sampling and a description of the outcrops are shown in Fig. 2.

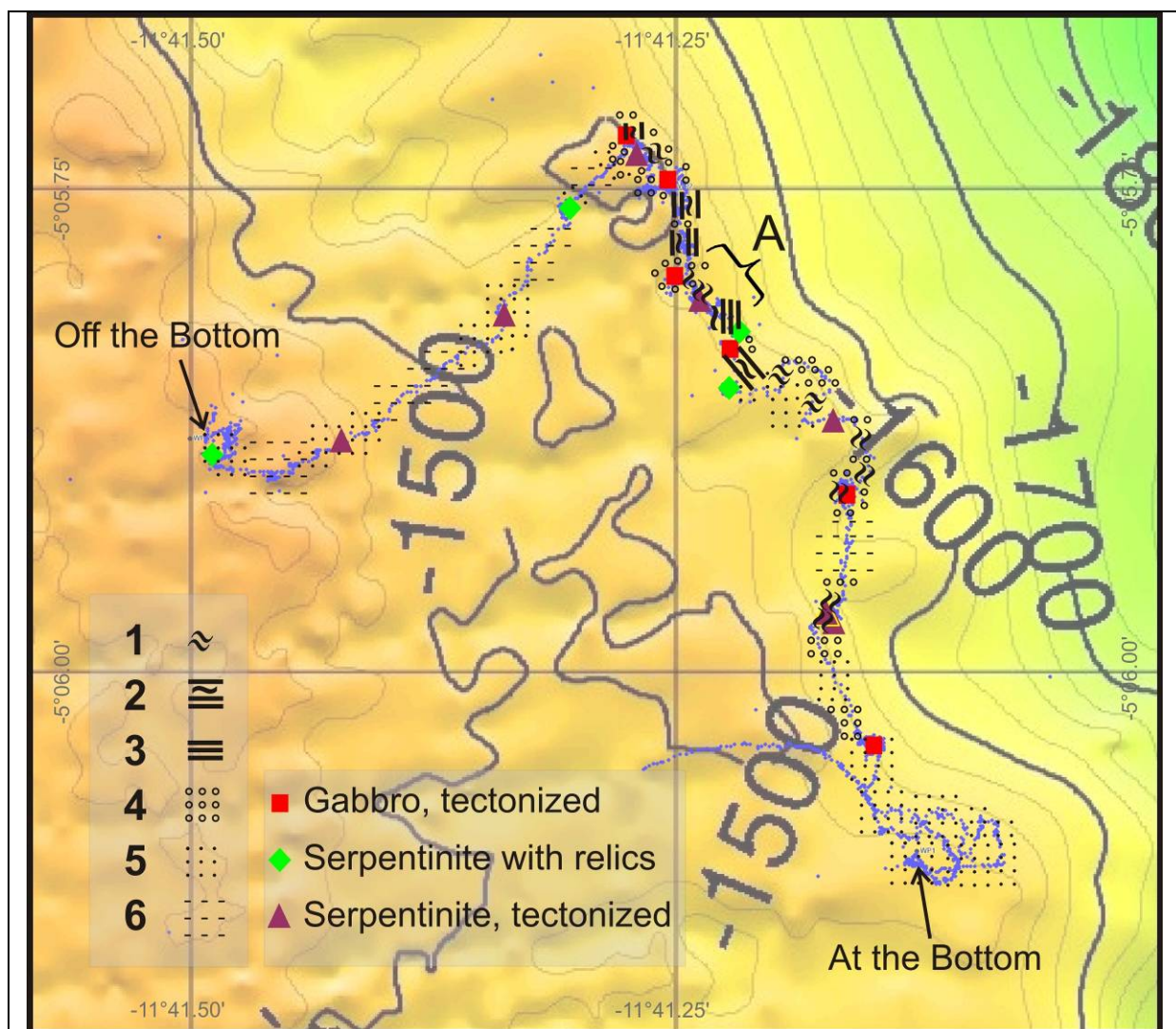


Fig. 2.4.3.2 Detailed map of the area covered by the ROV dive at station ROV310 (based on bathymetric map from Reston et al., 2002) including the ROV track (tiny blue points), description of the outcrops, and location of samples taken. Signatures: 1 – extremely tectonized and sheared zones (thickness: meter- to decameter range); formation of phacoids; 2 – steep cliff consisting of massive gabbro including individual shear zones in the decimeter to meter range; 3 – steep cliff consisting of massive gabbro; 4 – moderately steep slope with m-sized outcrops of massive rocks, talus and sediments; 5 – gently dipping slope with high amount of foraminiferous ooze, boulders, and pebbles; 6 – plateau, highly sedimented with boulders and pebbles; A – series of excellent outcrops from which the schematic profile in Fig. 4 was derived.

The travelled distance during our dive was 2.6 km. We started our dive at that point where we left sea bottom after the ATA_63ROV dive in 2008. We finished our profile at WP3, the highest point of the ICH plateau. We focused our observations mainly on the edge between the rift flank and the plateau and traversed this key horizon several times, in order to identify strongly sheared rocks in the outcrops corresponding to the presence of possible high-temperature shear zones including the mylonite horizon. Our work was hampered by the fact that it is nearly impossible to identify individual lithologies due to thick Mn-oxide-cover on all rocks, an experience we made already during the two ROV dives performed in 2008. But,

in many cases we were able to characterize structural details, as tectonized zones, joints, foliations, and the nature of the contacts between the neighboring lithologies. We collected 17 rock samples, which could be identified after the ROV recovery as ultramafic (11 samples) and mafic (6) in composition.

Thanks to the excellent features of the OFOP-protocol (Ocean Floor Observation Protocol), where all essential dive data like coordinates, depth, heading of the ROV, depth above seafloor, are included, we were able to study in detail the videos recorded by the ROV cameras (~ 17 hours video material in total for this dive) and to characterize the key lithologies at least from those outcrops from which samples were taken. Due to the knowledge of the ROV heading, it was even possible to obtain structural data from the recorded videos.

Results

During traversing the uppermost rift flank to the NW we passed several outcrops where the presence of marked shear zones could be observed, often with the formation of phacoidal bodies (Fig. 4). On the other hand, in the lowermost parts of our dive we observed outcrops of massive walls composed of gabbro, without any sign of deformation (Fig. 4).



Fig. 2.4.3.3 Outcrop images obtained with the still camera. Left: extremely sheared serpentinite sequence near the top of the plateau; from this outcrop, sample 310ROV-2 (tectonized serpentinite) was taken; visible are meter-sized phacoids; Lat -5.0995, Lon -11.6861; ROV heading 287. Right: massive gabbro wall in the deep part of the profile arranged in m-sized layers; perpendicular jointed; not far from this outcrop, rock 310ROV-11 was sampled; in the lower right, initiation of shear zone is observable (white arrow); accordingly the corresponding gabbro sample shows signs of deformation (sheared surface, micro-brecciation, but shows still domains of unstrained gabbro); Lat -5.0960, Lon-11.687, ROV heading 295.

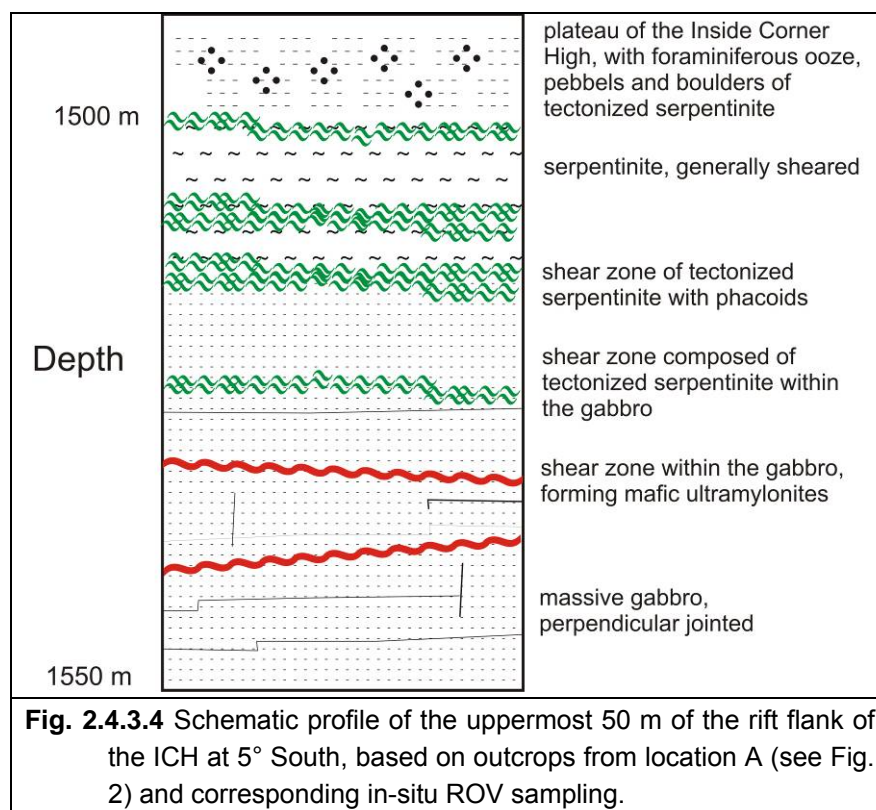
The macroscopic inspection of the 17 samples revealed that all rocks, both the ultramafic and the mafic, are tectonized. Some exhibit a record of strong shearing processes, with the formation of striations of the surface, foliation, and the development of phacoids. Among the samples taken, we identified three groups of rocks (Fig. 2): (1) tectonized gabbros, (2) tectonized serpentinites (no relictic peridotite minerals visible), and (3) serpentinites with relics of primary peridotite minerals. Details of the rock descriptions including photographs of the samples are presented in the Appendix. A key observation is that some of those rocks

characterized as tectonized gabbros are strongly foliated with domains characteristic of amphibolite. These show that fine, dense lamination which is typical for ultramylonite, which we know from our 2008 Atalante 63ROV dive. With the help of the recorded video information, we were able to localize a strongly sheared horizon including the mafic ultramylonites in the uppermost zone of the rift flank related to the last 50 meters below the plateau. At the northern part of our dive along this tectonized horizon we found excellent outcrops where it was possible to establish a schematic profile through the uppermost part of the rift flank, which is presented in Fig. 4.

The profile starts with massive, perpendicular jointed gabbro without record of strain in the lowermost position. This corresponds to the gabbroic core of the ICH complex, from which we recovered more than 20 samples during the Atalante Cruise Leg 2 in 2008. Moving upward, individual shear zones of decimeter to meter thickness within the gabbroic sequence become more and more prominent representing different lithologies: (1) extremely sheared gabbro now forming the finely laminated ultramylonite; (2) strongly tectonized serpentinites, often with the development of phacoids. Moving upward, a changing from mafic to ultramafic lithology can be observed, which is mostly strongly sheared in sub-parallel zones, often forming tectonites of serpentine, without any relics of the primary peridotite stage. Characteristic are blocks in decimeter to meter size with phacoidal shapes. Some meters above this sequence, the plateau starts with foraminiferous ooze and pebbles, blocks, and sometimes boulders of tectonized serpentinite. From this it is implied that the roof of the ICH

consists of tectonized peridotites.

An important result of our ROV work is the successful sampling of several mafic rocks corresponding obviously to ultramylonite, suggesting that high-temperature tectonic processes proceeded during the formation of the ICH complex. Moreover, we found that the occurrence of ultra-mylonites is not a local phenomenon, but that mylonites are present throughout a ~ 50 m thick zone beneath the roof of the



complex. Thus, our working hypothesis that "hot" instead of "cold" shearing was important during the tectonic evolution of the ICH at 5° S, seems supported.

2.4.3.4 ROV observations at 5°S

During M78/2, two dives were partly devoted to explore between previously known hydrothermal areas and to investigate the nature of features apparent on the detailed bathymetry previously obtained by the autonomous underwater vehicle (AUV) ABE from Woods Hole Oceanographic Institution (Fig. 5). Dive 297ROV started at Red Lion and showed a cone SE of Red Lion to be of volcanic origin. The dive then followed the eastern boundary of the detailed bathymetric map and documented the occurrence of abundant sheet flows and small areas of pillow lava, the latter mainly near the larger pillow mounds to the east of Red Lion and to the north of Sisters Peak. Additionally, another musselbed between Red Lion and Comfortless Cove was discovered suggesting that the area of diffuse hydrothermal fluid upflow is much larger than previously thought. The location of the Clueless field, discovered during a previous cruise, but without proper navigation, was specified as: 04°48.240'S / 12°22.245'W, placing it to the SE of Sisters Peak. It seems that most diffuse venting takes place in the vicinity of Comfortless Cove, six areas of diffuse flow and associated faunal communities are currently known here, however, the area to the east of the bathymetric map is completely unexplored.

Another dive, 308ROV, was used to map the area between Turtle Pits and Comfortless Cove, and to investigate the nature of three mounds apparent on the ABE bathymetry. These features proved to be of hydrothermal origin. The southernmost mound (04°48.455'S / 12°22.465'W) is larger than any other, presently active, hydrothermal feature in this area and sampling showed it to be constructed of massive sulfides overlain by Fe-oxyhydroxides. Minor diffuse fluid flow is evident in a small crater near the top of the structure. The two smaller mounds are likely also composed of sulfidic material underneath a thick Fe-oxide cover, but, since no samples were taken, visual inspection alone is no proof. The presence of old sulfide mounds and the discovery of additional inactive sulfide structures close to Sisters Peak are evidence for earlier episodes of hydrothermal activity at 5°S. The hydrothermal mounds are situated at a large NW/SE striking fracture and close to the northern extension with the fracture hosting the Turtle Pits site. Although the trace of this fracture in the bathymetric data disappears just north of Turtle Pits, the location of the mounds might imply the continuation of this fault to the north. The location of massive sulfide deposits at intersections of crosscutting faults is well known from ancient deposits and, due to enhanced fluid flow at those crosscutting faults, could also explain the large size of the mounds when compared to the presently active sites.

During the second part of the dive we approached the NNE/SSW striking terrain with numerous collapse features, including basalt pillars and skylights, between Turtle Pits and Comfortless Cove. Here we observed yet another musselbed and additional Fe-oxyhydroxides. It is very likely that even more diffuse vent sites occur all along this collapsed area connecting the Widewake field in the south with those diffuse sites at Comfortless Cove. This suggestion is confirmed by the finding of another musselbed just south of Sisters Peak. There is still a large potential for additional hydrothermal vent sites in this area, since no exploration north of Red Lion, south of Turtle Pits, or east of Sisters Peak has been undertaken.

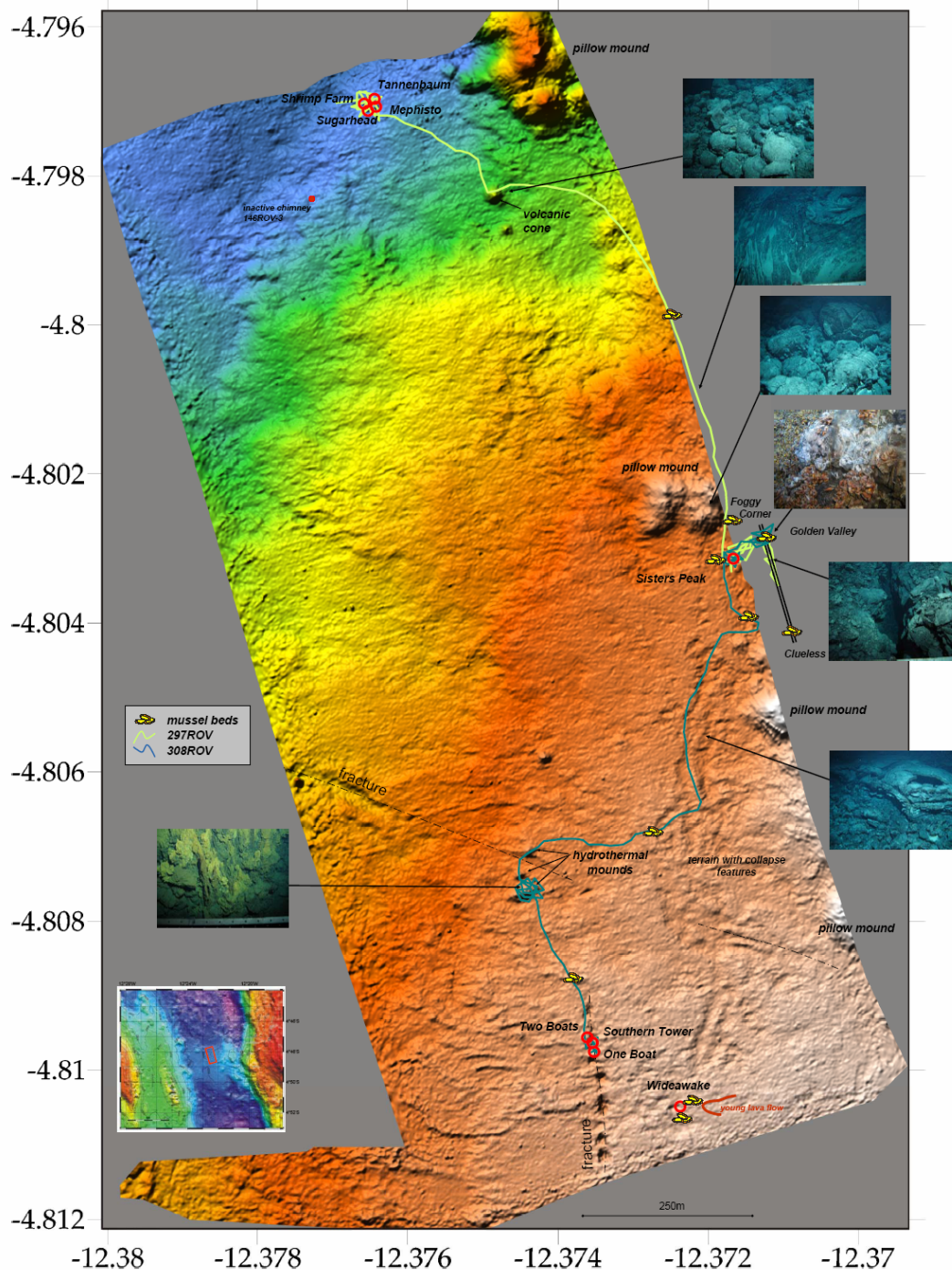


Fig. 2.4.3.5: ROV-tracks (stations 297ROV and 308ROV) posted on top of the existing AUV ABE (source C. German, WHOI) bathymetry. The original data has been reprocessed to provide more detailed information. Included are still images of selected geological features observed during this cruise. Three large hydrothermal mounds have been observed to the north of Turtle pits as well as several new mussel beds in the vicinity of the Comfortless Cove area. Note that no exploration north of Red Lion, south of Turtle Pits, or east of Sisters Peak has been undertaken leaving a large potential for additional hydrothermal sites in this area.

2.4.3.5 ROV observations at Lilliput

Four ROV dives took place in the Lilliput area. While sampling of diffuse fluids and mussels were the major activity at this site, exploration and geological mapping has been possible on several dives showing a distinct difference between the eastern parts of the area hosting the hydrothermally active sites and the western part mainly characterized by intensive fissuring

and pillow lava severely effecting the pillow mounds. This is clearly visible in the bathymetric map provided by the AUV Abyss during this cruise (Fig. 6). In the eastern part volcanic edifices are still intact and show only narrow fissures and cracks. The first dive, 319ROV, stayed in the eastern part, came down in to the west of the Main Lilliput site and crossed a NS fissure with some Fe-staining, before heading towards the mussel beds of Main Lilliput. During the dive two seamounts east of Main Lilliput were visited ($09^{\circ}32.72'S$ / $13^{\circ}12.48'W$ and $09^{\circ}32.94'S$ / $13^{\circ}12.42'W$; Fig. 6) that consists of pillow lava, that show intense fissuring in several crosscutting directions (star-like) resulting in block rotation and talus formation. While most fractures in the area run at 350° the seamounts to the east show also E/W and NW/SE trending fissures. The fractures can be several meters wide and expose massive flows; drainback is not visible. Additionally the large low lying mound to the northwest of Main Lilliput was investigated and was shown to consist of pillow lava cut by several small fissures. Selected images from the various lithologies are given in Fig. 7.

Dive 324ROV investigated the western fault block during the first part of the dive and showed that this area consists of intensely fractured and fissured pillow mounds. Individual fractures here are wider (Fig. 8) and show a higher throw when compared to those in the eastern part. Interestingly, this entire area does not show evidence for recent low-temperature venting implying that the fracture system and the volcanic edifices are older than those in the east. This is in agreement with the strong displacement of the volcanic edifices by the various faults in the area. The second part of the dive was devoted to the hydrothermally active part in the east where several areas of low-temperature Fe-oxyhydroxides were found in the Limtoc area and towards Main Lilliput. Collapse features including skylights, lava pillars, and collapsed roofs are abundant in this area. The final part of the dive was placed to the northeast of Main Lilliput passing by east of Candelabrum Meadows. Here a previously unknown site of tiny mussels was discovered. Close to finishing off the dive we passed the fissured terrain again in the very north of study area. The presence of Fe-oxyhydroxides in interstices of pillows indicates the potential for further hydrothermal activity to the north.

The next dive, station 329ROV, was dedicated to sampling at Main Lilliput before investigating the area of the Eh anomaly, located well outside the Main Lilliput area, found during previous CTD and AUV stations. During this dive sedimented pillow mounds, lobate flows and massive tilted blocks of basalt have been observed, that are very similar to those documented in the Lilliput area, however, the thick sediment cover indicates that the entire area is old and, since no evidence for low-temperature venting or Fe-oxyhydroxide formation has been found, is also hydrothermally inactive. The Eh-anomaly does not appear to be related to hydrothermal activity.

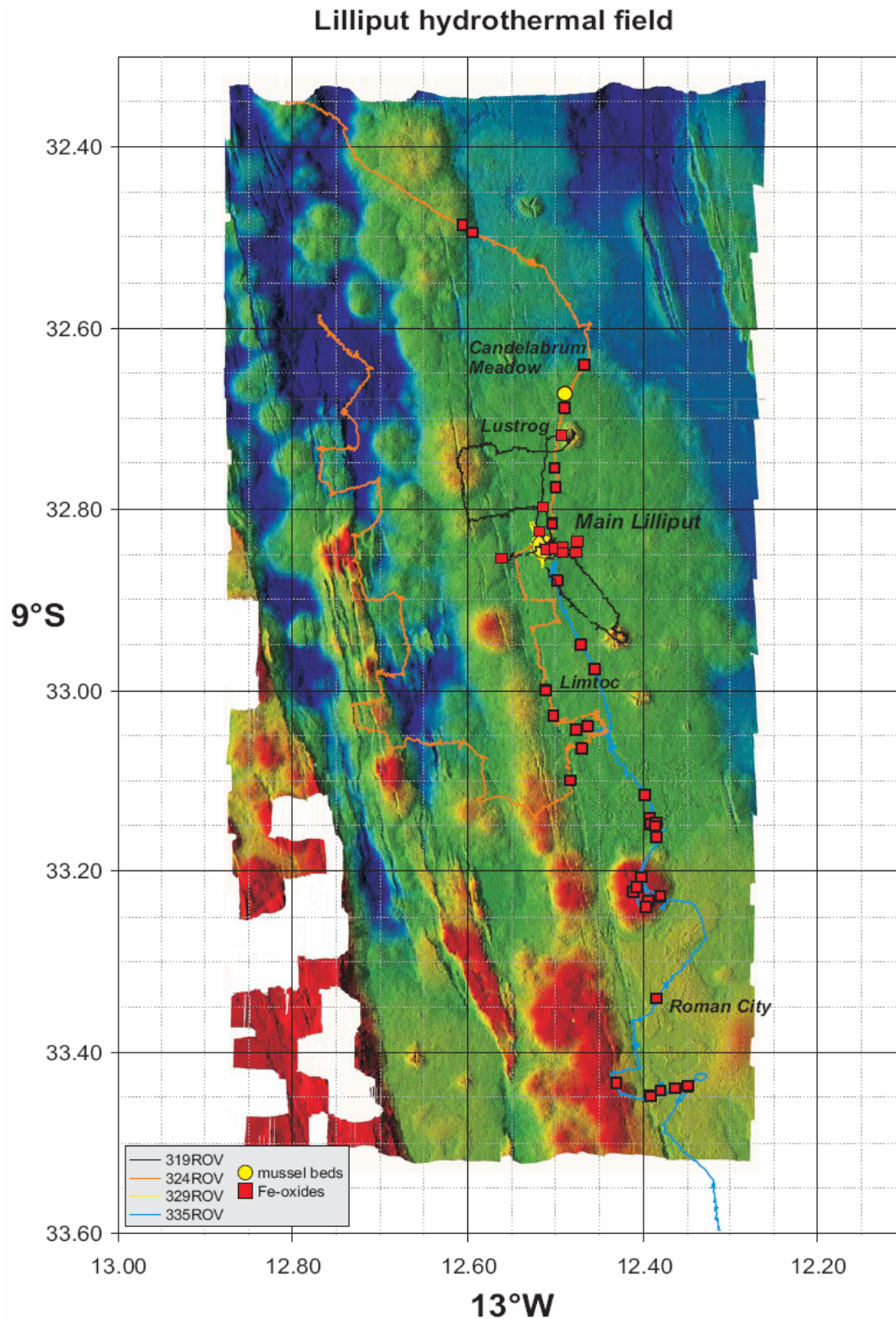


Fig. 2.4.3.6: Bathymetric map obtained by AUV ABYSS during this cruise overlain by edited ROV-tracks. The ROV positions („Posidonia“) obtained during the cruise showed various offsets to the map and have been edited to fit to the geological observations. The red squares denote the presence of Fe-oxyhydroxides indicating widespread venting of low-temperature hydrothermal fluids, mainly along younger fissures to the east of the central volcanic chain.

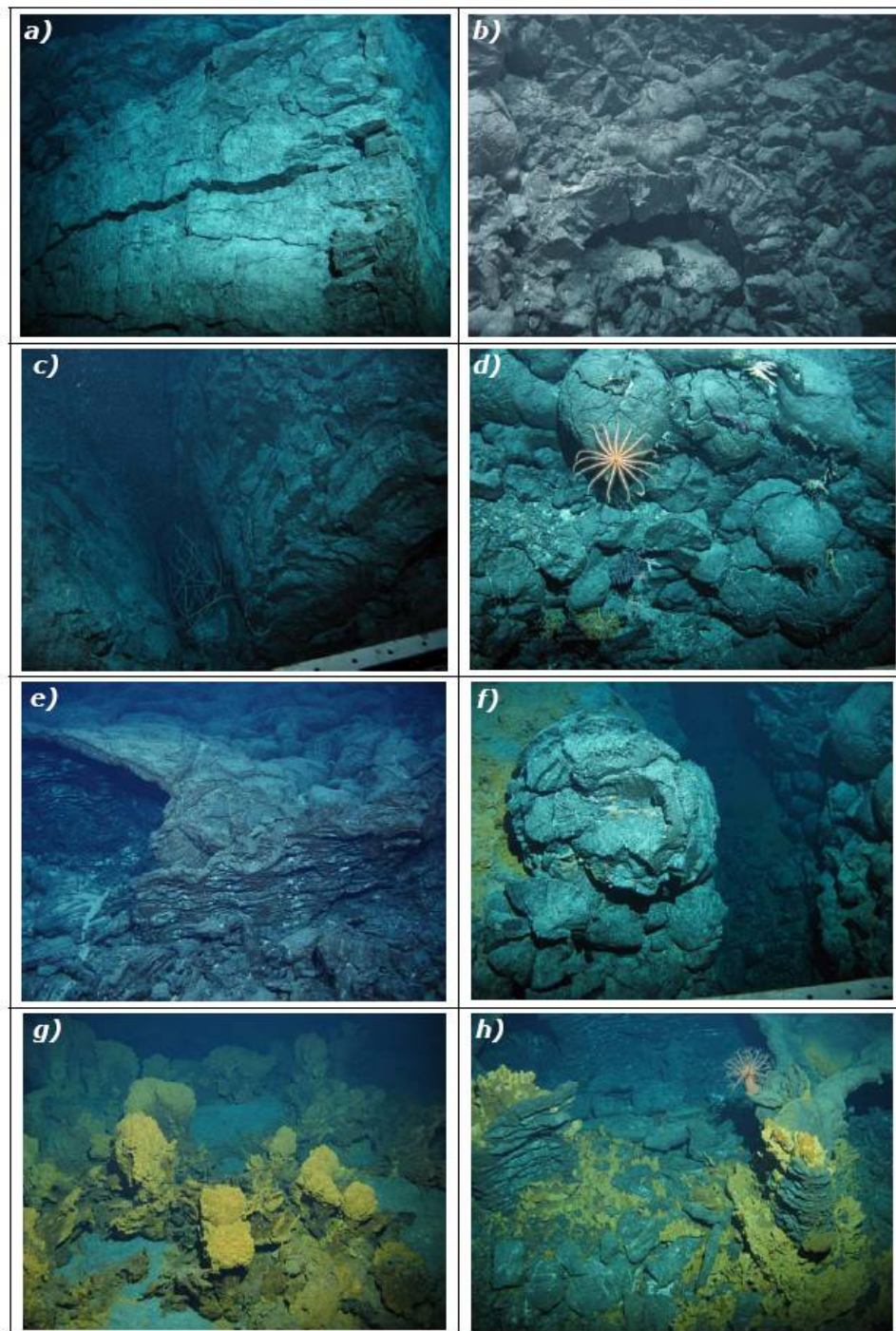


Fig. 2.4.3.7: Images of geological lithologies in the Lilliput hydrothermal field. a) massive rotated basalt block exposed by faulting at the top of a small seamount SE of Main Lilliput. b) Vertical section through a pillow mound exposed on a wall in the western fault block. c) E/W trending fissure in an elongated pillow mound at the northern limit of the mapped region. d) pillow lava and fauna exposed on an old pillow mound to the west of Main Lilliput (western fault block). e) Collapse features within lobate flows near Roman City. f) Fissure cutting pillow mound with associated Fe-oxyhydroxides along the fissure rim. g) Fe-oxyhydroxide chineys developed on top of lobate flows between Limtoc and Roman City. h) Fe-oxyhydroxides covering basalt pillars at Roman City.

The last dive, 335ROV started at Main Lilliput and investigated the area to the south, passing Limtoc and Roman City before exploring new ground further to the south, an area not covered by the AUV map. The discovery of Fe-oxyhydroxides outside the AUV map provides ample evidence for further hydrothermal activity in unexplored regions, albeit being less abundant

when compared to the Main Lilliput area. Interesting is the abundance of Fe-oxyhydroxides on a large seamount between Limtoc and Roman City.

In summary, it seems noteworthy that the occurrence of Fe-oxyhydroxides is limited to the eastern part of the working area and related to both, a recent, north/south trending fissure system and the tops of some younger pillow mounds. Especially the older mounds of the western fault block and to the east of Main Lilliput do not show evidence for recent hydrothermal activity. Additionally, drainback features only occur in the eastern part and seem to be an integral part of the geological setting of venting in this area. The discovery of Fe-oxyhydroxides well to the north and south of the previously known areas documents the potential of additional vent sites at Lilliput, that should be explored. During this and earlier cruises, no evidence was found of oxidizing massive sulfides suggesting that all Fe-oxyhydroxides are formed by upwelling „warm“ fluids ($< 100^{\circ}\text{C}$) that lost H_2S and metals in the subseafloor. The abundance of collapse features in the area of main Fe-oxyhydroxide occurrence could, if persistent at depth, potentially provide the porous substrate in which ascending high-temperature fluids are trapped underground only releasing cooler fluids to the seafloor.

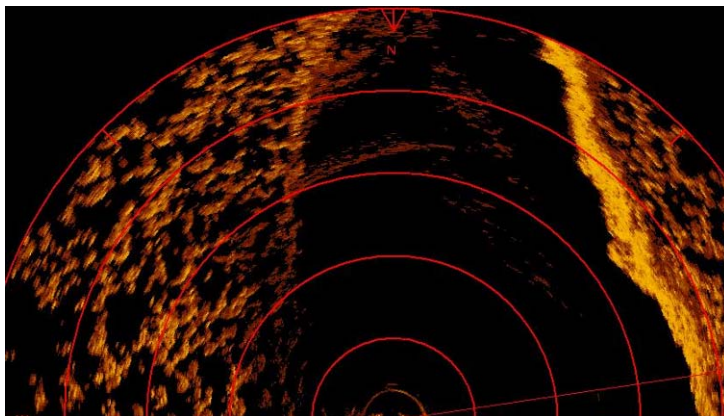


Fig. 2.4.3.8: Sonar image, looking south, showing the width (25 m) of one of the larger fissures in the western fault block while the ROV is hovering in the center of the fissure. Distance between red lines in this image is 5 m with a total range of 25 m. Note that individual pillows are visible in the left (eastern) part of the image and that the fissure is narrowing quickly towards the south. Dive 324ROV.

2.4.4 Physical Oceanography

(Christian Mertens, Janna Köhler)

The spreading of hydrothermal products into the deep ocean is controlled by background currents, tides, internal waves and turbulent diffusion. During METEOR cruise M78/2, near field measurements of temperature, salinity, turbidity, and velocity at the Turtle Pits and Lilliput hydrothermal sites were made to study the plume dispersal. Additionally, water samples were taken for later helium isotope analysis. A hydrothermal plume in the local background stratification should reveal itself by negative anomalies in temperature and salinity as well as an increase in turbidity and drop of oxygen reduction potential. In addition to plume mapping, the temperature and density field, as well as the vertical shear of the horizontal velocity field, will be analyzed to determine the strength and distribution of turbulent vertical mixing in the water column above the Mid-Atlantic ridge.

Conductivity-temperature-depth (CTD) casts were carried out using a Sea-Bird Electronics, Inc. SBE 911plus system that was equipped with a custom build Seapoint Turbidity Meter (5x normal gain). The underwater unit was attached to a SBE 32 carousel water sampler with 24 Niskin bottles. Two bottles were left out for a lowered acoustic Doppler current profiler system (LADCP), hence a maximum of 22 bottles was used. The complete system worked properly throughout the cruise, except for bad turbidity data on stations 282 and 327 caused by a stained sensor. Salinity samples, typically three on each cast, were collected for later analysis at home. In total 23 CTD casts were carried out, including three towed transects (tow-yo) at Lilliput (Fig. 2.4.4.1).

Two RD Instruments 300 kHz Workhorse Monitor ADCPs, were used for velocity

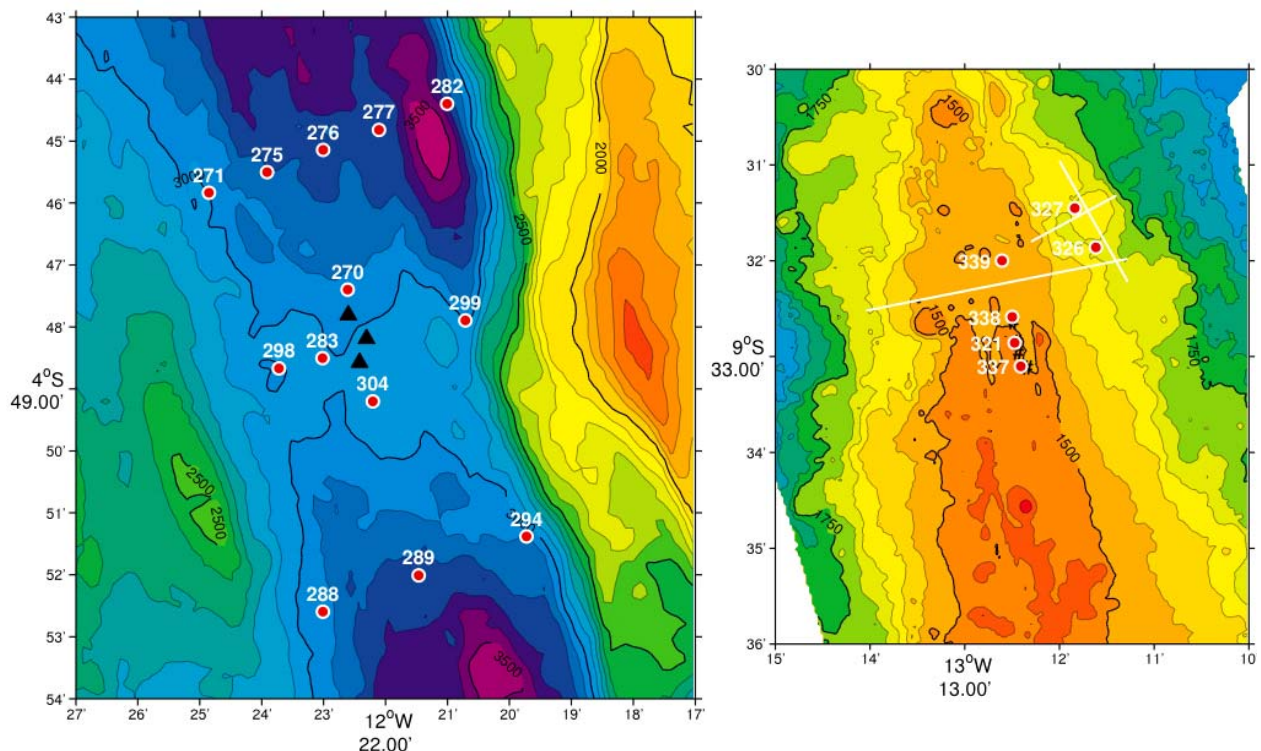


Fig. 2.4.4.1: Maps of the working areas at Turtle Pits (left) and Lilliput (right) showing the CTD/LADCP stations (dots). White lines denote the tow-yo tracks in the Lilliput area.

profiling. The instruments worked in a synchronized master-and-slave setup, where the downward looking master (S/N 7915) triggers the upward looking slave (S/N 2161). The instruments were powered by an external battery supply, that consists of 35 commercial quality 1.5 V batteries assembled in a pressure resistant Aanderaa housing.

An inverse method incorporating the bottom track velocities was used for the post processing of the raw data. The overall performance of the two instruments was very good: The range of each instrument was typically 150 m in the upper parts of the water column and 60 to 70 m at depths exceeding 1500 m. Thus, the total range of the package varied from 150 to 300 m. With lowering and heaving velocities of 1 m/s, this range amounts to 100-200 estimates of current shear in each depth cell in the deep water, and more in the shallow layers, depending on the abundance of backscatterers.

To collect redox potential (Eh) data, a miniature autonomous plume recorder (MAPR, E. Baker, NOAA, PMEL) was attached to the CTD on eight of the stations. MAPRs are self-contained instruments, that record data at pre-set time intervals (5 seconds) from temperature (thermistor mounted in a titanium probe, resolution 0.001°C), pressure (0-6000 psi gauge sensor, resolution 0.2 psi), and nephelometer (Sea Tech Light Backscatter Sensor) sensors. The Eh probe was build by K. Nakamura (AIST, Japan). Only one MAPR (S/N 41) was used on this cruise, that worked properly except for occasional hang-ups during data recovery.

For measurements of the helium concentrations and isotopic signature, water samples were collected from the Niskin bottles. In total 237 samples were taken, 181 of them at stations around the Turtle Pits vent sites and the remaining 56 at Lilliput. The samples were sealed free of head space and gas tight in copper tubes (sample volume 40 ml). Helium isotope measurements will be carried at the University of Bremen with a fully automated UHV mass spectrometric system. The sample preparation includes gas extraction in a controlled high vacuum system. Helium and neon are separated from permanent gases in a cryo system at a temperature of 25 K. A split of the sample is analyzed for ^4He , ^{20}Ne and ^{22}Ne with a quadrupole mass spectrometer. At 14 K He is separated from Ne and released into the sector field mass spectrometer for analysis of ^3He and ^4He . The facility achieves about $\pm 0.2\%$ precision for $^3\text{He}/^4\text{He}$ ratios, and $\pm 0.5\%$ or better for helium and neon concentrations. The primordial components of helium isotopes are ideal tracers for large-scale distribution of vent fluids in the water column. Samples collected during this cruise are supposed to provide the regional distribution of dispersing vent fluids in the water column leading to an estimate of its volume.

Attempts were made to collect helium samples directly at the vents with the ROV. Special tools, that prevent phase separation of vent fluids and gases, were developed for the sampling of vent fluid. However, despite the positive experiences on previous cruises were several samples were successfully collected, the helium sampling with the ROV on this cruise was an utter failure. The first attempt was to collect a helium sample was made von April 18 (station 281) at the black smoker One Boat of the Turtle Pits vent field. A newly developed sampler was used, that was intended to reduce handling difficulties and sampling time compared to the old sampler. The idea of the new design was that only one trigger has to be pushed to close the sampler instead of closing the two valves at the upper and lower end of the sampler manually. However the mechanism did not work thus leaving the sampler open, although it

appeared in the camera that the trigger was pushed several times. However, during ascend the sampler slipped out of the Rigmaster and was lost. The second attempt was made on April 21 (station 297), using the old type of sampler. The sampling site was the smoker Mephisto of the Red Lion vent field. The sampling went well, although it took about one hour to take the sample. Unfortunately one of the valves was opened again during stowing, which made the sample unusable. Further attempts to collect helium samples with the ROV were not scheduled.

During a L'ATALANTE cruise in January 2008 a mooring, with CTD and acoustic current meter profiling along the wire (IFM-GEOMAR), was deployed half way between Turtle Pits and Red Lion ($4^{\circ} 48.20'S$, $12^{\circ} 22.51'W$). Messages from its Argos watchdog were received in July 2008, indicating a loss of at least the top-most floatation. Several tries from different directions were made to locate the releases acoustically, but even with all other acoustic equipment of the ship switched off not a single response was received. Nevertheless release commands were sent on April 23, 2009 at 07:20 UTC but as no signs of the mooring were spotted after one hour of lookout it has to be concluded that the mooring is completely lost. However, this was already the second mooring lost in this area. The first mooring with three Aanderaa RCM11 current meters (Univ. Bremen) was deployed on METEOR cruise 68/1 in May 2006, and could not be recovered during the L'ATALANTE cruise in January 2008, but it was possible to locate the releases acoustically on the sea floor. This location was confirmed on the present cruise, which indicates the proper functioning of the acoustic equipment.

Two hydrographic sections were made at Turtle Pits, one north (five stations, Fig. 2.4.4.2) and one south (three stations) of the vents. The local bathymetry is closed to the sides below a depth of 2800 m, which coincides with the upper boundary of the hydrothermal plume. Hence

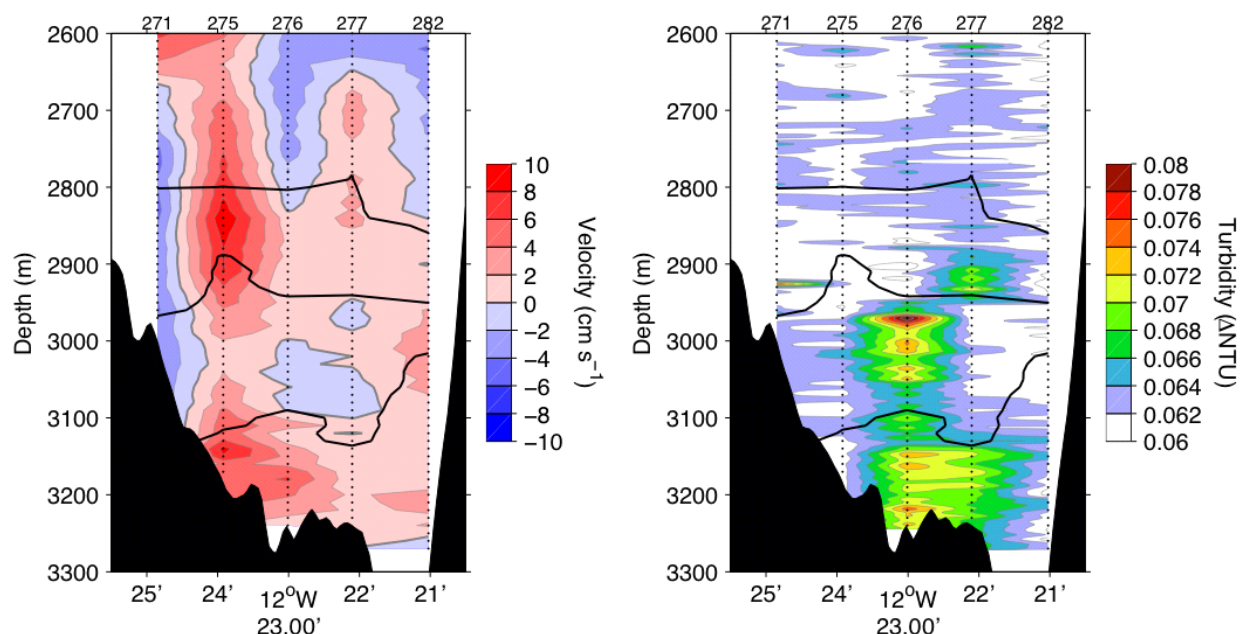


Fig. 2.4.4.2: Current velocity (left) and turbidity (right) along a cross-valley section north of the Turtle Pits vent sites. Thick black lines denote density surfaces that separate the different plume layers ($\sigma_3 = 41.465, 41.468, \text{ and } 41.471 \text{ kg m}^{-3}$).

the two sections form a closed box where measurements of the current field and the

stratification allow to calculate fluxes of volume, heat and helium into and out of the vent field area.

The area is dominated by along-valley northward currents, which are modulated in strength by tides. The average current velocity below a density of $\sigma_3=41.465 \text{ kg m}^{-3}$ (that coincides roughly with the upper boundary of the side wall) was 1.7 cm/s , but maxima exceeded 15 cm/s (Fig. 2.4.4.3). The strongest currents are orientated northward, while southward currents are weaker and occur only in the effluent plume layer. The volume transport associated with

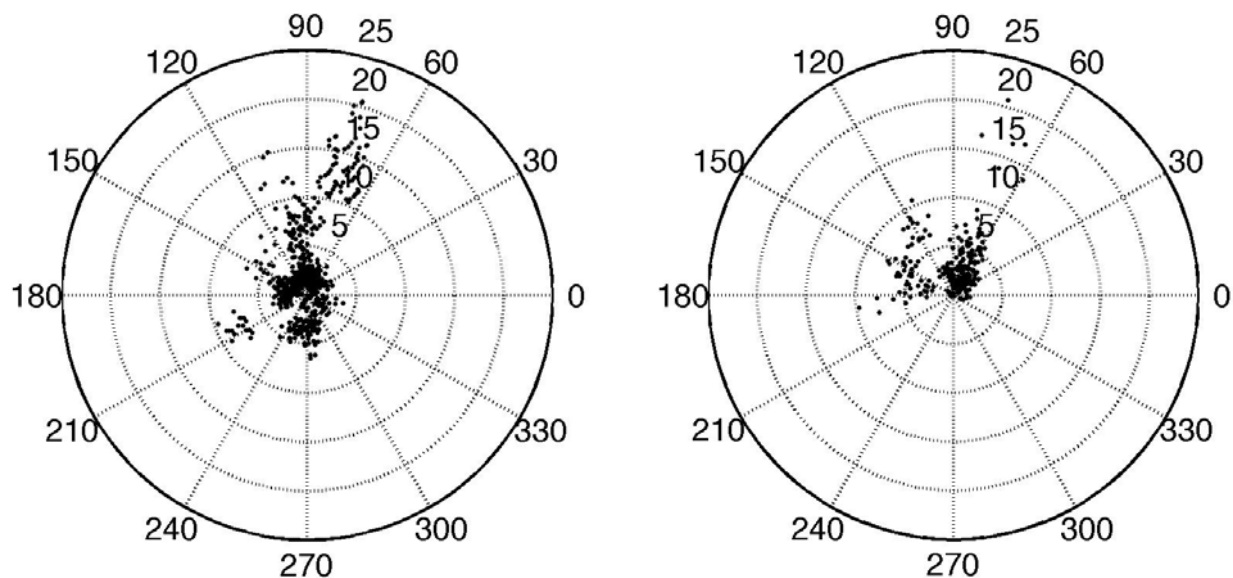


Fig. 2.4.4.3: Scatter plot of amplitude and direction of the currents from all stations in the Turtle Pits area in two different density layers. The density range of the upper layer (left hand side, $\sigma_3=41.465\text{--}41.471 \text{ kg m}^{-3}$) corresponds to the effluent plume layer, and velocities below $\sigma_3=41.471 \text{ kg m}^{-3}$ are shown in the right hand side panel. Most of the data points in both layers have a northward component, i.e. fall into the E-N-W segment of the diagram ($N=90^\circ$). The amplitude of these currents (distance from the centre of the plot) ranges from a few centimeters per second to more than 15 cm s^{-1} .

the flow amounts to 0.021 Sv ($10^6 \text{ m}^3 \text{ s}^{-1}$) across the section north of the vent sites, 0.011 Sv of the total volume transport were observed in the effluent layer.

The distribution of turbidity along the northern section exhibits three distinct layers with local maxima backscatter signal within each of them. The top-most layer ($\sigma_3=41.465\text{--}41.468 \text{ kg m}^{-3}$) shows maximum backscatter at station 277 in a depth of about 2900 m . The source of the signals in this layer are presumably the vents at Turtle Pits and Comfortless Cove. The maximum plume signal of the intermediate layer ($\sigma_3=41.468\text{--}41.471 \text{ kg m}^{-3}$) was located at station 276, thus westward of the maximum in the upper layer. In the bottom layer ($\sigma_3 \geq 41.471 \text{ kg m}^{-3}$) the turbidity is still high, but less focused and maximum signals were found at stations 276 and 277. Although about 300 m below the depth of the hydrothermal vents, there is virtually no density contrast between the bottom layer at the vents and the northern section, hydrothermal signals in the bottom layer may therefore, at least partially, also originate from diffuse venting.

Further CTD stations were made in the vicinity of the vent sites itself, two of them are shown in Fig. 2.4.4.4 (stations 283 and 304). Station 283, east of Turtle Pits, shows a strong

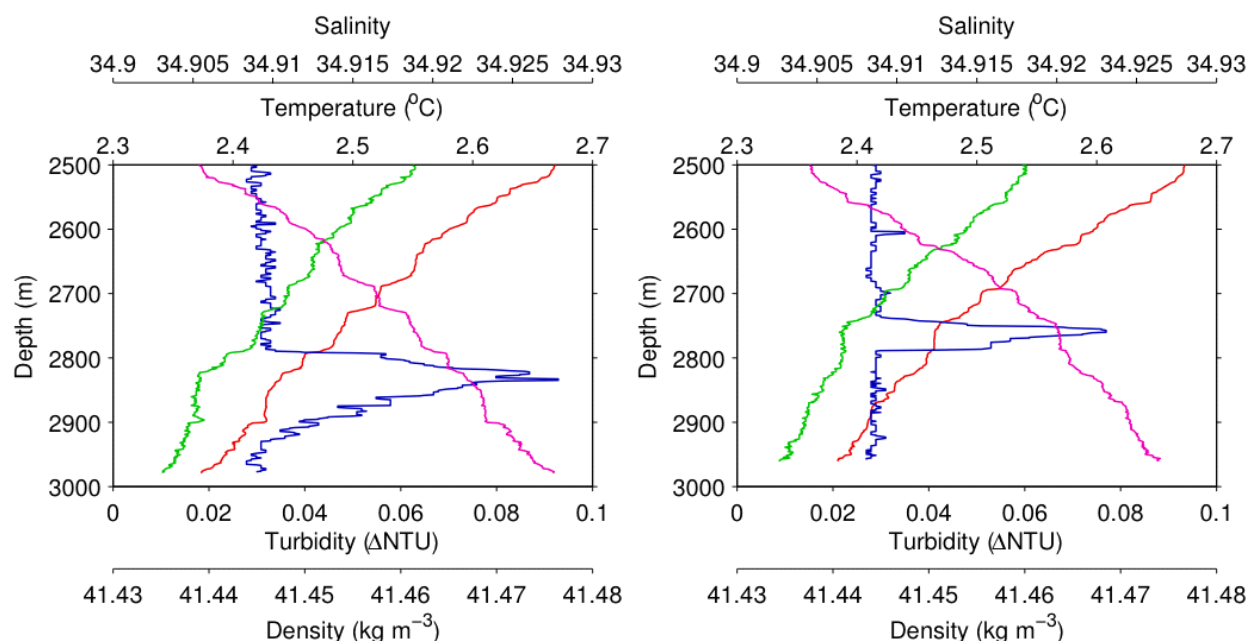


Fig. 2.4.4.4: Vertical profiles of temperature ($^{\circ}\text{C}$, red), salinity (green), turbidity (blue), and density anomaly (σ_3 , kg m^{-3} , magenta) at two CTD stations near the Turtle Pits hydrothermal field. Station 283 (left hand side) was located east and station 304 (right hand side) was located south of the vents.

turbidity signal between 2800 and 2900 m and at station 304, in the south, a slightly weaker signal was found between 2750 and 2800 m. Although it appears likely that the plume signals found at these two stations originate from the known vents of Turtle Pits, this is not supported by the direction of the observed currents, that point to the opposite direction. Thus it cannot be ruled out that these signals originate from a different, yet unknown, source. Similar spurious signals had been found on previous cruises, but a detailed AUV survey would have been necessary to clarify the situation.

In contrast to Turtle Pits and Nibelungen, the Lilliput hydrothermal site ($9^{\circ} 33' \text{ S}$) is quite shallow (about 1500 m), which makes plume anomalies in the water column difficult to observe. Hydrothermal fluids in shallower areas have lower maximum temperatures and lower metal contents and hence often carry only a weak or no turbidity signal. Further, the background variability of temperature is high in this depth range because it is situated between the shallow Antarctic Intermediate Water and the upper North Atlantic Deep Water as well as subject to strong mixing above the Mid-Atlantic Ridge. The hydrographic work at this site was therefore restricted to four CTD casts in the vicinity of the known diffuse venting locations of Lilliput. Two additional CTD casts (stations 326 and 327) and two tow-yo tracks were made northwest of Lilliput in search of a possible new vent location. The largest turbidity signals were found on stations 327 and 339 (Fig. 2.4.4.5) and during a ridge-crossing tow-yo north of Lilliput (Fig. 2.4.4.6). The turbidity and redox potential signals found on the stations close to Lilliput were small and decreased southward. Thus it is not clear whether they originate from the diffuse venting at Lilliput or from an other source north of Lilliput where the strongest signals were found. Motivated by relatively strong Eh signals on the eastern flank of the ridge, that were found on the ridge-crossing tow-yo (Fig. 2.4.4.6), a search for new vent

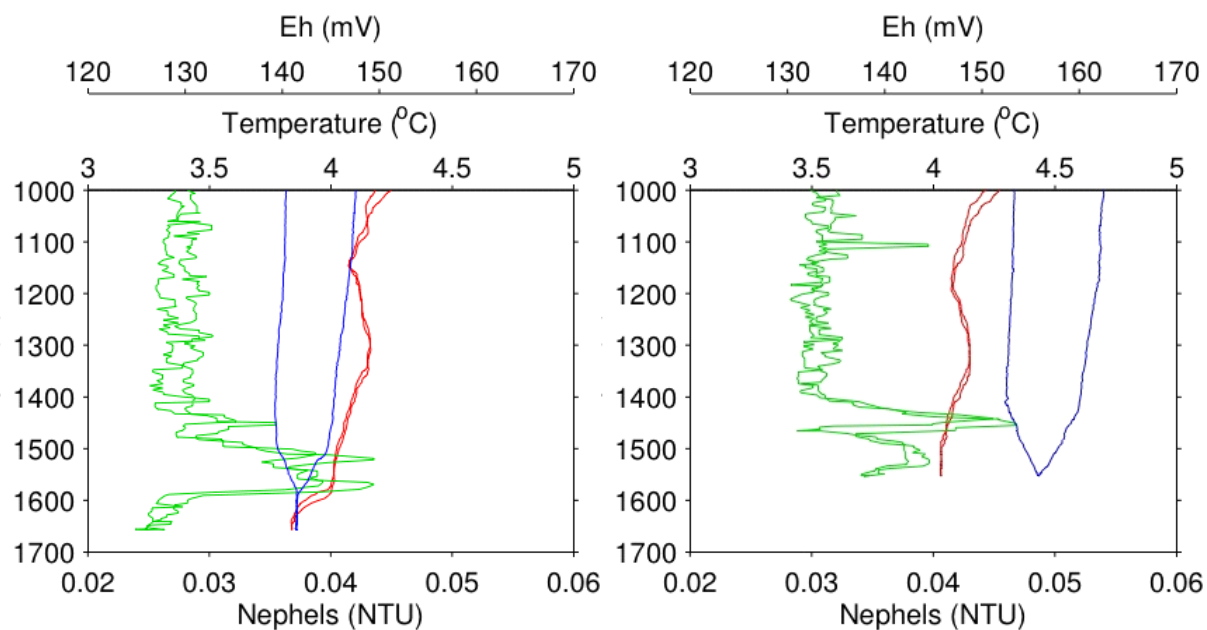


Fig. 2.4.4.5: Vertical MAPR profiles of temperature (°C, red), turbidity (green), and redox potential (mV, blue) at two stations near the Lilliput hydrothermal field. Station 327 (left hand side) was located northeastward of Lilliput and was carried out in search of a possible new vent location and station 339 (right hand side) was located north of the known Lilliput field.

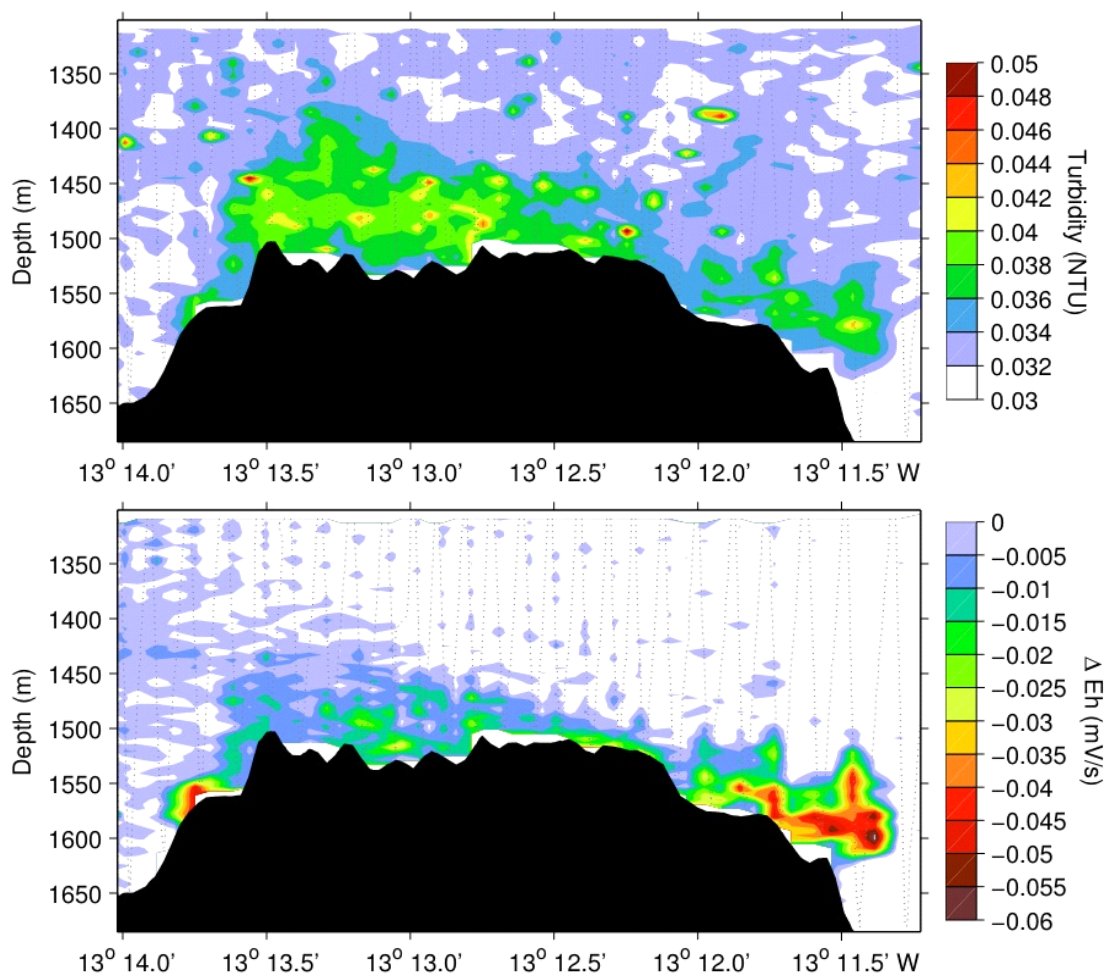


Fig. 2.4.4.6: Horizontal distribution of turbidity (upper panel) and the rate of change of redox potential (lower panel) along a tow-yo track north of the Lilliput field (cf. Fig. 2.4.4.1).

sites was conducted near a shallow mound northwestward of Lilliput. But despite the two further tow-yos and two AUV surveys that confirmed the turbidity and Eh signals of the tow-yos, no vent site could be found during a ROV dive. The source of the signals thus remains unclear, but it may however have been caused by re-suspension of sediments.

2.4.5 Fluid Chemistry

(D. Garbe-Schönberg, V. Klevenz, D. Meißner, H. Strauss, C. Breuer)

Scientific objectives for the fluid geochemistry group were (i) to continue the monitoring of temporal variability of elemental and isotopic compositions in hydrothermal fluids at the southern Mid-Atlantic Ridge, in particular at the vent sites at 4°48'S: Turtle Pits and Red Lion (started in 2005), Sisters Peak (started in 2006), and Clueless (started in 2008); at 8°55'S with Drachenschlund (data from 2006); and at the Lilliput area at 9°33'S (started in 2005); (ii) to identify spatial heterogeneity between different hot fluid vent sites, and (iii) to determine temporal and spatial variability within individual mussel fields. From these long-term observations a quantitative understanding of temporal and spatial variations in fluid chemistry at the slow spreading Mid-Atlantic Ridge will be developed. It is anticipated that the resulting model will be in strong contrast to our current understanding of respective processes that is based largely on results from the East Pacific Rise.

Fluid sampling of both diffuse warm, and focused hot fluids was achieved using the ROV-based fluid sampling system "KIPS" (Kiel Pumping System, KIPS-3). Compared to previous cruises, the design of the KIPS system has been significantly modified with the objective to (1) improve the tightness of sample containers and avoid gas-induced leakage of samples causing cross-contamination of gases; (2) develop a more compact, self-contained unit which can easily be mounted and dismounted on the ROV tool sled; (3) use a deep sea peristaltic pump for *in situ*-fixation by adding reagents into a sample container; (4) use a combination of different temperature sensor technologies to improve accuracy of temperature data. The new KIPS fluid sampling system was successfully used during the entire cruise. A more detailed description of the system components is given in the Appendix. In addition to the KIPS, two titanium syringes ("Majors" after von Damm et al., 1985; manufactured by IFREMER/BREST-MECA) were used to collect hot hydrothermal fluids (see Appendix for details).

On-board measurements comprised pH, concentrations of oxygen, sulfide, Mg, as well as Cu, Zn in diffuse fluids. Analyses were performed in order to ascertain the quality of sampled hydrothermal fluids (i.e., the degree of admixed seawater) and to provide an initial characterization of fluid composition. Details of on-board sub-sampling and sample preparation as well as analytical methods used are summarized in the Appendix.

2.4.5.1 Chemistry of hydrothermal fluids

Twenty-four hot fluid samples were collected at four locations, and first results are being presented in the following paragraphs.

Turtle Pits – One Boat. Two fluid samples of the black smoker chimney "One Boat" were collected during station 281 ROV with titanium syringes. Fluid was blackened by sulphide particles, indicating a certain degree of seawater entrainment. Ex-situ measurements yielded pH values of 2.44 and 2.62. The Mg concentration indicates a fluid proportion of 74 and 63%, respectively (Tab. 2.4.5.1). Sulphide concentrations of 4.3 and 3.1mM were measured for both samples.

Red Lion – Mephisto. Fluid from “Mephisto”, a black smoker at the Red Lion vent area, was sampled during station 297 ROV using the KIPS. Due to an unstable sampling position of the nozzle (see Fig 2.4.4-2 in the Appendix depicting a variable fluid sampling temperature) entrainment of seawater during sampling was relatively high, resulting in precipitation of “black smoke” particles. A broad range of Mg concentrations in the six samples indicates variable fluid proportions between 6 and 80%. Ex-situ pH values ranged from 3.8 to 7.3. Dissolved sulphide concentrations ranging from 1.1 to 4.7mM were determined.

Comfortless Cove – Sisters Peak. The ultra-high temperature fluids of the black smoker chimney “Sisters Peak” were sampled during station 302 ROV using a titanium syringe and during station 308 ROV with KIPS. Sample 302 ROV-1 was of poor quality having a fluid proportion of only 8%. The respective pH is 6.7. The 308 ROV samples have fluid percentages between 29 and 70% and pH values ranging from 2.4 to 4.2. The hot vent fluids from Sisters Peak showed dissolved sulphide concentrations between 2.8 and 7.2mM.

Nibelungen – Drachenschlund. Hot hydrothermal fluid with a constant temperature of 371.6 °C venting from an orifice directly on the seafloor was sampled during station 314 ROV. At this site, sampling was most successful yielding samples with the highest fluid proportions (up to 87%) of all sites. For three of the 9 samples, however, the objective was to sample fluids from the mixing zone between pure fluid and seawater at temperatures around 100 °C for subsequent gene expression studies. Consequently, samples have relative low proportions of 16 – 20% hydrothermal fluid. In the samples with high fluid percentages the pH was measured at values ranging from 2.9 to 3.3 and in the low-fluid samples from 5.3 to 5.8. Sulphide concentration of 0.5 – 1.1mM were measured for hot fluids emanating from the Drachenschlund.

A total of forty-six diffuse vent fluid samples were collected, with twenty-one from different sites at Comfortless Cove and twenty-five at the Main Lilliput vent field. First results are being presented in the following paragraphs.

Comfortless Cove – Foggy Corner. At the diffuse venting site “Foggy Corner” three KIPS bottles and one Niskin bottle were taken during station 267 ROV and one Niskin bottle was taken at station 287 ROV. Acidity was determined to pH values between 7.7 and 7.9 and Mg concentrations indicate fluid proportions between 0 and 4.6 %. Dissolved sulphide concentrations between 0.5 and 1.5µM were measured for three diffuse fluids at Foggy Corner.

Comfortless Cove – Clueless/Desperate. At the diffuse vent site “Clueless” KIPS was used for sampling during station 302 ROV. Fluid percentages were higher than at Foggy Corner with values between 4.6 and 7.4 %. pH values ranged from 6.1 to 6.6. At the vent site “Desperate” KIPS samples were taken during station 287 ROV, with fluid percentages ranging from 0.9 to 4.3%. pH values were determined at 6.7 to 7.4. Thirteen samples of diffuse fluids emanating from different sites at the Clueless mussel fields yielded concentration for dissolved sulphide between 237 and 266µM (Clueless) and 0.6 and 22.3µM (Desperate). In-situ fixation of dissolved sulphide at the Clueless site yielded a concentration of 313.0µM. In two of the Clueless fluids Zn was measured at concentrations of 87 and 254 nM and Cu at concentrations of 13 and 27 nM, respectively. Two other samples from the

Desperate mussel field displayed Zn concentrations at 62 and 41 nM and Cu concentrations of 22 and 28 nM, respectively. These values – as the following ones for other diffuse sites - are only slightly elevated in comparison to seawater concentrations which is caused by the non-conservative behaviour of these metals during mixing with seawater (precipitation of minerals).

Comfortless Cove – Sisters Peak. Fluids were sampled at a diffuse site close to the black smoker Sisters Peak during station 302 ROV. For these, pH values between 6.5 and 6.7 were measured and fluid percentages were determined at 6.1 to 8.3%. Concentration of dissolved sulphide ranges from 69 to 107 μ M for diffuse fluids at Sisters Peak. One of these samples was analysed for Zn and Cu yielding 85 and 20 nM, respectively.

Lilliput – Main site. The Main site of Lilliput was sampled four times during stations 319, 324, 329 and 335 ROV. pH values for these samples ranged from 5.99 to 6.58, and fluid proportions from 0 to 7.1%. Repeated sampling of diffuse fluids from the Main Lilliput site at the Lilliput mussel fields (25 samples in total) yielded sulphide concentrations ranging from 22-53 μ M. For two in-situ fixations dissolved sulphide concentrations of 49 and 74 μ M were measured.

Four of these samples were analysed for Zn and Cu with concentrations ranging from 91 to 431 nM and 19 to 39 nM, respectively.

Table 2.4.5.1: Results from on-board chemical analyses (not endmember corrected)

Stat. No.	Description	Sample ID	Bottle	Date	T (°C)	pH	O ₂ (µM)	H ₂ S (µM)	Mg (mM)	Mg (mM) ^a	% EM Fluid	Zn (nM)	Cu (nM)
267 ROV	Foggy Corner	1	A2	16.04.2009	3.0-3.5		252						
		2	A3		3.0-3.5	7,9		1,4	51,6	54,3	-0,6		
		3	B4		3.0-3.6	7,9	228	0,5	51,5	54,4	-0,7		
		4	Niskin			7,7	209	1,5	52,2	54,9	-1,7		
281 ROV	Turtle Pits, One Boat	1	D1	18.04.2009	max. 425	2,4		4300	14,0	3,4	93,6		
		2	D2		max. 425	2,6		3120	20,0	0,4	99,2		
287 ROV	Foggy Corner	1	Niskin	19.04.2009	5 - 8	7,7		264	0,8	54,0	54,4	-0,7	
		2	A1+ZnAc		5 - 8	6,7			26,4	53,0	53,9	0,2	
		3	A2		5 - 8					53,7			
		4	A3		5 - 8	7,2	226	1,8	53,2	54,1	-0,2		
		5	B4		5 - 8	6,9	224	8,3	52,8	53,9	0,3	62	22
	Desperate	6	B5		5 - 8	7,2	215	14,1	53,0	53,7	0,5	41	28
		7	B6		5 - 8	7,2	225	15,2	52,0	53,6	0,8		
		8	C7		5 - 8	7,3	225	0,6	51,7	52,6	2,7		
		9	C8		5 - 8	7,3	227	22,3	53,5	53,3	1,4		
		10	C9		5 - 8	7,4	229	0,6	53,3	53,4	1,1		
297 ROV	Red Lion, Mephisto	2	A1(ZnAc)	21.04.2009	320 - 348	4,6		2654	22,8	23,1	57,3		
		3	A2		348	5,3		1553	36,6	39,3	27,2		
		4	A3		348	4,1		4534	22,3	17,9	66,8		
		5	B4		348	7,3			50,5	50,5	6,5		
		6	B5		348	3,8		4746	11,3	10,7	80,1		
		7	B6		348	5,4		1095	40,4	40,9	24,2		
302 ROV	Sisters Peak	1	D1, Major	22.04.2009		6,7		31	49,5	51,8	4,1		
		5	C8		9.4 - 12.6	6,6			50,7	52,8	2,2		
	Sisters Peak, diffus	6	C7		8 - 12.9	6,7	141	69	49,5	53,0	1,8		
		7	C9		5 - 12	6,7	162	69	50,5	53,1	1,6		
		8	B6		10.5 - 16.2	6,5	122	107	50,5	53,3	1,2	85	20
		9	A1		13	6,1		313	50,0	52,2	3,4		
	Clueless	10	A2		13	6,5			50,0	52,8	2,2		
		11	A3		13	6,6		266	51,0	53,2	1,4	87	13
		12	B4		13	6,5		237	51,5	49,2	8,9		
		13	B5		13	6,5		261	50,0	53,1	1,6	254	27
308 ROV	Sisters Peak	2	A2	23.04.2009	375	3,1			20,8	17,8	66,9		
		3	A1 + ZnAc		375	2,9		6438	17,7	16,7	69,1		
		4	A3		375	2,9		6864	20,1	16,2	70,0		
		5	B4		375	3,8		4009	32,4	18,7	65,3		
		6	B5		375	2,7		4691	18,5	18,5	65,8		
		7	B6		375	2,4		7205	16,0	11,0	79,5		
		8	D2 Major		375	4,2		2753	38,5	36,8	31,8		
314 ROV	Nibelungen Drachenschlund	1	A1+ZnAc	27.04.2009	368 - 370	5,4		477	31,6	29,0	46,3		
		2	A2		369	3,1		1003	7,0	4,6	91,5		
		3	A3		368	2,9		1147	7,0	3,0	94,5		
		4	B4		368	3,2		612	8,9	5,9	89,1		
		5	B5		368	3,1		945	7,2	5,0	90,8		
		6	B6		368	3,3		1106	12,5	5,3	90,1		
		7	C7		90 - 120	5,3	25	7	43,0	45,7	15,4		
		8	C8		90 - 120	5,7		12	45,2	44,9	16,8		
		9	C9		90 - 120	5,8	87	6	44,0	46,0	14,8		
319 ROV	Lilliput main	2	C7	29.04.2009	9,2	6,34		42	53,0	53,4	1,1		
		3	C8		9,2	6,28	90	48	50,8	54,0	0,0	181	33
		4	C9		9,2	6,3	210	42	50,9	53,8	0,4		
		6	A2		9,2	6,37		60	52,5	54,1	-0,3	105	19
		7	A3		9,2	6,33		43	52,8	54,1	-0,1		
		11	B4		9,2	6,35		38	52,8	53,5	0,9		
		12	B5		9,2	6,25	80	50	51,1	53,6	0,7		
		13	B6		9,2	6,35	109	24	52,5	53,9	0,3		
		14	A1+ZnAc		9,2	6,4		58	52,7	53,9	0,2		
324 ROV	Lilliput main	1	A2	30.04.2009	9	6,30		53	52,8	54,1	-0,1		
		2	A3		9	6,34	93	34	52,8	53,5	0,9	91	30
		3	B4		9	6,44	91	35	52,3	53,6	0,8		
		4	B5		9	6,35	84	36	52,0	53,9	0,1	431	39
		5	B6		9	6,32	71	38	52,0	54,0	0,0		
		6	C7		9	6,31		52	51,8	53,7	0,6		
		7	C8		9		69	45	52,5	53,5	0,8		
		8	C9		9	6,30	72	52	51,5	53,8	0,3		
		9	A1+ZnAc		9	6,24		74	50,2	53,1	1,6		
329 ROV	Lilliput main	1	C7	01.05.2009	9	6,48	89	12	52,8	54,3	-0,5		
		2	C8		9	6,58		6	53,4	54,2	-0,3		
		3	C9		9	6,52		25	54,1	53,9	0,1		
335 ROV	Lilliput main	1	A2	02.05.2009	9,8	6,12		29	50,2	48,6	10,1		
		2	A3		9,8	6,13	92	22	50,5	53,5	1,0		
		3	B4		9,8	6,27		20	51,0	53,5	0,8		
		4	A1		9,8	5,99		49	50,2	52,0	3,6		

^a measured on-shore by ICP-OES at IfG Kiel

2.4.6 Gases in Hydrothermal Fluids and Plumes

(M. Warmuth and S. Herrlich)

2.4.6.1 Introduction

Objective of the work during M78/2 was to characterise hydrothermal fluids and plumes to compare them with data gathered during former MARSUED cruises (M64/1, M68/1 and Atalante leg 2) to monitor the temporal variations within these hydrothermal fields. Subjects of the study were hydrothermal fluids and plumes of three areas along the MAR - Red Lion / Turtle Pits / Wideawake (04°48'S), Nibelungen (8°17'S) and the Liliput hydrothermal field (9°30'S). CH₄, H₂, CO, and CO₂ were measured on board by gas chromatography. Focus was given to hot fluids to obtain information on the sub-surface hydrothermal processes and on diffuse vents emphasizing on the energy and food supply of vent organisms. In addition, the stable carbon and hydrogen isotope ratio of methane from the fluid samples will be measured in the isotope laboratory at the IfBM. The water samples for these analyses were collected from 6 CTD stations and 11 ROV dives. For ROV dives, samples were obtained by three different advices namely the KIPS, titanium in situ gas samplers (MAJORS) and a niskin bottle attached to the front porch of the ROV. To elucidate the transformation of carbon species and reduced gases brought along by hydrothermal fluids, a comprehensive set of samples was secured for on shore analysis of stable isotope contributions (H and C) of fluid components.

In addition, hydrogen was monitored within incubation experiments conducted in cooperation with M. Perner (Biozentrum, Klein Flottbek, Hamburg).

2.4.6.2 Samples and Methodology

For on board measurements of dissolved methane and hydrogen up to 320ml of sample is connected to a high grade vacuum using a technique modified from the method described by Schmitt et al. (1991). Aliquots of the released gas are transferred via a septum from the degassing unit into the analytical system. A gaschromatograph (THERMO TRACE) equipped with a packed stainless steel column (Molecular sieve 5A, carrier gas: He) and a pulse discharge detector (PDD) is used to separate, detect and quantify Hydrogen. Recording and calculation of results is performed using a PC operated integration system (THERMO CHROM CARD A/D). Analytical procedures were calibrated daily with commercial gas standards (LINDE).

CO, CO₂, and CH₄ concentrations of extracted gas were determined using a gas chromatograph (CARLO ERBA, 8000 top). 0.1 to 1 ml of gas was injected on and separated by a 10m long packed column, passed a thermal conductivity detector to a methanizer transforming all oxidized carbon species into CH₄ subsequently quantified by a flame ionization detector. Data are recorded for both detectors by a PC based commercial integration software. Carrier gas was helium, oven temperature was 3 min isotherm 60°C, 40°/min to 120° kept for 10 min.

Samples for the determination of *carbon and hydrogen stable isotope compositions of the dissolved light hydrocarbons* were obtained by degassing the water samples with a vacuum technique (see above). Aliquots of the released gas were transferred by gas tight syringe via a septum from the degassing unit into, gastight glass vials filled with NaCl-saturated water for later on shore analysis by GC-Isotope-Ratio-Mass-Spectrometry. Afterwards the septum is sealed with silicone on the outside.

2.4.6.3 Preliminary Results

The maximum values of hydrogen and methane concentrations measured in a hydrocast (CTD 283) in the plume of the Turtle Pits field were 1278 nM and 51 nM, respectively. That hydrocast must have hit the rising zone of the plume, as the highest values are measured just 50 m above ground in a depth of 2930 m. Concentrations decrease rapidly with decreasing water depth (see fig. 2.4.6.1). Also the H_2/CH_4 ratio in the sample is nearly that of the emanating fluids with 25 in the water sample and 27 in the fluids.

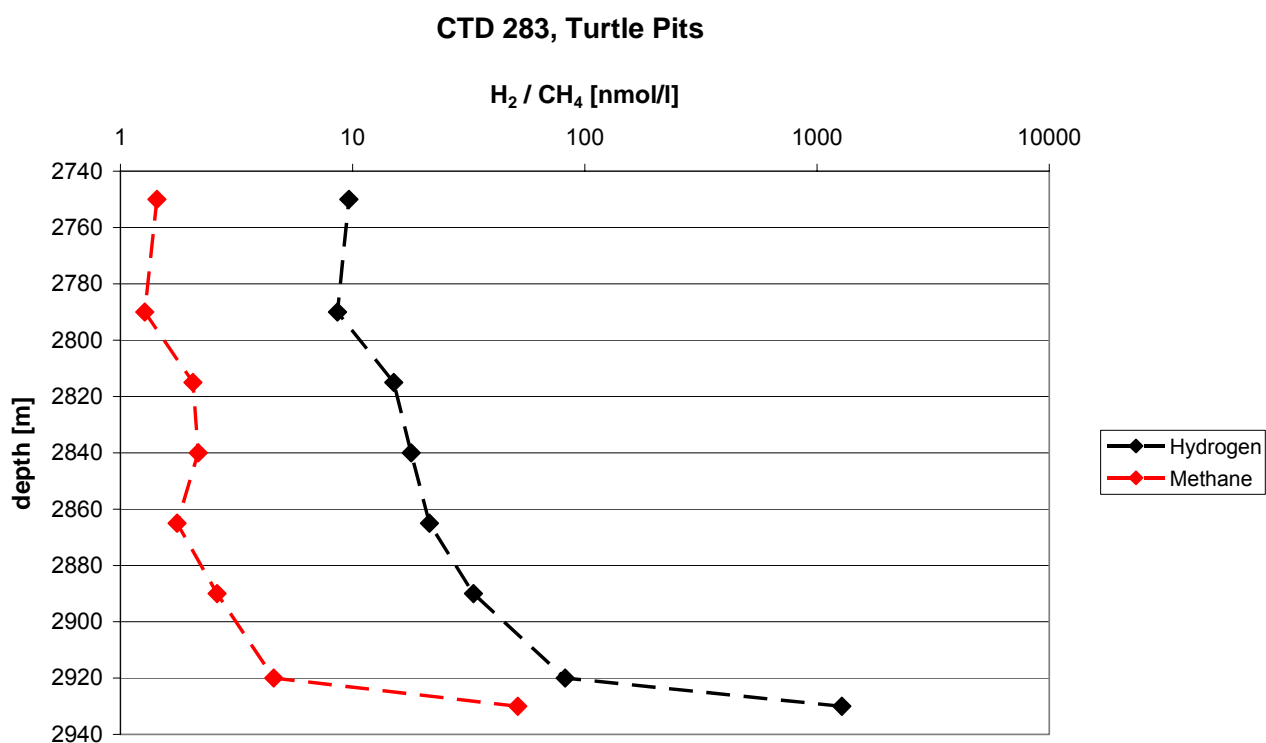


Fig. 2.4.6.1: CH_4 and H_2 concentrations at station 283 CTD

Samples obtained by the ROV directly at the fluid emanations revealed very high concentrations of dissolved hydrogen and Methane. Maximum concentrations found accounted for 0.85 mmol/l and 0.03 mmol/l of hydrogen and methane, respectively. These high values are uncommon for basaltic hosted hydrothermal systems. The resulting H_2/CH_4 ratio of about 27 is still as high as that we measured in 2008 on the “Atalante” cruise (H_2/CH_4 =26) and even exceeds those we found for fluids of the Logatchev field (see Table 2.4.6.1).

Tab. 2.4.6.1: **CH₄ and H₂ concentrations found in MOR hydrothermal fluids.**

	H ₂ [mmol/l]	CH ₄ [mmol/l]	H ₂ /CH ₄ molar ratio	ref.
<u>Atlantic</u>				
<u>Peridotitic host rocks</u>				
Rainbow 36°14'N, MAR	13, 16	2,5	5.2-6.4	1, 2
Logatchev 15°N, MAR	12	2.1	5.7	2, 13
<u>Basaltic host rocks</u>				
Broken Spur 29°N, MAR	0.43 – 1.03	0.07 – 0.13	6.6 – 7.9	3
Menez Gwen 37°17'N, MAR	0.02 – 0.05	1.35 – 2.63	0.01 – 0.02	6
TAG 26°N, MAR	0.15 – 0.37	0.12 – 0.15	1.2 – 2.47	8, 2
MARK 23°N, MAR	0.19 – 0.48	0.02 – 0.06	7.7 – 8.3	10, 11
Lucky Strike 37°17'N, MAR	0.02 – 0.07	0.0 – 0.97	0.03 – 0.07	8
Turtle Pits 04°49'S, MAR	0.85	0.03	27.3	14
Red Lion 04°47' S, MAR	0.4	0.06	6.4	14
Lilliput 09°33' S, MAR	0.003	0.08	0.03	14
<u>Pacific</u>				
Endeavour. JdF, EPR	0.16 – 0.42	1.8 – 3.4	0.1 – 0.12	12
Southern JdF, EPR	0.27 – 0.53	0.08 – 0.12	3.3 – 4.5	9
21°N EPR	0.23 – 1.7	0.06 – 0.09	3.5 – 20	4
Galapagos	0.001 – 0.004	0.1 – 0.4	0.01 – 0.03	5
1: Donval et al., 1997; 2: Charlou et al., 2002; 3: James et al., 1995; 4: Welhan & Craig, 1979; 5: Lilley et al., 1983; 6: Charlou et al., 2000; 7: Kelley et al., 2001; 8: Charlou et al., 1996; 9: Evans et al., 1988; 10: Campbell et al., 1988; 11: Jean-Baptiste et al., 1991; 12: Butterfield et al., 1994; 13: own data M60/3; 14: This work				

In the Red Lion field the H₂ concentrations (0.41 mmol/l) were stable since our last visit in 2008 (0.43 mmol/l) (see fig. 2.4.6.2). But CH₄ concentrations increased from 0.02 mmol/l in 2008 to 0.06 mmol/l, thus resulting in a lower H₂/CH₄ ratio of 6.4. Since 2006 gas concentrations of both fields increased and at least doubled. Reasons for this change are still unknown but maybe onshore analysis of the stable isotopes of methane will give further indications.

In the diffuse Lilliput field we took samples during high and low tide to determine if there is a tidal influence to the chemistry and biology of the fluids. Therefore we visited and sampled the exact fluid outlet at different times on four following days. During this time period no correlation between tidal intervals and gas concentration could be determined. For further description and other parameters measured during this experiment see section 2.4.7.2

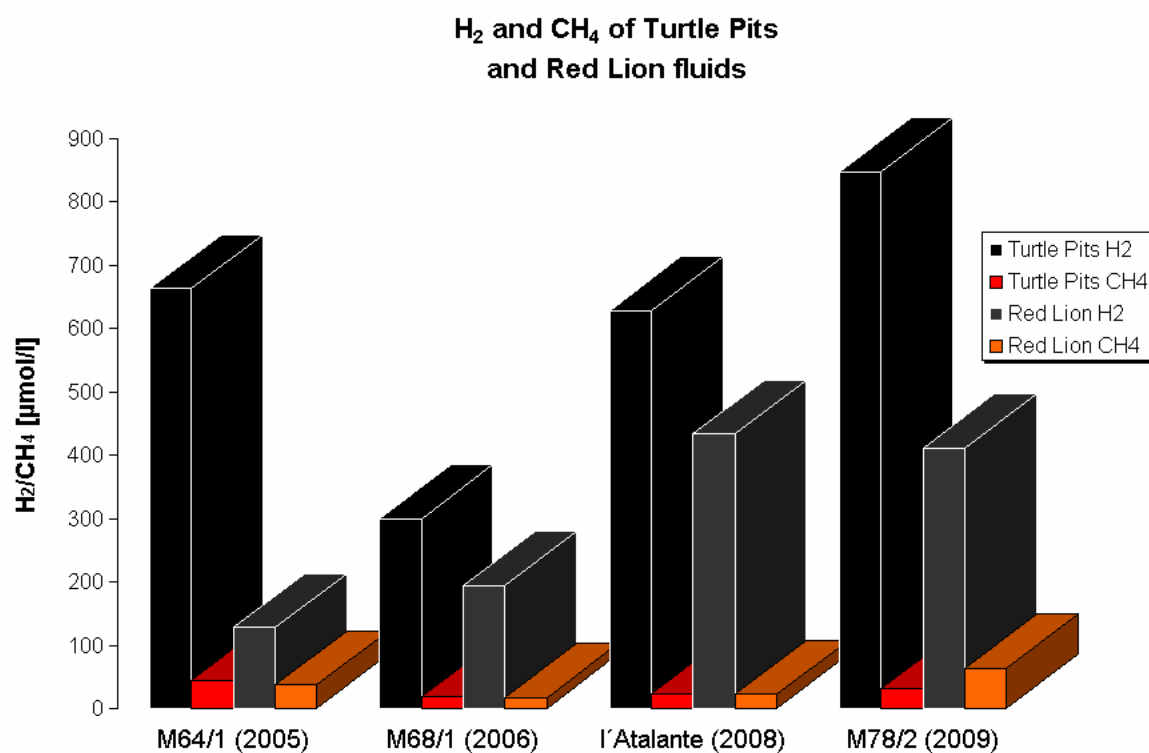


Fig. 2.4.6.2: Methane and hydrogen concentrations of Turtle Pits and Red Lion since 2005.

2.4.7 Microbial Ecology

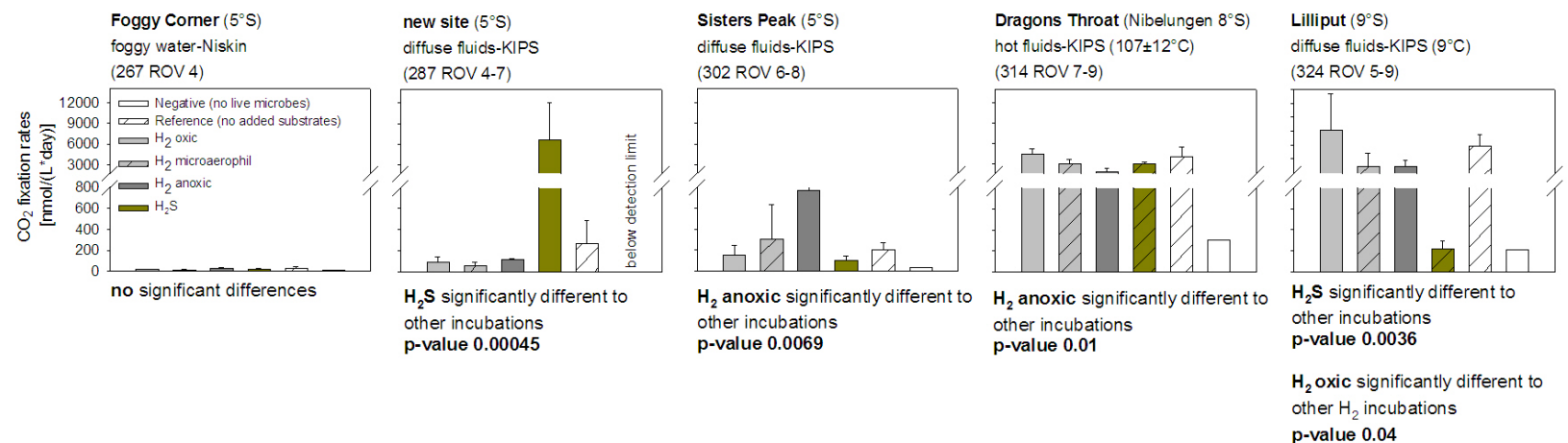
The main objective of the microbiology group during this cruise was to collect low-temperature, diffuse and hot hydrothermal fluids as well as chimney pieces from the hydrothermal fields located at 5°S, 8°S and 9°S along the Mid-Atlantic-Ridge to investigate:

- *the functioning of the microbial community, specifically focusing on microbial H_2 - and H_2S -oxidation coupled to CO_2 fixation*
- *short term temporal variability of microbial community compositions in diffuse fluids*

2.4.7.1 Microbial community composition and its functionality

(Mirjam Perner & Nicolas Rychlik)

We repeated experiments conducted on previous cruises (MSM 06/2, 06/3, 10/3) for investigating the influence of hydrogen and sulfide on microbially mediated autotrophic CO_2 fixation. Here fore, foggy water (Foggy Corner, 5°S, 267 ROV 4), low-temperature, diffuse hydrothermal fluids from the mussel patch from a new site (5°S, 287 ROV 4-7), from Sisters Peak (5°S, 302 ROV 6-8), from Lilliput (9°S, 324 ROV 5-9) and hot fluids from Dragons Throat (8°S, 314 ROV 7-9) were sampled. We supplemented the hydrothermal fluids/plume with either hydrogen (oxic, microaerophilic or anoxic conditions) or sulfide, added the inorganic radioactively labeled carbon, and incubated the liquids for 9-12 hours. Hydrogen uptake (M. Warmuth, University of Hamburg), sulfide concentrations (H. Strauss and C. Breuer, University of Münster), and incorporated amounts of inorganic carbon were determined. Some of this material was collected for microautoradiography and in situ hybridization. Also, parallels were performed for later 16S rRNA community analyses. The highest carbon incorporation rates were mostly determined for the hydrogen supplemented fluids (Fig. 2.4.6.1). However, at the newly discovered site at 5°S (287 ROV 4-7) the substrate consumption and incorporation of CO_2 was the greatest in sulfide amended fluids (Fig. 2.4.7.1). In contrast, at Lilliput hydrogen stimulated CO_2 fixation to the greatest extent and was consumed rapidly. Independent of the inorganic electron donor added to the fluids from Dragon Throat, all incubations with live microbes showed a stimulation of CO_2 fixation, suggesting that the oxidation of a yet unknown energy source, available in the fluids, must be responsible for providing the energy for CO_2 fixation.

CO₂ Fixation Rates

Consumption Rates

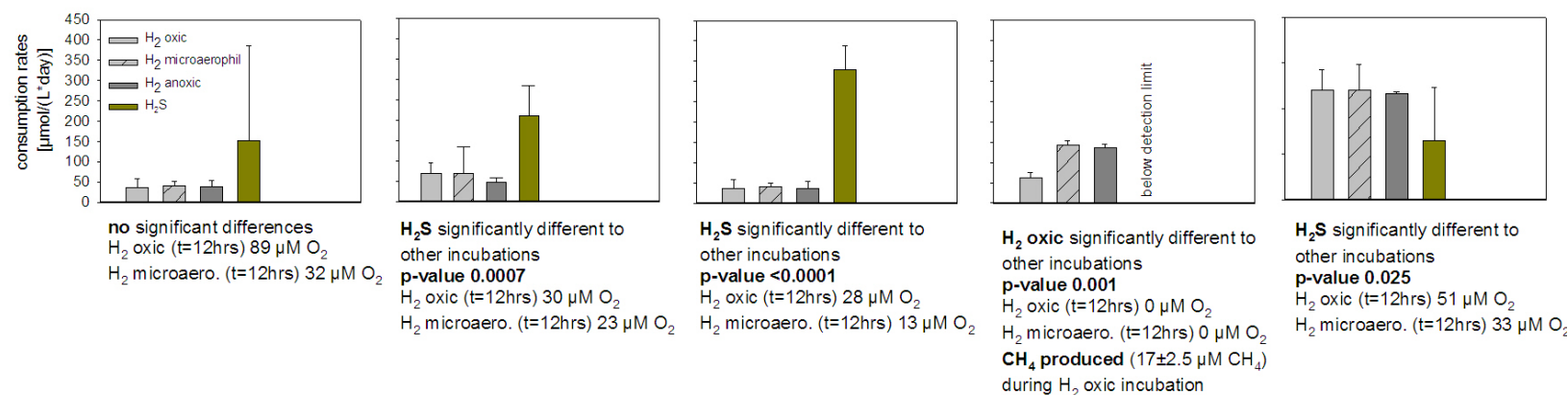


Fig. 2.4.7.1: CO₂ incorporation and consumption rates measured for the fluids without live microbes, with live microbes but without adding substrates and with amending fluids with hydrogen or sulfide. Hydrogen was measured by M. Warmuth (University of Hamburg) and sulfide concentrations were determined by C. Breuer & H. Strauss (University of Münster).

2.4.7.2 Fluid dynamics in chemistry & microbial communities in diffuse fluids

(Mirjam Perner, Dieter Garbe-Schönberg, Harald Strauss, Christian Breuer, Marco Warmuth, Sven Petersen & Christian Mertens)

We collected four diffuse fluid samples from the same spot in the mussel bed at Lilliput (9°S) over different days to investigate the influence of tidal phases on the temperature, chemistry and microbiology. Three KIPS bottles (see also section 1.4.8) were collected from the same site at tidal heights and tidal lows (fig. 2.4.7.2A). Temperature was monitored for this period of time by means of SMoni (Fig. 2.4.7.2B). Hydrogen, methane, sulfide, oxygen and pH were determined on board. Major, trace, and rare earth elements, and microbiology data will be analyzed in the home laboratory.

The temperatures recorded for the diffuse fluids reflect the sea level height (compare Fig. 2.4.7.2A and B) in that during tidal highs temperature decreases. Generally, sulfide and oxygen display the same trend: concentrations are slightly elevated during tidal lows and decreased at tidal highs (Fig. 2.4.7.3A). In contrast, hydrogen and methane concentrations do not correlate with the tidal intervals. In fact, the hydrogen decrease and methane increase (Fig. 2.4.7.3B) could be related to biological processes such as methanogenesis, by which hydrogen and carbon dioxide are microbially used as a substrate with methane as the final product. Methane isotope values determined by R. Seifert and microbiology analyses conducted in the home laboratories will reveal whether this is the case.

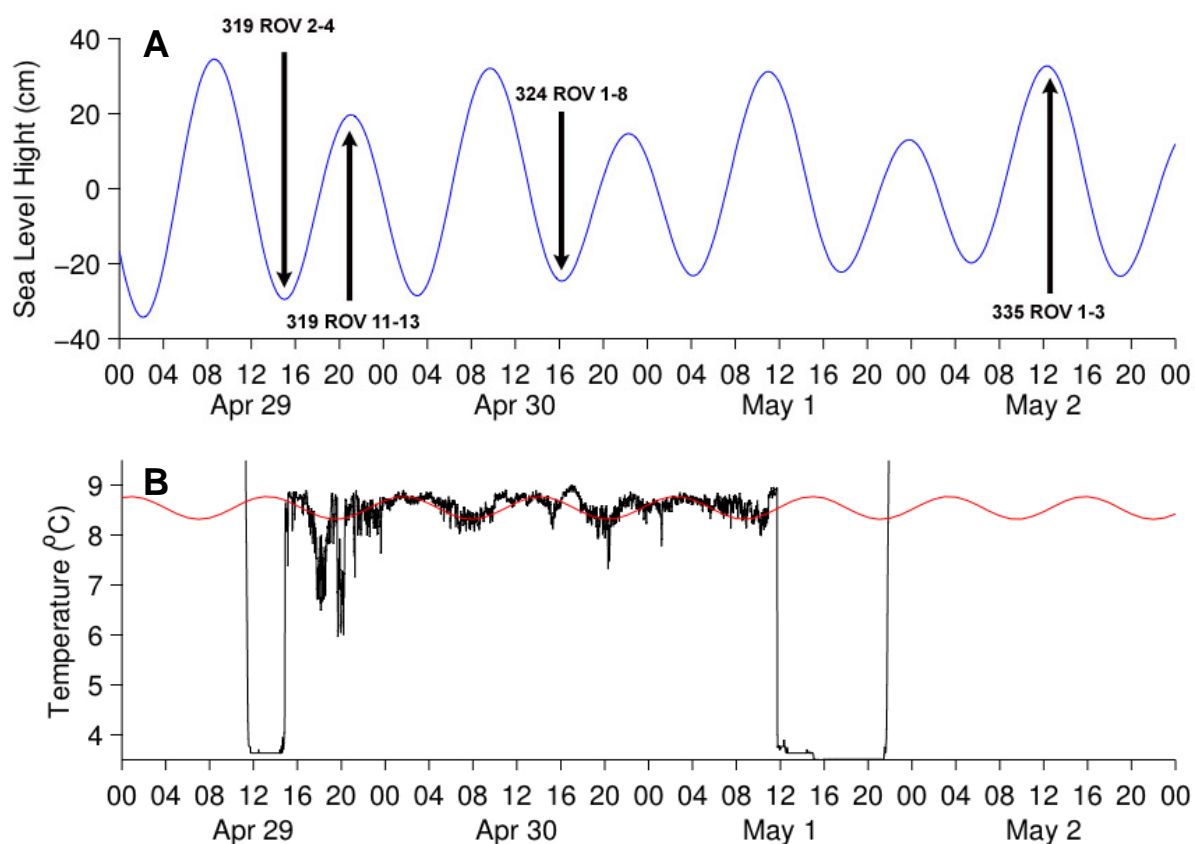


Fig. 2.4.7.2: Sampling of the diffuse fluids during different tidal heights (A) and corresponding temperature of the emanating fluids monitored during this time (B).

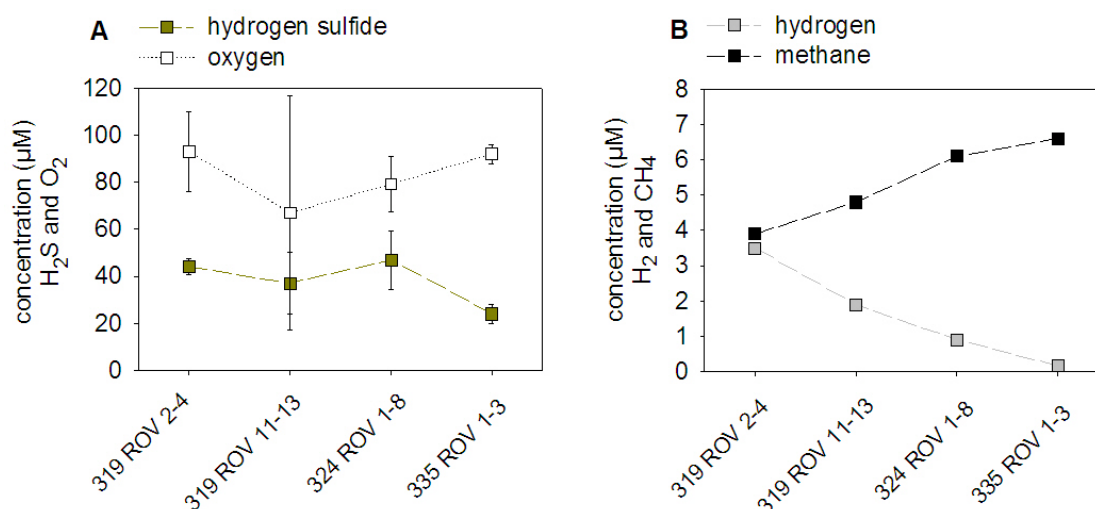


Fig. 2.4.7.3: Sulfide and oxygen (A) and hydrogen and methane (B) concentrations determined for the emanating fluids at Lilliput from the same spot at different tidal intervals.

2.4.7.3 Metal-Complexation Experiments Using Cultures

(Verena Klevenz & Mirjam Perner)

Microbial life at deep-sea hydrothermal vents is exposed to high concentrations of metals present in the venting fluids. Although some of them are biologically essential at low levels, these metals are toxic at high levels. However, toxicity of a metal for the microbes depends on its chemical speciation, as speciation determines the metal's bioavailability.

In order to study the influence of amino acids (AAs) as possible ligands for copper (Cu), with impact on the bioavailability of both (AAs constitute an energy source to microbes) and on the copper's toxicity we have designed a culture experiment: Microbes derived from diffuse fluids of Lilliput (from sample 319 ROV 6-7) were cultured along Cu gradients (from 0 to 10 µM) and with three different concentrations of a mixture of 19 proteinogenic AAs (0, 100 nM and 1 µM).

Shifts in the microbial communities will be monitored, and the concentration of labile Cu, i.e. not complexed by strong organic ligands, of total Cu and of Cu-ligands in the cultures, as well as of the vent sample the microbes are derived of, are measured by voltammetric methods (see section 2.4.5). Furthermore, the AA concentration in the fluid sample will be determined by the use of an HPLC-FD system. The total Cu concentration of the sample was determined after UV-digestion (2h) on board: [Cu] = 19 nM. The rest of the analyses will be carried out in the geochemistry lab at Jacobs University Bremen (voltammetric and HPLC analyses) and in the microbiology lab at University Hamburg (microbial communities).

2.4.8 Hydrothermal Symbioses

(Christian Borowski & Karina van der Heijden)

Metabolic pathways of the symbionts and symbiont activity patterns

One of our main goals within the SPP 1144 is to understand the interactions between hydrothermalism and biology. The vent mussel *Bathymodiolus* sp. harbors two coexisting types of symbionts in its gill tissues: chemolithoautotrophic bacteria that use reduced sulfur compounds such as sulfide as an energy source and fix CO₂ as a carbon source, and methanotrophic bacteria that use methane as both an energy and a carbon source.

In order to study symbiotic activity patterns in relation to the geochemical environment we closely coordinated the collection of symbiotic animals with sampling of diffuse fluids which will be analyzed by the fluid geochemistry groups for dissolved compounds. Mussels were collected in four locations in the 5°S hydrothermal vent area (Foggy Corner, Clueless, Desperate, Golden Valley) and in the Lilliput hydrothermal vent field at 9°S. Animals were dissected as soon as possible upon recovery and symbiont containing tissues were preserved according to the various molecular analyses including DNA and RNA analyses, Fluorescence In Situ Hybridizations (FISH), immunohistochemistry, transmission electron microscopy and analyses for stable isotopes and trace metals.

One of our ongoing projects focuses on the interaction between the composition of dissolved volatiles in the diffuse fluids and the abundances and relative compositions of the symbionts in the host tissues. In previous in situ experiments with *B. puteoserpentis* specimens in the Logatchev Hydrothermal Vent Field (LHF), a shut-off from diffuse fluid flow caused significant decrease of symbiont abundances within only a few days suggesting that abundances and distribution patterns of symbionts directly reflect the availability of reduced compounds in the fluids. With respect to this, we preserved dissected gill tissues throughout the entire gill lengths and separately for inner and outer demibranches for quantitative determinations of symbiotic biovolume and cell numbers. Later 3D FISH based on confocal laser scanning fluorescence microscopy, mRNA FISH and immunohistochemistry will allow to quantify symbionts and to reveal the patterns of their distributions and their specific activities throughout the host body. These data will be compared with quantitative analyses of 16S gene copy numbers using q-PCR and with cell counts using transmission electron microscopy. Correlation with geochemical data of the diffuse fluids at the various collection sites will reveal interaction between fluid composition and symbiotic activity. Further comparisons to similar data obtained from *B. putoserpentis* collected in the ultramafic-hosted LHF will reveal the influences of different concentrations of sulfide, methane in hydrogen in the contrasting environments.

For analyses of the metabolic pathways of the symbionts, we use FISH methods directly targeting specific functional genes (single gene FISH) or their transcription products (mRNA FISH) and immunohistochemistry methods. A problem for such analyses arises when the animals experience physiological stress due to strong decompression and temperature changes during the ascent of the ROV and long time spans between sampling in the habitat and fixation of the tissues. Changes in the transcription of genes to messenger RNA can occur within minutes, changes in the protein level within hours. We have therefore designed in situ

fixation chambers, called “DieFasts”, for fixing mussels or other biological samples directly on the seafloor within minutes of their collection (Fig. 2.4.8.1). DieFast 1 was already deployed during the MARSUED IV cruise in 2008. The ROV manipulator loads 5-10 mussels in a 3-L fixation chamber and triggers 1 to 3 100-ml syringes that inject concentrated formaldehyde solution into the chamber (end-concentrations in the chamber 1.3, 2.6 or 4%). DieFast 2 uses a saturated salt solution called “RNA Later” instead of formaldehyde and was deployed for the first time in this cruise. RNA Later rapidly penetrates into the cells, inactivates enzymes by denaturation and thereby prevents enzymatic degradation of nucleic acids and proteins

The two DieFasts fit together on the porch of the ROV, and we successfully deployed them simultaneously during dives 302 ROV (Clueless) and 319 ROV (Lilliput). In both locations, we shared out mussels from the same sampling spots to the two DieFasts and an additional batch of mussels that was fixed “conventionally” on board. Animals fixed in formaldehyde solution will later serve for FISH analyses while RNA Later fixations will allow detailed analyses studies of mRNA and enzymes. Comparative analyses of specimens fixed conventionally and in the DieFasts and will reveal the importance of in situ fixation.



Fig. 2.4.8.1: In situ fixation chambers. Left: DieFasts 1 (right) and 2 (left) sitting on the seafloor in “Clueless”. Left: Loading of mussels into a seawater-filled top chamber of DieFast 2. After closing the top lid, a trapdoor opens and the mussels slide down into the RNA Later-filled main chamber (white drum). The two-chamber design was chosen to minimize mixing of the saturated RNA Later solution with seawater during the loading with mussels.

Biogeography and population genetics of hosts and symbionts

The morphology of *Bathymodiolus* sp. specimens collected during previous cruises from the Southern MAR hydrothermal resembled *B. puteoserpentis* from the northern MAR suggesting that they most probably belong to the same species (von Cosel, pers. communication). Our preliminary phylogentic analyses based on the mitochondrial COI and ND4 genes confirmed closest relationship between *Bathymodiolus* specimens from the Wideawake vent field at 4°48' S and *B. puteoserpentis* from the Logatchev Hydrothermal Vent Field at 14°45' N. Surprisingly, specimens collected in the Lilliput vent field at 9°31' S clustered with *B. azoricus* from the Rainbow hydrothermal vent field next to the Azores. This throws new light on the possible migration pathways of *Bathymodiolus* along the Mid-

Atlantic Ridge and gives rise to the hypothesis that *Bathymodiolus* possibly colonized the northern MAR at low latitudes and has migrated bidirectional. Our collections from vent sites at 5° S and 9° S contain heterogeneous shell morphologies including specimens that resemble the oval-wedge shaped Logatchev mussels and other elongate ones that appear more similar to *B. azoricus* (not yet analysed in detail). All these findings call for a detailed study of population genetics based on multiple mitochondrial and nuclear gene loci that includes northern and southern MAR populations. This study on host population genetics will be combined with a detailed study of the biogeography of the chemolithoautotrophic and methanotrophic symbionts based on diagnostic microbial genes in order to unravel the biogeography of the *Bathymodiolus* symbiosis on the MAR. For this purpose, we sampled *Bathymodiolus* sp. from all visited diffuse vent sites including Foggy Corner, Clueless, Desperate, Golden Valley and Lilliput. Five to fifteen specimens from each diffuse vent site were dissected as soon as possible upon recovery. Symbiont containing gill tissues will serve for extractions of DNA from the hosts and their symbionts. Additional specimens were entirely frozen.

Growth patterns of Bathymodiolus

When the Lilliput vent field was discovered in April 2005 with Meteor cruise 64/1, recently settled juveniles dominated the mussel populations (Haase et al, 2005), and in 2006, 80% of all individuals were < 10 mm long (Koschinsky et al 2006). In our collections, the size frequency distribution again suggests that 90% of the population is less than one year old and that the supply with settling juveniles was continuous during the recent months (Fig. 2.4.8.2). With respect to the large amount of juveniles in Lilliput in 2005 and 2006, one would have expected to find in 2009 considerable numbers of mid-sized individuals or, in the case of high mortality of the juveniles, large amounts of empty shells. Surprisingly none of this was observed, and the question arises whether Lilliput *Bathymodiolus* grow slower than animals in other populations. We will analyze this with determinations of age and growth patterns on the basis of micro-increment measurements in the shells and compare these with similar data expected from the 5°S sites and from the LHF at 15°N.

Video explorations to the north of Lilliput revealed extended beds of exclusively juvenile mussels covering the pillow lavas, while larger individuals were not observed. This may indicate that the activity of diffuse hydrothermal venting has strongly increased in the entire area since earlier visits by SPP cruises.

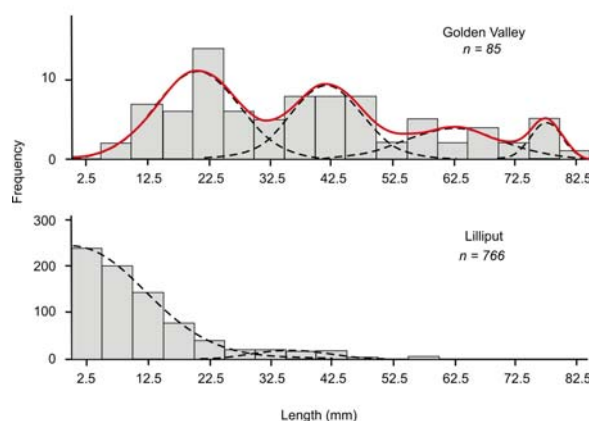


Fig. 2.4.8.2: Size frequency distributions of *Bathymodiolus* sp. in Golden Valley (5°S) and Lilliput (9°S). Modal decomposition of the size-frequency data into Gaussian components (calculated with NORMSEP) indicates several groups that have settled during recent years in Golden Valley, while the majority of Lilliput mussels is < 30 mm long and is therefore suggested to be less than one year old.

2.4.9 Volatile Organohalogens in and Over the Tropical Atlantic Ocean

(F. Laturus, S. Herrlich, R. Seifert)

2.4.9.1 Introduction

The widespread use of chloro- and chlorofluorohydrocarbons (CFCs) and other volatile organohalogens in our industrialised society cause a large annual release of these compounds into the environment. Besides atmospheric pollution, some of these compounds, for example chloroform, tri- and tetrachloroethene, also constitute a risk for drinking water resources as they can be transported to the groundwater from contaminated field sites or even from atmospheric deposition. These volatile organohalogens have been under scrutiny the recent years as they are a source for halogen radicals involved in various catalytic atmospheric reaction cycles, including the destruction of the stratospheric ozone layers. To avoid a total collapse of the protecting ozone layer against solar ultraviolet radiation, the production and consumption of man-made ozone depleting substances is now controlled by international regulations (e.g. UNEP 1987). Therefore, identification and quantification of sources and sinks are a topic of particular interest. In line with the industrial emissions, also a natural emissions of volatile organohalogen compounds has been identified and several marine and terrestrial sources of volatile organohalogens were discovered (e.g. Khalil et al. 1999, Laturus 2001, Laturus et al. 2002). Extrapolations of global emissions of volatile organohalogens from natural sources into the atmosphere revealed sources strengths comparable to the industrial input (e.g. McCulloch et al. 1999, Keene et al. 1999). For the terrestrial environment several natural sources, such as wetlands, peatlands, salt marshes, rice fields, soil, forests, volcanos have been found to release mainly chlorinated compounds (e.g. Isidorov et al. 1990, Goodwin et al. 1995, Redeker et al. 2000, Yokouchi et al. 2002/2007, Laturus 2001, Laturus et al. 2002, Rhew et al. 2002, Scheeren et al. 2003, Manley et al. 2007, Gebhardt et al. 2008). The emission of volatile organobromine and organoiodine compounds from natural terrestrial sources apparently is negligible. Although the terrestrial environment is only 29% of Earth's surface, it is an important major contributor to the occurrence of chloroform and other volatile reactive chlorine-containing compounds in the environment. In the marine environment, the oceans are major sources for volatile organohalogens released into the atmosphere, the origin of these compounds inside the oceans is not yet fully explored. At present, marine macroalgae and microalgae have been identified as a producer of volatile organohalogens. However, they are responsible for only 0.7 to 16% of the annually total released amounts of volatile organohalogens emitted from the oceans. Thus, other so far unknown sources must still exist to balance the global halogen budget.

The aim of this study was to measure the concentrations of volatile organohalogens in air and surface water along a transect from the coast of Guyanna to the Middle Atlantic Ridge to the coast of Brazil. Therefore, possible coastal impacts on volatile organohalogen concentrations may be determined. In a second part of the study, hydrothermal vents in the Middle Atlantic Ridge have been investigated as a possible source for volatile organohalogens.

2.4.9.2 Volatile Organohalogenes in air and surface water of the Middle Atlantic

The sampling along the transect started after leaving the exclusive economic zone (EEZ) of Guyana at 10° 13.07' N, 56° 38.16' W. The transect ended with entering the EEZ of Brazil at 17° 11.81' S, 27° 48.14' W. Figure x1 shows the sampled transect, which consisted of a total of 56 sampling points. The first part of the transect until 2° 16.98' N, 35° 42.32' W went parallel to the coast of Northern Brazil to investigate possible influence of the terrestrial environment on the concentration of volatile halocarbon in air and surface water.

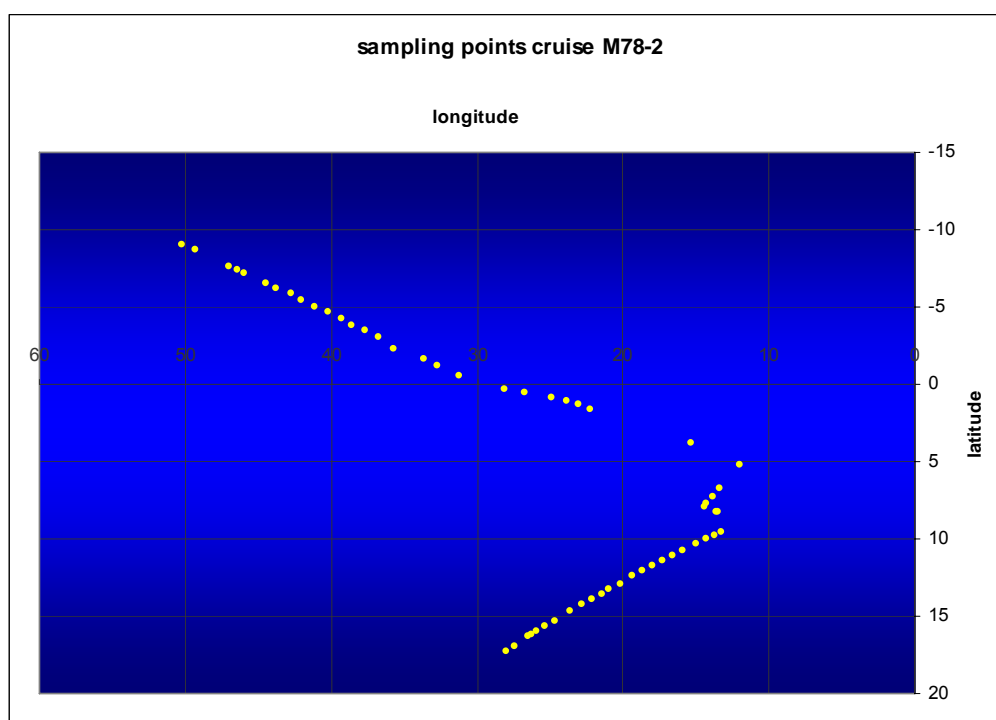


Fig. 2.4.9.1: Sampling points on cruise M78-2 for the determination of volatile organohalogenes in air and surface water of the equatorial atlantic ocean.

At every sampling point of the transect an air sample, a surface water sample and a sample for chlorofyll a was taken. Air and water samples have been analyzed directly after sampling by purge-and-trap gas chromatographie with dry electrolytic conductivity detection (p&t-GC-DELCD). The volatile organohalogenes identified were methyl chloride (CH_3Cl), methyl bromide (CH_3Br), dichloromethane (CH_2Cl_2), tetrachloromethane (CCl_4), trichloromethane (C_2HCl_3), bromodichloromethane (CHBrCl_2), tetrachloroethene (C_2Cl_4), bromoform (CHBr_3), and 1,2-dibromoethane (1,2-EtBr₂). Chlorophyll concentrations will be determined in the home laboratory first. The average concentrations in air determined for CH_3Cl , CH_3Br and CH_2Cl_2 were 37.3 pmol L⁻¹, 7.29 pmol L⁻¹, 0.37 pmol L⁻¹, respectively. Comparison of the average air concentration between the sampling transect close to the coast and the sampling transect in the Middle of the Atlantic Ocean revealed slightly higher average concentrations for the area with coastal influence (Table 2.4.9.1). Especially for CH_2Cl_2 a coastal influence on air concentration is visible.

Table 2.4.9.1: Mean concentrations of selected volatile organohalogens in the sampling area closed to the Northern Brazilian coast and the open Atlantic Ocean. The open ocean was defined starting from 2° 6.99'N, 35° 42.32'W.

	CH ₃ Cl	CH ₃ Br	CH ₂ Cl ₂
	[pmol L ⁻¹]		
mean concentration air			
- coastal influence	37.8	7.81	0.70
- open ocean	36.5	7.05	0.25
mean concentration surface water			
- coastal influence	126.1	2.88	43.2
- open ocean	136.1	2.30	25.3

In surface water, the average concentration of the three volatile organohalogens were 136.6 pmol L⁻¹, 2.47 pmol L⁻¹, 30.6 pmol L⁻¹, respectively. The detected concentrations were well in the same range than previous measured concentrations in the marine environment (see Koppmann et al. 1993, Khalil et al. 1999). Compared to their occurrence in ambient air, the concentrations of CH₃Cl and CH₂Cl₂, respectively, in surface water showed around 4 and 82 times, respectively, higher concentrations while CH₃Br revealed an almost three times lower occurrence in the surface water. Furthermore, the concentrations of CH₃Cl and CH₃Br were higher in the coastal influenced air mass of the sampling transect (Table 2.4.9.1). Similar results have been found for surface water except for CH₃Cl, which showed higher concentration in the open ocean area (Table 2.4.9.1).

Table 2.4.9.2: Correlation between the concentrations of chloromethane, bromomethane and dichloromethane in air and surface seawater.

	CH ₃ Cl		CH ₃ Br		CH ₂ Cl ₂	
	air	sea	air	sea	air	sea
CH ₃ Cl						
air		0.158	0.558		0.197	
sea				0.510		0.112
CH ₃ Br						
air				0.213	0.590	
sea						0.506
CH ₂ Cl ₂						
air						0.344
sea						

Correlation of the concentration of CH₃Cl, CH₃Br and CH₂Cl₂ are given in Table 2.4.9.2. A high correlation coefficient *r* for a pair of compounds is a first indication for possible similar sources. The first interesting results was an obviously non-correlation between the surface water and air concentrations of all three compounds evaluated. Apparently, the concentrations in air and surface water are not directly related to each other through simple exchange processes. On the other side, the concentrations of CH₃Cl and CH₃Br in air and surface water, respectively, showed a slight correlation indicating that either their sources or their formation/degradation are related to each other. In literature, for example a similar formation pathway for CH₃Cl and CH₃Br through a methyl transferase is discussed (*e.g.* Wousmaa and Hager 1990) suggesting similar natural sources for both compounds. Whether or not the origin of both compounds is natural or anthropogenic can not be answered at present. To answer this question, we took samples to investigate the carbon isotope composition of the

volatile organohalogens. However, the results are not yet available. Interesting is that between the concentrations of CH_3Br and CH_2Cl_2 in air and surface water a slight correlation have been found too, while a correlation is missing between the concentrations of CH_3Cl and CH_2Cl_2 . This is surprising as so far no similar formation mechanisms have been reported for CH_3Br and CH_2Cl_2 . At present, an answer for these findings can not be given.

Other volatile organohalogens, such as CCl_4 , C_2HCl_3 , CHBrCl_2 , CHBr_3 and 1,2-EtBr₂, determined during this study have not yet been evaluated.

2.4.9.3 Release of volatile organohalogens by hydrothermal vents of the Middle Atlantic Ridge

Investigation of fluid samples directly sampled by an a pumped flow-through system (Kiel Pumping System "KIPS", for details refer to Garbe-Schönberg et al 2006) mounted on a remote operating vehicle (ROV Kiel6000, IfM-GEOMAR). The samples were collected from the KIPS directly after the ROV has emerged from the sea and was fixed on the deck of the research vessel. The samples were filled without headspace in 120mL glass bottles closed with aluminium locks with PTFE covered rubber septum. The samples were stored in a refrigerator until analysis. Determination of volatile organohalogens was achieved within 4 hours after sampling by p&t-GC-DELCD. The volatile organohalogens identified were CH_3Cl , CH_3Br , CH_2Cl_2 , CCl_4 , C_2HCl_3 , CHBrCl_2 , C_2Cl_4 , CHBr_3 and 1,2-EtBr₂. The concentrations of CH_3Cl , CH_3Br , CH_2Cl_2 determined in the fluids are given in Table 2.4.9.3. CCl_4 , C_2HCl_3 , CHBrCl_2 , CHBr_3 and 1,2-EtBr₂ have not yet been evaluated.

Table 2.4.9.3: Release of selected volatile organohalogens by hydrothermal vents of the Middle Atlantic ridge. The results are corrected to 100% fluid.

vent field	type	fluid [%]	sample name	CH_3Cl	CH_3Br [nmol L ⁻¹]	CH_2Cl_2
Red Lion						
- Mephisto	hot	79.1	297 ROV	2.06	54.4	0.21
Comfortless Cove						
- Sisters Peak	hot	8.3	302 ROV MA.	21.70	5.46	54.10
- Sisters Peak	hot	62.8	308 ROV 4	5.07	32.80	0.32
- Sisters Peak	diffuse	6.1	302 ROV 2	0.90	1.62	0.25
- Golden Valley	diffuse	0	287 ROV 1	-	-	-
-unknown	diffuse	0.9	287 ROV 9	6.37	42.0	5.16
Turtle Pits						
- One Boat	hot	74.1	281 ROV 1	2.52	0.06	22.10
Nibelungen						
-Drachenschlund	hot	87.0	314 ROV 2/5	3.87/3.28	0.30/0.17	0.60/0.35
Lilliput	diffuse	51.6	319 ROV 6	1.73	0	0.016

The results showed a high input of volatile organohalogens from fluid released from hydrothermal vents into seawater. The concentration for CH_3Cl , CH_3Br and CH_2Cl_2 found in the fluid were between 0.117 and 54.4 nmol L⁻¹, and well above the concentration of the surrounding seawater (0.02 pmol L⁻¹ for CH_3Cl , 0 pmol L⁻¹ for CH_3Br , 0.003 pmol L⁻¹ for CH_2Cl_2). The impact of hydrothermal vents on the concentration of volatile organohalogens were visible through the depths profiles taken above different hydrothermal vents (Figure x2). At the example of CH_3Cl a decrease in the seawater concentration has been found from the surface water down to deep seawater. Close to the hydrothermal vents the CH_3Cl concentrations increased again. The other compounds investigated showed similar distribution.

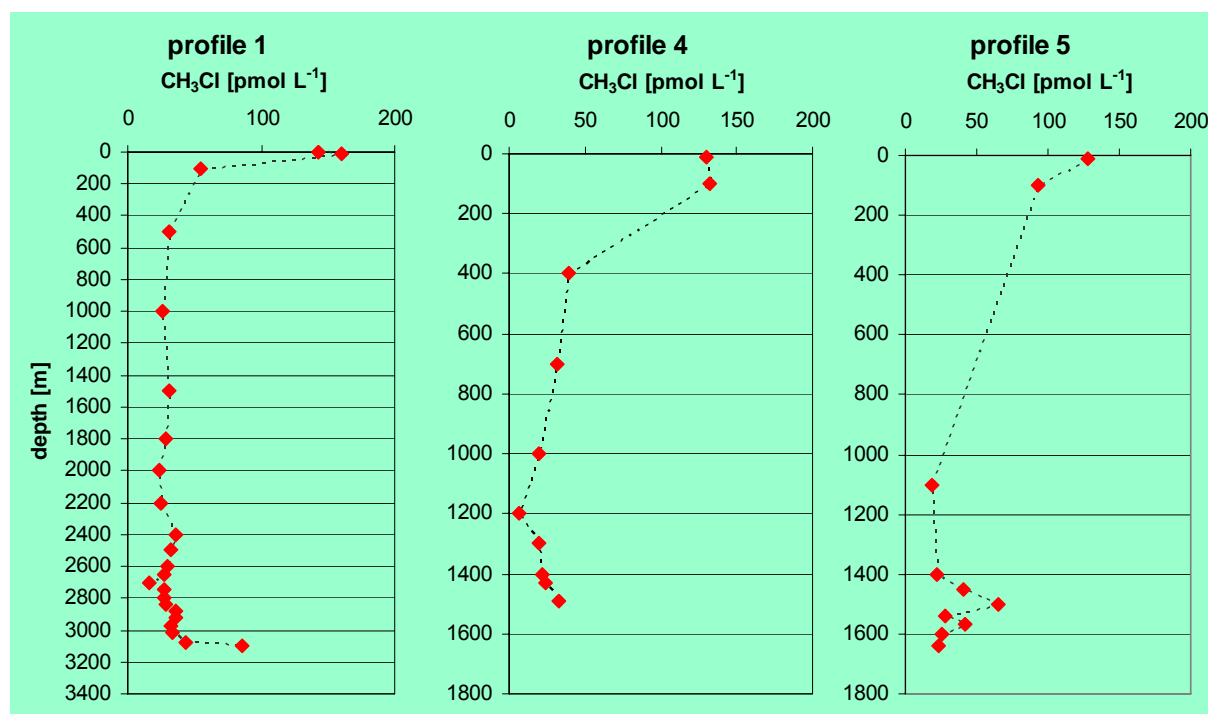


Fig. 2.4.9.2: Depth profiles of CH_3Cl concentrations in the water column at Sisters peak (profile 1, n=23), Nibelungen (profile 4, n=10) and Lilliput (profile 5, n=10).

The sources strength of hydrothermal vents regarding their contribution to the global occurrence of volatile organohalogenes still needs to be estimated. However, it is obviously that a novel and important sources for volatile organohalogenes has been found, which may close the gap between the determined concentrations of volatile organohalogenes in the marine environment and the input by biogenic sources so far identified, such as micro- and macroalgae.

2.4.9.4 Conclusion

Natural sources have been found to be significant contributors to the environmental input of volatile organohalogenes. However, compared to industrial sources, natural sources can hardly be controlled. Thus, it is important to complete the picture of natural sources contributing to the environmental input of volatile organohalogenes. It has been shown that changes of abiotic factors, such as nutrient concentration, temperature, salinity, ultraviolet radiation, can alter the release of volatile organohalogenes by natural sources. Therefore, human influences on the environment resulting in uncontrolled eutrophication or further global warming can change the emission of volatile organohalogenes by natural sources. For example, the investigations of marine macroalgae showed evidence for a significant increase in the release of these substances when the macroalgae are exposed to elevated levels of ultraviolet radiation. Therefore, increasing emission of volatile organohalogenes may be expected in future from natural marine and terrestrial sources, when ultraviolet radiation levels reaching the Earth's surface still elevates due to a weakening stratospheric ozone layer. This would alter the global atmospheric input and in turn the stratospheric ozone chemistry, and has to be considered when predicting future scenarios in global climate changes.

2.4.10 Temperature Measurements of Hydrothermal Fluids

(D. Garbe-Schönberg)

The mafic-hosted hydrothermal system at 5° S MAR hosts, at present, black smokers venting the hottest fluids ever recorded on the seafloor (Koschinsky et al., 2008). In the southern part of the system at Turtle Pits and Comfortless Cove hydrothermal fluids with lower salinity than seawater originate from a vapor phase after “supercritical” brine condensation and phase-separation. Since discovery of the system in 2005 a constant fluid temperature of ~407 °C has been recorded during the previous cruises. This temperature corresponds to a water depth of 3000m and marks the critical point terminating the boiling curve of seawater. Consequently, all reactions in the sub-seafloor hydrothermal system occur entirely at p,T conditions above the critical curve of seawater. Moreover, short high-temperature pulses >425 °C and a highly variable chemical fluid composition have been identified at these vents. On the other hand, lower temperatures of ~360 °C being too low for phase separation processes characterize the northern part of the hydrothermal system at Red Lion. Main objective for this cruise was the unambiguous reconfirmation of the high temperatures and transient temperature pulses using dedicated sensor and data transfer technology (see Methods in the Appendix). This data will provide the basis for estimates of heat flow of the entire system and a new understanding of the evolution of high-pressure hydrothermal systems in slow-spreading crust. At Nibelungen/Drachenschlund near 8°55 S a new type of hydrothermal activity in an off-axis position had been discovered but could not be sampled (Melchert et al., 2008). Objective for this cruise was the first sampling and in-situ temperature measurement of the hot fluids from ultramafic host rocks. Besides this, temperature being one parameter for the characterisation of the habitat of biological communities in musselfields was to be measured in diffuse fluids.

2.4.10.1 Hot Fluids from Black Smokers

Turtle Pits – One Boat. During station 281 ROV at the Turtle Pits hydrothermal field all black smoker chimneys - Two Boats, Southern Tower, and One Boat - were surveyed for changes in appearance and activity since our last visits, and for accessibility of orifices. All chimneys were found to be as highly active as in the previous years, venting fluids and black smoke vigorously, but from few small outlets only. Black smoke distributed by bottom currents and accessibility of orifices for the ROV, however, limited sampling to the One Boat chimney. A small orifice in the top region of the ~7m tall chimney was measured and sampled with 2 Major's samplers. The temperature-versus-time plot over seven minutes (Fig. 2, Appendix 2.8) illustrates the challenge to keep the temperature sensor within the fluid. Temperatures change very rapidly during different trials with the ROV'S manipulator to bring the T-probe into the cm-sized fluid outlet with maximum temperature. The maximum temperature recorded was 426 °C, the average temperature was 407 ± 2 °C over a time interval of two minutes (Table 2.4.10.1). These temperatures compare well to temperatures recorded in 2008 and 2006 (Koschinsky et al., 2008).

There is a remarkable difference in the temperature readings from the two sensor types built into the T-probe that has only been observed at the high-temperature vents of Turtle Pits and Comfortless Cove: When the T-probe's temperature rises very rapidly from low to high

temperature, and vice versa, the NTC sensor rises to higher and lower temperatures, respectively, than the simultaneously measuring Pt-1000 sensor. Moreover, the temperature readings from the NTC sensor appear to be more “fine-structured” than readings from the Pt-1000 sensor, with the latter having the appearance of an averaged, smoothed data record.

Table 2.4.10.1: Measured temperatures of hot hydrothermal fluids venting from black smokers

Area	Site	2008	2009	2009	Fluid sample No.
		T_{max} (°C)	T_{max} (°C)	T_{avg} (°C)	
Turtle Pits	One Boat	451 ¹	426	407 ± 2	281 ROV-1/-2
Comfortless Cove	Sisters Peak	(379)	(375) ²		308 ROV-2/-8
Red Lion	Mephisto	364	358	353 ± 2	297 ROV-2/-7
Nibelungen	Drachenschlund	(192) ³	372	371.6 ± 0.1	314 ROV-1/-9

¹ Two Boats was sampled in 2008; ² No temperature logging for this site, NTC on-line data only. ³ Sampled in 2006, in mixing zone. – Note: Numbers in brackets certainly do not reflect maximum temperatures of undiluted hydrothermal fluid

It is hypothesized that the NTC sensor has a faster response (i.e., reaction time after a temperature change) than the Pt-1000 sensor and, hence, is able to record also very short, transient high-temperature pulses that cannot be “seen” by the Pt-1000 sensor. These pulses probably originate from immiscible ultra-hot fluids (superheated fluid?) ascending with the “normal” 407 °C fluid. This compares to our observation that fluids with different chemical composition vent from the same chimney within short time intervals (Schmidt et al., subm.).

Red Lion – Mephisto. With station 297 ROV all four chimneys at the Red Lion site - Tannenbaum, Shrimp Farm, Sugarhead, Mephisto – were surveyed in the same way as described above before sampling started in the top region of the Mephisto black smoker. Our sampling point was almost the same as in 2008. The maximum temperature measured was 358 °C comparing to 364 °C recorded in 2008 (Tab. 2.4.10.1). The temperature plot (Fig. 2, Appendix 2.8) shows highly variable and unstable temperatures. This indicates that nozzle and temperature probe were not perfectly located within hot venting fluid and, probably, the true maximum temperature of the fluid has been missed.

Comfortless Cove – Sisters Peak. Fluid outlets in the top region of the Sisters Peak chimney appeared to be extremely difficult to reach with the ROV'S manipulator during station 308 ROV. Finally, a small orifice could be sampled and measured. The fact that no clear hydrothermal fluid but only black smoke could be observed at this outlet is also reflected in relatively low maximum fluid temperatures of 375°C. It can be assumed that maximum temperatures of clear undiluted hydrothermal fluid from this chimney would be significantly higher, comparable to the 407 °C as measured at Turtle Pits. Unfortunately, measured temperatures during the dive have been noticed in the protocol as on-line readings only but have mistakenly not been logged.

Nibelungen – Drachenschlund. For the first time, undiluted hydrothermal fluid from the vent Drachenschlund at 8°55 S could be sampled and measured in-situ. Details of the special technical set-up for KIPS and ROV operation at this station 314 ROV are given in the methods section in the Appendix. At Drachenschlund hydrothermal fluids are venting directly from the seafloor without building chimney structures from precipitating sulfides. Scanning the T-probe across the orifice revealed extremely homogenous fluid temperatures indicating

that fluids must leave the orifice with a very high flow rate across a diameter of approx 30 cm. During KIPS fluid sampling the in-situ fluid temperature was measured to 371.6 ± 0.1 °C over a time interval of 20 minutes. Later, samples were taken for microbial diversity studies in a mixing zone between fluid and seawater at 107 ± 12 °C (Fig. 2, Appendix 2.8)

2.4.10.2 Diffuse Fluids in Mussel Fields

Comfortless Cove – Foggy Corner. During stations 267 ROV and 287 ROV diffuse fluids were sampled at Foggy Corner for microbial gene expression studies. Warm “shimmering” water with high turbidity and bacterial flocks was venting from cracks between pillow lava at this site. The nozzle and T-probe were held too high above the fluid outlet, thus yielding temperatures of only 3-3.5 °C during station 267 ROV (Fig. 3, Appendix 2.8), but re-sampling during station 287 ROV was at 7-8 °C (Table 2.4.10.2).

Table 2.4.10.2: Measured temperatures of diffuse hydrothermal fluids in mussel fields

Area	Site	2008	2009	Fluid sample No.
		T_{max} (°C)	T_{max} (°C)	
Comfortless Cove	Foggy Corner	9	8.2	267 ROV-2/-4 287 ROV-1/-10
	Clueless, Desperate	10.0 ¹	13.6	302 ROV-5/-8
	Sisters Peak	-	16.2	302 ROV-9/-13
				319 ROV-2/-14
Liliput	Liliput Main	6.5	10.6	324 ROV-1/-9
				329 ROV-1/-3
				335 ROV-1/-4

¹ Clueless sampled in 2008 (cruise ATA-2)

Comfortless Cove – Clueless/Desperate. The Clueless mussel fields were investigated during dive 302 ROV. A small pond with a distinct active flow of warm hydrothermal fluids was sampled at a very constant temperature of 12.9 ± 0.2 °C.

Comfortless Cove – Sisters Peak. A small mussel patch within a few meters distance from the Sisters peak black smoker chimney was sampled for the first time, the logged fluid temperature varied between 10 and 16 °C (station 302 ROV).

Liliput – Main site. At the Liliput Main musselfields a dedicated experiment was performed by re-sampling diffuse fluids during both high tide and low tide with stations 319 ROV (low and high tide 1), 324 ROV (low tide 2, no temperature logging), and 335 ROV (high tide 2). A significant correlation of fluid temperature with the tide cycle has been recorded by means of the SMoni autonomous temperature logger (for details see section 2.4.7.2). Sampling temperatures during the four stations were 9.74 ± 0.03 °C (Low Tide 1), 8.3 ± 1.6 °C (High Tide 1), 9.7 °C (Low Tide 2, no logging), and 9.75 ± 0.05 °C (High Tide 2) (Fig. 4, Appendix 2.8).

2.4.11 Bathymetry

(Sven Petersen, Pablo Rodriguez & Carsten Schirnack)

Multibeam mapping was carried out with the Kongsberg Simrad EM120 multibeam system. The main objective was to obtain a detailed bathymetry of the Turtle Pits area as well as of the Inside Corner High, Nibelungen, and Lilliput areas. Additionally long stretches of the transits from and to the working area have been logged. In total 460 nautical miles of lines have been mapped in the working areas during M78/2. The echo sounder system consists of 2 transmitter/receiver units coupled with a Motion Reference Unit installed on RV Meteor. System settings of 12 kHz, 2 x 45° opening angle and 191 beams per ping allowed a swath width of about 6500 m at 3000 m water depth corresponding to a theoretically resolution of ~30 x 30 m. Ship's speed was set to 8 knots during surveys.

Data acquisition has been done with the software SIS[®] by Kongsberg. General data editing and data post processing was performed on board using the software Neptune[®], also provided by Kongsberg as well as with the open source software MB-System (vers. 5.1.1; Caress and Chayes, 2008) and Generic Mapping Tools (GMT; Wessel and Smith, 2009). Selected maps are shown in Figures 2.4.11.1 to 2.4.11.4. Backscatter information is also available and will be combined with bathymetric data after the cruise. The resolution of a bathymetric measurement on the seafloor is determined by the covered swath width, the number of available beams, ship speed, and the physical resolution which equals mainly the footprint size of a single beam (i.e. in 3000 m water depth ~ 30 m in across- and along-track directions at 1° single beam angle). Beams within one footprint area do not resolve separate seafloor features, and the potential for increasing resolution by narrowing the swath width is therefore limited. In order to increase the resolution we choose a 0.5 nm line spacing for the Turtle Pits and Lilliput working areas, resulting in a multifold overlap of the surveyed area. We kept a line spacing of 1 nm for the Inside Corner High and 1.5 nm for the Nibelungen area. The final grid resolution was chosen to be between 10 and 50 m, depending on data coverage of the respective area. Detailed maps were prepared, mainly as pre-dive information for ROV-dives and proofed to be very helpful in areas of no detailed information.

During transit from Trinidad/Tobago, Ascension, and towards Rio de Janeiro bathymetric data was collected during parts of the transit. Ship's speed during these transits varies between 10 and 13 knots.

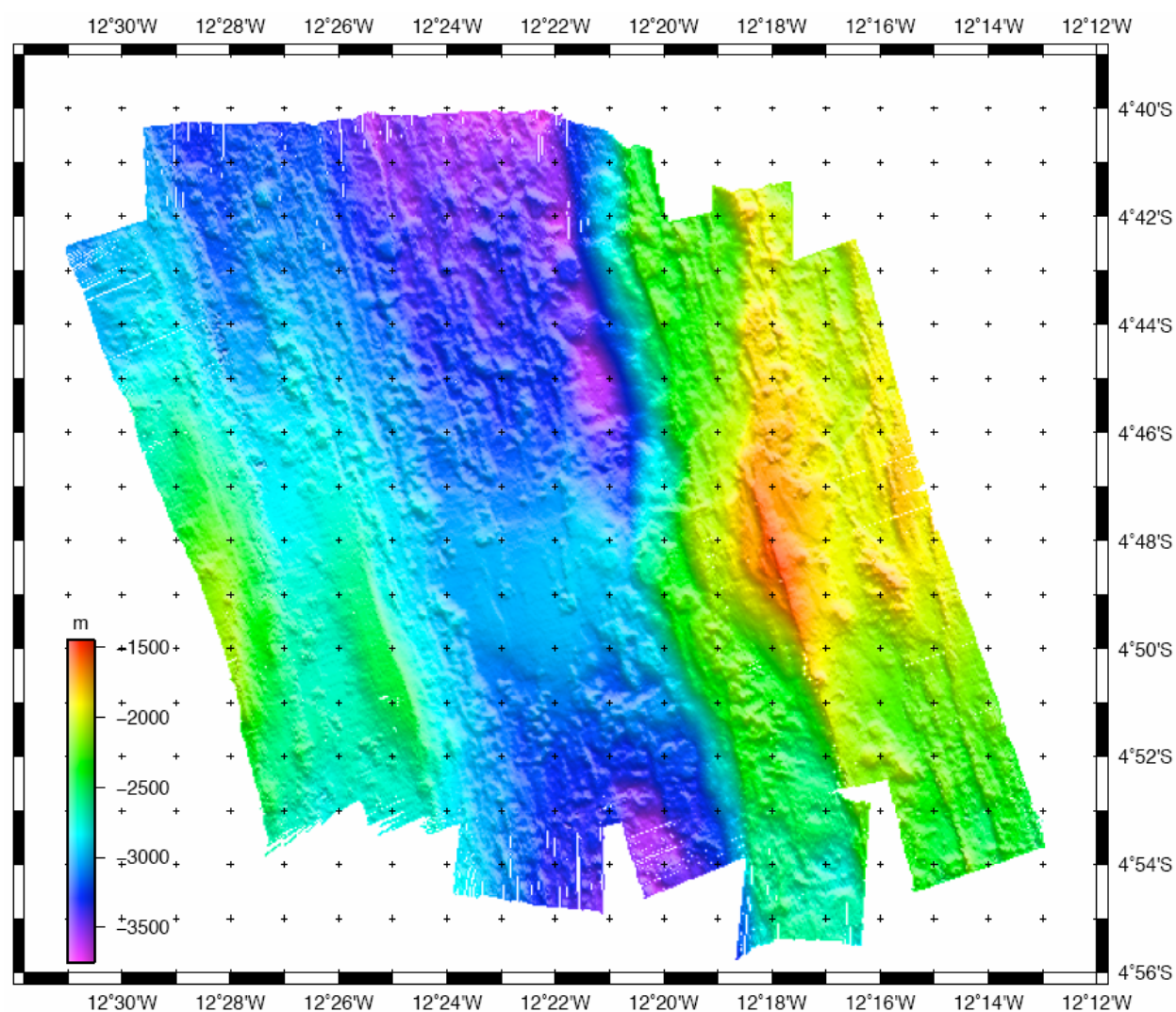


Fig. 2.4.11.1: Bathymetric map of the Turtle Pits area. The map was obtained by profiling 157 nm with, mainly, a line spacing of 0.5 nm (stations 273MB, 293MB, and 309MB). The underlying grid cell size is 30 m.

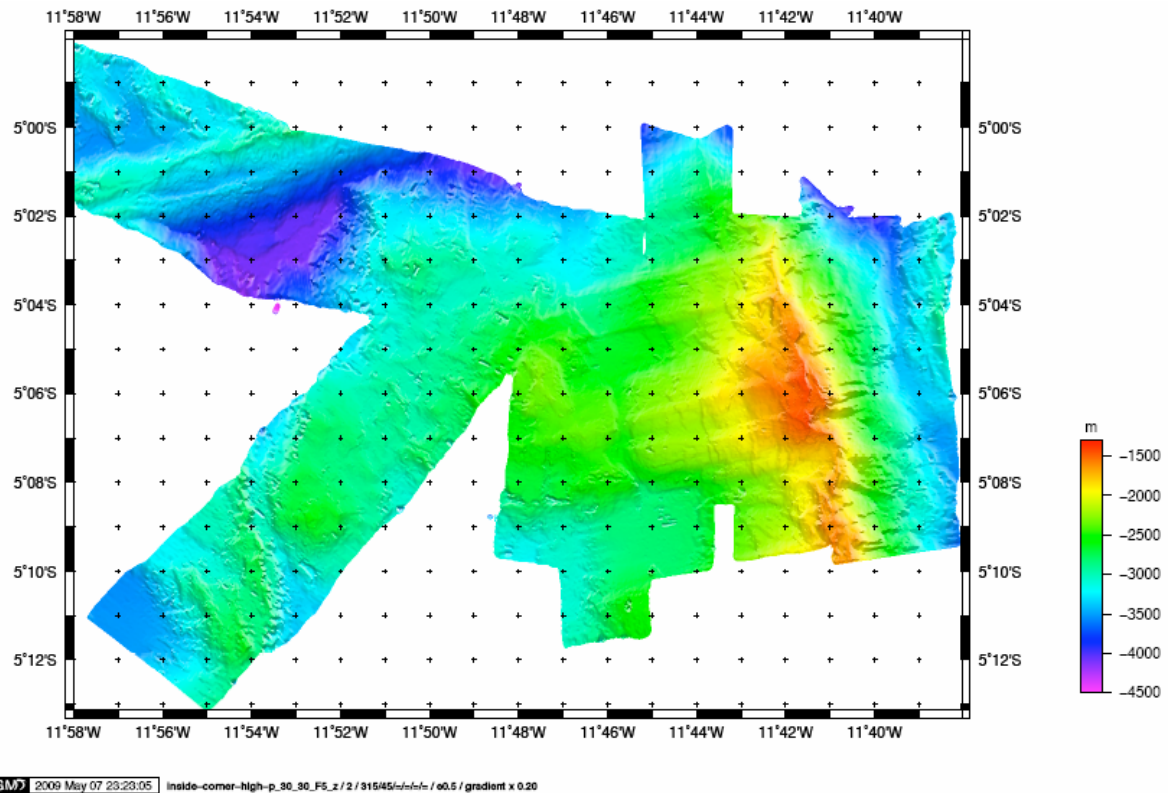


Fig. 2.4.11.2: Bathymetric map of the Inside Corner High. The map was obtained by profiling 57 nm with a line spacing of 1 nm (station 311MB). The underlying grid cell size is 30 m. Included into this image are parts of the transit to and from the working area.

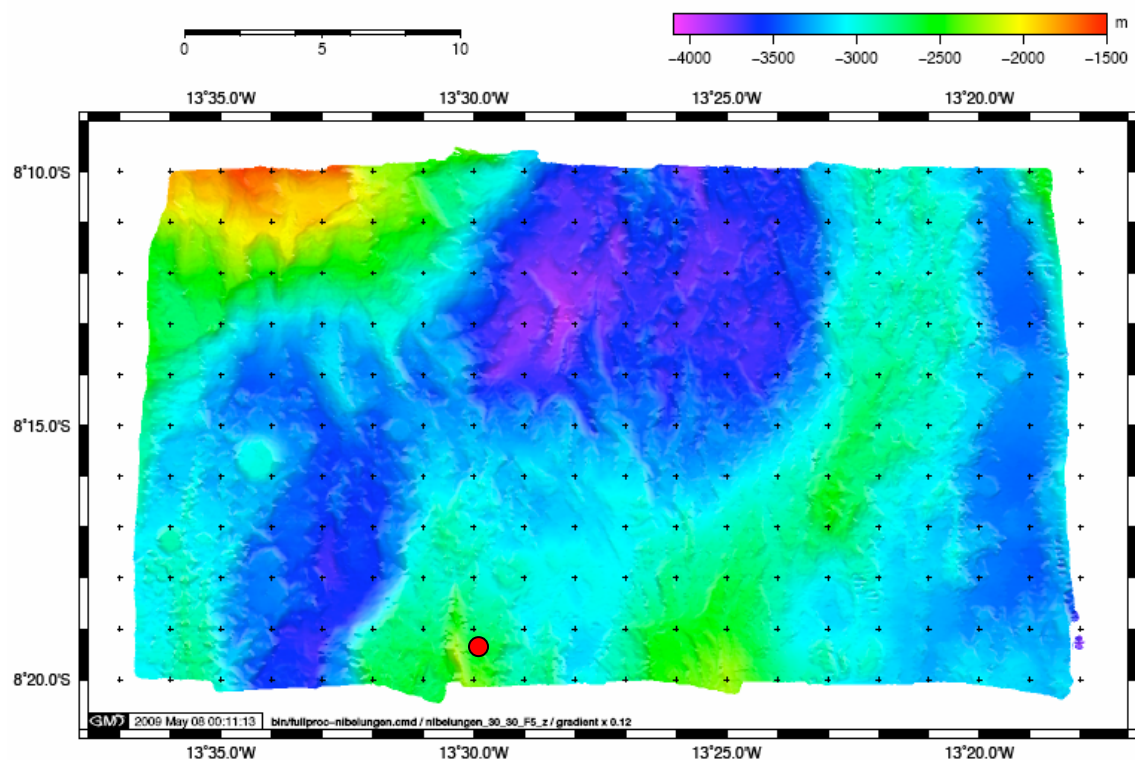
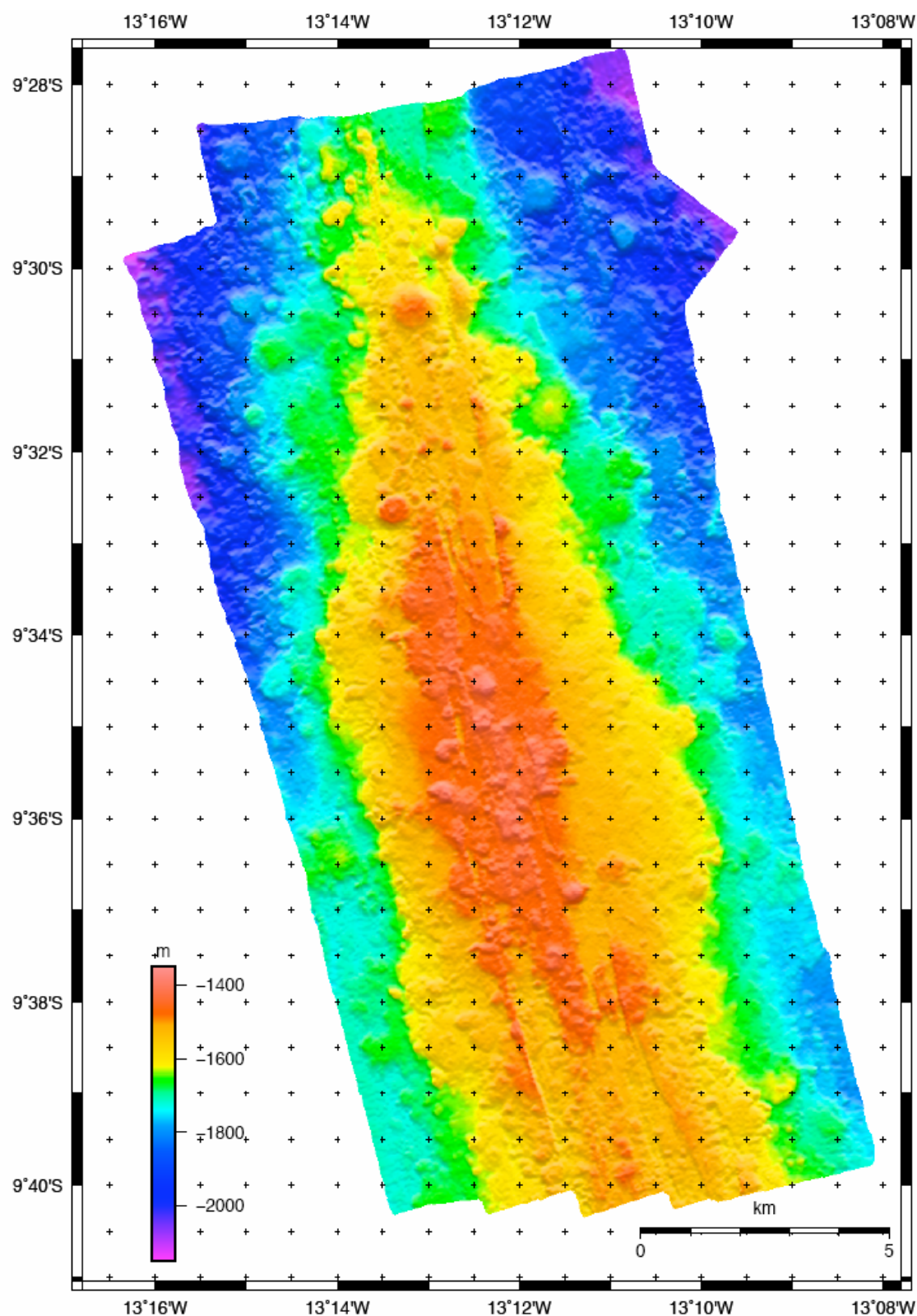


Fig. 2.4.11.3: Bathymetric map of the ridge axis north of the Nibelungen field (red dot). The map was obtained by profiling 137 nm with a line spacing of 1 nm (stations 313MB, and 315MB). The underlying grid cell size is 30 m.



GM 2009 May 07 23:53:53 lilliput_20_20_F5_z::2:::

Fig. 2.11.4.4: Bathymetric map of the Lilliput area. The map was obtained by profiling 110 nm with a line spacing of 0.5 nm (stations 328MB, 333MB, and 340MB). The underlying grid cell size is 20 m.

2.5 Journey Course and Weather

(Harald Rentsch)

The RV "Meteor" left the harbor of Port of Spain one day delayed, in the 4/2/2009 at 13 o'clock local time. At this time a high with 1022 hPa lay with 28N 50 W, his wedge still reached up to the southern Antilles. It was cloudy, nearly 30° Celsius hotly, in the harbor we had wind from 10 to 15 knots, however, it was very quietly and the continual north-east trade wind blew us around the nose. The ship went to the north of Trinidad by a strait in the Atlantic by which nozzle effects generated gusts to 25 knots and a swell of 1.5 m appeared. Our first destination was the area of operation with 4°48' S („Turtle Pits“), which should be reached with an average of 10 knots in 4/15/2009. On the next day a low-pressure area with 1014 hPa shifted with 32N 42W eastward and weakened a little. A matching cold front turned eastward and reached the middle Antilles in weakened form. The journey area itself lay in the area of the north-east trade wind under trouble-free weather. Also during the following two days we remained on the edge of deep atmospheric pressure and a upper-level trough in the zone of the steady north-east trade wind which blew with wind force 4 to 5. The swell running out from north-east reached 2.5 to 3 meters and 1.5 meters of wind sea. The equatorial current (330 degrees, one knot) stood directly opposite the way of the ship. On 4/5/2009 a wedge of subtropical high (1025 hPa, N37 W19) turned away from the day course of the ship "Meteor". With the further approach to the ITCZ cloudiness and shower probability increased. So, in the afternoon, the first shower cells reached us, initiated by conventional processes of the ITCZ. With gusts up to 28 knots, the temperature degreased about 3° within 5 minutes and the visibility decline to 3 km, the compact shower cloudiness moved later from south to the north across the ship's way. The caps of the Cb-cloudiness were measured with 14 km from an infrared satellite image.

A wedge of this subtopic high with approx. N40 W35 with central pressure about 1030 hPa also determined on the subsequent days the weather for the "Meteor". At the same time the period of the shower and thunderstorm probability raised within the ITCZ and moved to the afternoon and evening hours. Therefore it was often sunny dry below a dropping trade wind inversion in the mornings, up to 5 Beaufort and 2.5 m of sea height included.

4/11/2009 ("Equator – Christening"): Meteor had reached the ITCZ, that is why the instability of the atmosphere increased during the day steadily, however, "Meteor" remained still spared from tropical thunderstorms which stroked only in a wide distance of the ship. Near by the equator only low pressure differences existed, so that bringing weak winds from northern directions. The sea remained quiet, swell from 1.5 to 2 m, also still dry, tropical-hot and marvelous weather and a lot of sun during our "Equator – Christening". Within the ITCZ the labiality totally increased in all layers of the atmosphere and thunder clouds could study on the 12.4 in the evening.

On the 11.4, "Meteor" had crossed the equator and moved slowly into the area of the southeast trade winds. With it a stable southeaster direction was based hesitantly. At the same time the high labiality in the atmosphere continued. However, "Meteor" was spared by showers furthermore, in addition the sea remained relatively quiet, and with nearly 28°C maximum temperature, a cloudy sky on Easter day. From here "Meteor" went in the zone of equatorial low-pressure that means with weak winds. Before the southeast trade wind properly

formed up, and also the swell became stronger, sunny-hot and dry weather continued with an easily moved sea. The day maximum of air temperature and water temperature further lay within 28°C. On 4/15/2009 we reached our first area of operation (4° 48'S, 12° 22'W) in the trade wind zone. Up to 19.4 by the high water temperature released thermally caused zones of lability and an ITCZ far shifted to the south single showers or thunderstorms occurred mostly during the evening or night hours particularly with light increase of winds. During the morning hours a passing stabilization and dispersal of clouds could often be observed. Culmination of the instable weather character was on Saturday, 19.4., with huge cloud-clusters, which caused long continual rain-showers and a rain sum of 5 to 10 mm per hour. Only in 2nd day half there was the crossing to a friendlier sun-cloud-mix with only isolated showers. Besides, the southeast trade wind remained weak, the sea relatively quietly. After this rainy Sunday (total sum nearly 10 l / m² / h) a friendly sun-cloud-mix with 28 to 29 degrees as a maximum temperature once more expected us on Monday. In the area of the southeast trade wind and light increase of atmospheric pressure occurred, at the same time drier and warmer air masses reached us which contributed to a general weather stabilization namely in higher atmosphere layers. From this date (21.4.) there were only weak showers (0.4 mm / h) in the south edge of the ITZC. The wind remained solidly with wind force 4 from southeast, the sea hardly reached 2 m. On our way to „Inside Corner High“ we were already so far away from the ITCZ that the stable, dry subtropics weather of the trade winds asserts itself. With it we had a fine barbecue on this Saturday evening. - Ascension Island expected us on Sunday morning, 26.4., at a picture book sunrise, while we took aboard the film team of the ZDF. Up to the achievement of the next area of operation "Nibelungen" (9 S. 13 W) accompanied us southeast wind with 4 to 5 Beaufort and a parallel swell of 2.5 m. Two days later the desired picture book sundown (17:47 board times) at the shot time for the film team was no experience, because every evening arising clouds covered everything. On the last day of the photographs of ROV and AUV by the ZDF-film team the sun was so hot and the UV radiation charge was so high that sunbathe had to be well measured to get not sunburned. Under influence of a ground high wedge of the subtropics high to the south of 35 S we went with full speed to our last area of operation "Lilliput" together with a consistently, slightly moved sea. Last day of April thicker Sc-fields moved on which had formed below the trade wind inversion. An increasing of pressure-gradient and breezing winds with varying directions stood in connection with a low-pressure area with 30S 18 W which moved eastward and brought showers over the ship. Also the May weather began under influence of the southern subtropics high with 50S. 15 E and the trade wind was diverted by the low-pressure area with 25S 15W temporarily to a more eastern component of force 4 and a swell of 2, later to 3 m. During the following days "Meteor" remained in the area of the subtropics high with 1030 hPa on her journey towards Rio. Because some days before low- pressure-developments took place south of 35 S, a steadily rising swell 3.5 to 4 m reached us up to the 4th of May with periods from 12 to 14 seconds, in the beginning from southeast direction, later from 220 degrees. In addition the wind reaches nearly 5 wind forces. This complicated the work aboard and the drive by the rubber dinghy near by position (16° 20'S, 26° 5'W). On the last part of the trip a high-pressure area with 28S 34 W remained for us weather-determining. Inversion cloudiness, a moderately moved sea with a 3.5-m-high swell, 4 to 5 wind forces from north-east and only a day maximum of 27° Celsius accompanied us in the

territorial waters of Brazil. Together with the equatorial current which turned round here in the Brazil-current and a low-pressure area with 29S 37 W led to tail wind for the “Meteor” which strove with steadily sinking swell with on an average 11 knots against Rio. The journey segment M78 / 2 ended in the morning of the 5/11/2009 with the entrance in the harbor of Rio de Janeiro.

2.6 References

- Garbe-Schönberg D, Koschinsky A, Ratmeyer V, Jähmlich H, Westernströer U (2006) KIPS—A new multiport valvebased all-Teflon fluid sampling system for ROVs. Paper presented at EGU General Assembly, Eur Geosci Union, Vienna
- Gebhardt S, Colomb A, Hofmann R, Williams J, Lelieveld J (2008) Halogenated organic species over the tropical South American rainforest. *Atmos Chem Phys* 8-12, 3185-3197
- Goodwin KD, North WJ, Lidstrom ME (1997) Production of bromoform and dibromomethane by giant kelp: factors affecting release and comparison to anthropogenic bromine sources. *Limnol Oceanogr* 42, 1725-1734
- Haase, K., C. Flies, S. Fretzdorff, O. Giere, A. Houk, S. Klar, A. Koschinsky, J. Küver, H. Marbler, P. Mason, N. Nowald, C. Ostertag-Henning, H. Paulick, M. Perner, S. Petersen, V. Ratmeyer, W. Schmidt, T. Schott, M. Schröder, R. Seifert, C. Seiter, J. Stecher, H. Strauss, J. Süling, D. Unverricht, M. Warmuth, S. Weber, U. Westernströer 2005: MARSÜD 2. Meteor Berichte 05, Cruise No. 64, Leg 1. Institut für Meereskunde der Universität Hamburg. 59 pp.
- Isidorov VA (1990) Organic chemistry of the Earth's atmosphere. Chapter 3 – Natural sources of organic components of the atmosphere. Springer, Berlin 215p
- Keene WC, et al. (1999) Composite global emissions of reactive chlorine from anthropogenic and natural sources – reactive chlorine emissions inventory. *J Geophys Res* 104, 8429-8440
- Khalil MAK, Morre RM, Harper DB, Lobert JM, Erickson DJ, Koropalov V, Sturges WT, Keene WC (1999) Natural emissions of chlorine-containing gases – reactive chlorine emissions inventory. *J Geophys Res* 104, 8333-8346
- Koppmann R, Johnen FJ, Plass-Dülmer C, Rudolph J (1993) Distribution of methyl chloride, dichloromethane, trichloroethene and tetrachloroethene over the North and South Atlantic. *J Geophys Res* 98, 20517-20526
- Koschinsky, A., A. Billings, C. Devey, N. Dubilier, A. Duester, D. Edge, D. Garbe-Schönberg, C. German, O. Giere, R. Keir, K. Lackschewitz, H.A. Mai, H. Marbler, J. Mawick, B. Melchert, C. Mertens, W.-T. Ochsenhirt, M. Peters, S. Sander, O. Schmale, W. Schmidt, R. Seifert, C. Seiter, U. Stöber, I. Suck, M. Walter, S. Weber, D. Yoerger, M. Zarrouk, F. Zielinski, 2006, Fluid geochemistry, biology and geological setting of hydrothermal systems at the southern MAR (4°S - 10°S) (MAR-SÜD III). METEOR Berichte 06, Cruise No. 68, Leg 1. Institut für Meereskunde der Universität Hamburg. 89 pp.
- Koschinsky A, Garbe-Schönberg D, Sander S, Schmidt K, Gennerich HH, Strauss H (2008) Hydrothermal venting at pressure-temperature conditions above the critical point of seawater, 5°S on the Mid-Atlantic Ridge. *Geology*, 36, 615–618, doi: 10.1130/G24726A.1
- Laternus F (2001) Marine macroalgae in Polar Regions as natural source of volatile organohalogenes. *Environ Sci Pollut Res* 8, 103-108
- Laternus F, Haselmann KF, Borg T, Grøn C (2002) Terrestrial natural sources of trichloromethane (chloroform, CHCl₃) – an overview. *Biogeochemistry* 60, 121-139
- Manley SL, Wang NY, Walser ML, Cicerone RJ (2007) Methyl halide emissions from greenhouse grown mangroves. *Geophys Res Lett* 34, L01806, doi:10.1029/2006GL027777
- McCulloch A, Aucott ML, Benkovitz CM, Graedel TE, Kleiman G, Midgley PM, Li YF (1999) Global emissions of hydrogen chloride and chloromethane from coal combustion, incineration and industrial activities – reactive chlorine emissions inventory. *J Geophys Res* 1004, 8391-8403
- Redeker KR, Wang NY, Low JC, McMillan A, Tyler SC, Cicerone RJ (2000) Emissions of methyl halides from rice paddies. *Science* 290, 966-969
- Rhew RC, Miller BR, Bill M, Goldstein AH, Weiss RF (2002) Environmental and biological controls on methyl halides emissions from southern California coastal salt marshes. *Biogeochemistry* 60, 141-161
- Scheeren HA et al. (2003) Measurements of reactive chlorocarbons over the Surinam tropical rain forest: indications for strong biogenic emissions. *Atmos Chem Phys Discuss* 3, 5469–5512
- Schmidt K, Garbe-Schönberg D, Bau M, Koschinsky A (subm.) Rare earth element distribution in >400°C hot hydrothermal fluids from 5°S, MAR: Controls on anomalous and highly variable distribution patterns. - *Geochim. Cosmochim. Acta*

- Schmitt M, E. Faber, R. Botz & P. Stoffers, 1991: Extraction of methane from seawater using ultrasonic vacuum degassing. *Anal Chem* **63**: 529–531
- UNEP (1987) The Montreal protocol on substances that deplete the ozone layer. United Nations Environmental Programme (UNEP) 192p
- Wousmaa AM, Hager LP (1990) Methyl transferase – a carbocation route for the biosynthesis of halometabolites. *Science* 249, 160-162
- Yokouchi Y, Ikeda M, Inuzuka Y, Yukawa T (2002) Strong emission of methyl chloride from tropical plants. *Nature* 416, 163-164
- Yokouchi Y, Saito T, Ishigaki C, Aramoto M (2007) Identification of methyl chloride-emitting plants and atmospheric measurements on a subtropical island. *Chemosphere* 69, 549–553

2.7 Acknowledgments

We would like to thank Captain Baschek and his crew on R/V Meteor for their excellent cooperation as well as T. Ohms and D. Quadfasel at the "Leitstelle Meteor" for the professional patronage.

We wish to thank the German Science Foundation (DFG) for funding the cruise and the subsequent scientific work in the framework of the priority program SPP 1144 "From Mantle to Ocean: Energy-, Material-, and Life Cycles at Spreading Axes".